

Investigating the Interactions of Polymeric Excipients with Poorly Water-Soluble Drugs as Means for Pharmaceuticals Bioavailability Enhancement

A Thesis

SUBMITTED TO THE FACULTY OF

UNIVERSITY OF MINNESOTA

BY

Anatolii Purchel

IN PARTIAL FULLFILLMENT OF THE REQUIREMENTS

FOR THE DEGREE OF

DOCTOR OF PHYLOSOPHY

Theresa M. Reineke

February, 2019

© Anatolii Purchel

Acknowledgements

The author would like to acknowledge the contributions from other authors from his prior published papers, the guidance of Dr. Theresa Reineke who played a significant role in the research projects, the members of the committee, collaborators from the Dow project and the funding that made this work possible.

The author would also like to thank former Reineke group members Swapnil Tale, Yogesh Dhande, Haley Phillips, Jeff Ting, Bharat Wagh, Leon Lillie, Mammad Nasiri, Victoria Szlag, Lakmini Widanapathirana, Susith Wickramaratne, Quanxuan Zhang, Seyoung Jung, Will Boyle, Pranav Agrawal, Lindsay Robinson, Rui Ding, and Mitra Ganewatta. Additionally, the author would like to extend his gratitude to the current Reineke group members Naree, Matt, Ramya, Piril, Rishad, Ethan, Ngoc, Annie, Monica, Snain, Derek, Zhe, Craig, Cameron, George, Julia, Mckenna, Erin, Christian, Mayuri, Cristiam, and Andy. Thank you, Letitia, for help with NMR kinetics and DOSY experiments, Nancy for help with regulatory, and Joe for proof reading and editing.

This project was partially funded by the Department of Chemistry at the University of Minnesota and partially funded by The Dow Chemical Company (Dow) through Agreement 224249AT with the University of Minnesota. Parts of this work were carried out in the Characterization Facility, University of Minnesota, which receives partial support from NSF through the MRSEC program.

To my family and all the curious minds

Abstract

Oral administration is the most preferable route of drug delivery, especially during prolonged therapy of chronic diseases. Unfortunately, many effective pharmaceuticals are poorly water-soluble, which leads to decreased bioavailability and shelf life. One of the ways to improve drug solubility and efficacy is to prepare an amorphous solid dispersion (ASD) with a polymer excipient. It is important that the polymer matrix of an ASD will stabilize the drug in the amorphous state and maintain its supersaturated concentration long enough in the dissolution media. Some of the commercial polymeric systems have shown a positive impact on drug dissolution, but most of them are difficult to characterize due to high polydispersity and system complexity. Most of the available excipients that improve dissolution of poorly water-soluble drugs tend to form nano-aggregates in the solution. Thus, in order to understand structure-property relationships better, various polymers were explored, which self-assemble into micelle-like structures or exist as free polymer chains in the solution, as excipients for dissolution of a model drugs such as probucol and phenytoin. Reversible addition-fragmentation chain transfer (RAFT) polymerization was used as a controlled polymerization technique to obtain well-defined polymers of polystyrene, poly(acrylic acid), N-isopropylamide, 4-vinylpyridine, N,N-dimethylacrylamide, and trehalose-derived monomers. The polymers were characterized by nuclear magnetic resonance (NMR) spectroscopy and size exclusion chromatography (SEC). The effects of nano-aggregation in ASDs, polymer charge, H-bonding and hydrophobic interactions on drug dissolution were determined. Caco-2 cell permeability assay was applied to determine cell permeability of drugs in some of the obtained formulations.

Table of Contents

<i>Abstract</i>	<i>iii</i>
<i>List of Figures</i>	<i>vi</i>
<i>List of Tables</i>	<i>xiv</i>
Chapter 1. General Introduction	1
1.1 Oral drug delivery	2
1.2 Reversible addition-fragmentation chain transfer polymerization (RAFT)	6
1.3 Block copolymer applications in oral drug delivery	10
1.4 Applications and limitations of the Caco-2 cell permeability assay	17
1.5 Thesis outline	20
1.6 References	21
Chapter 2. Diblock Terpolymers are Tunable and pH Responsive Vehicles to Increase Hydrophobic Drug Solubility for Oral Administration *	31
2.1 Introduction	32
2.2 Results and Discussion	35
2.2.1 Synthesis of the diblock terpolymers	35
2.2.2 Synthesis of the PDMA homopolymer.....	39
2.2.3 Solid dispersions preparation and solid-state characterization	42
2.2.4 Drug dissolution testing.....	46
2.3 Conclusion	52
2.4 Materials and Methods	53
2.4.1 Materials	53
2.4.2 Polymer synthesis.....	54
2.4.3 Methods	57
2.5 References	63
Chapter 3. Aggregated Solution State Morphology of Poly(acrylic acid)-Poly(styrene) Block Copolymers Improves Drug Supersaturation Maintenance and Cell Membrane Permeation *	67
3.1 introduction	68
3.2 Results and Discussion	71
3.2.1 Polymer synthesis	71
3.2.2 Polymer solution-state properties in organic solvents.....	74
3.2.3 Solid-state properties of the spray dried dispersions.....	77

3.2.4 Aqueous solution behavior of the spray dried polymer/drug dispersions	79
3.2.5. <i>In Vitro</i> Caco-2 cell assay permeation studies	85
3.3 Conclusion.....	88
3.4 Materials and Methods.....	89
3.4.1 Materials	89
3.4.2 Polymer synthesis.....	90
3.4.3 Methods	95
2.5 References	103
<i>Chapter 4. Star Architectures of Polymeric Excipients and Their Effect on Drug Supersaturation Maintenance.....</i>	<i>110</i>
4.1 introduction.....	111
4.2 Results and Discussion.....	116
4.2.1 Synthesis of the chain transfer agent.....	116
4.2.2 Synthesis of the multi-functional CTAs	118
4.2.3 Synthesis of the star polymers	120
4.2.3 Solid dispersions preparation with BCS Class II drug probucol	123
4.2.4 Drug dissolution testing.....	124
4.3 Conclusion.....	130
4.4 Materials and Methods.....	130
4.4.1 Materials	130
4.4.2 Polymer synthesis.....	131
4.4.3 Methods	134
4.5 References	136
<i>Chapter 5. Summary and Outlook.....</i>	<i>142</i>
5.1 Dissertation summary.....	143
5.2 Future directions.....	145
<i>Bibliography.....</i>	<i>148</i>

List of Figures

Figure 1.1. Percentages of marketed vs. pipeline drugs: trends towards low solubility. Many pipeline drugs are not brought to the market due to solubility problem. Adapted from reference ¹	4
Figure 1.2. Equilibria of reversible-addition fragmentation chain transfer (RAFT) polymerization. I stands for the initiator, P – for the polymeric radical, M – monomer, R – RAFT agent derived radical. The Z group of the RAFT agent affects the stability of C=S bond and the stability of the adduct radical (3) where the R group must be able to produce a stable enough radical such that will favor the formation of the growing polymer chain P _n , but unstable enough to reinitiate growth of a new polymer chain P _m . Adapted from reference ³³	9
Figure 1.3. Guidelines for selection of the macro-R group for the preparation of block copolymers. Dashed lines indicate poor control over polymerization (high dispersity due to inferior hemolytic group ability or retardation due to slow re-initiation of polymerization). Abbreviations: MMA – methyl methacrylate, HPMAM – N-(2-hydroxypropyl) methacrylamide, St – styrene, DMAM – N,N-dimethylacrylamide, NVC – N-vinylcarbazole, VAc – vinyl acetate, NVP – N-vinylpyrrolidone. Reproduced from reference ³³	10
Figure 1.4. Different amphiphilic copolymer types and architectures lead to different micelle structures by self-assembling. Initial structure of a block copolymer determines the morphology of a micelle. Adapted from reference ³⁹	12

Figure 1.5. Drug–polymer formulations and their advantages. A: Drug formulations prepared with polymeric excipients by either simple mixing to obtain a polymer-drug solution, encapsulating the drug in micro- or nanoparticles, or by synthesizing a covalent drug–conjugate. B: The different formulations should enhance drug stability in the GI tract and shield the drug from the acidic pH, GI enzymes, and bile salts. C: Adequate drug release is required at the targeted site. D: Transport across the intestinal membrane can occur via the paracellular and/or transcellular pathway through epithelial or M cells. Adapted from reference⁵⁴ 17

Figure 2.1. ¹H NMR spectrum recorded for PNIPAAm-CTA in CDCl₃ 36

Figure 2.2. ¹H NMR spectrum recorded for PDEAEMA-CTA in CDCl₃ 37

Figure 2.3. ¹H NMR spectrum recorded for PNIPAm-*b*-P(DMA-*grad*-MAT) in d₆-DMSO 38

Figure 2.4. ¹H NMR spectrum recorded for PDEAEMA-*b*-P(DMA-*grad*-MAT) in CDCl₃ 39

Figure 2.5. Synthesis of the diblock terpolymers. Reagents and Conditions: a) AIBN, 70 °C, Toluene b) 1.25M HCl in methanol 40

Figure 2.6. Powder XRD patterns of crystalline probucol comparing SDDs with A) PEP-*b*-P(DMA-*grad*-MAT), B), B'), B'') PNIPAm-*b*-P(DMA-*grad*-MAT) (18, 32, 48 kDa, respectively), C) PDEAEMA-*b*-P(DMA-*grad*-MAT), and D) PDMA as the matrices at 25 weight percent. SEM image is of the SDD created by spraying a THF:MeOH (15:2) solution of probucol with PEP-*b*-P(DMA-*grad*-MAT). 43

Figure 2.7. MDSC thermograms of total heat flow from SDDs containing 50 weight percent of probucol A) PEP-*b*-P(DMA-*grad*-MAT), B) PNIPAm-*b*-P(DMA-*grad*-MAT) – 32 kDa, B)’ – PNIPAm-*b*-P(DMA-*grad*-MAT) – 18 kDa, B)’’ – PNIPAm-*b*-P(DMA-*grad*-MAT) – 48 kDa, and C) PDEAEMA-*b*-P(DMA-*grad*-MAT). 44

Figure 2.8. Dissolution data of the SDDs with 10 and 25 weight percent of probucol. PNIPAm-*b*-P(DMA-*grad*-MAT) – 32 kDa showed excellent rapid initial dissolution and supersaturation maintenance profile for probucol at pH 6.5. PDEAEMA-*b*-P(DMA-*grad*-MAT) showed a controlled release profile for probucol at pH 3.1. The target concentration of probucol was 1000 µg/mL (denoting 100% drug solubility) whereas the aqueous solubility of crystalline probucol (without an excipient) is very poor (0.042 µg/mL). Data points denote the mean of two dissolution experiments and error bars denote the range of measured data (*N*=2). 48

Figure 2.9. Dissolution data of the SDDs with three differing DMA-*grad*-MAT lengths with 10 and 25 weight percent of probucol and controls. The target concentration of probucol was 1000 µg/mL (denoting 100% drug solubility) whereas the aqueous solubility of crystalline probucol (without an excipient) is very poor (0.042 µg/mL). Data points denote the mean of two dissolution experiments and error bars denote the range of measured data (*N*=2). 49

Figure 2.10. Area under the curve (AUC) as calculated at 360 min from the dissolution data of SDDs with 10, 25, and 50 weight percent probucol (PRB) loading. The calculated AUC is the average of two trials and error bars denote the range of measured data (*N*=2). The data for the homopolymer of PDMA with probucol SDD was obtained from previously published work.¹⁰ 50

Figure 2.11. REPES analysis of data obtained from intensity correlation function at a 90° angle for the solutions in THF:MeOH (15:2, v/v) of a) PNIPAm-b-P(MAT-*grad*-DMA) – 32 kDa, b) PDEAEMA-b-P(MAT-*grad*-DMA), c) PEP-b-P(MAT-co-DMA), and d) PNIPAm-b-P(MAT-*grad*-DMA) – 18 kDa. Polymer concentration is at 1 wt %..... 59

Figure 2.12. SEM images of the SDDs created by spraying a THF:MeOH (15:2) solution of probucol with (a) PEP-b-P(DMA-*grad*-MAT), (b) PNIPAAm-b-P(DMA-*grad*-MAT) – 32 kDa, (c) PDEAEMA-b-P(DMA-*grad*-MAT), (d) PNIPAAm-b-P(DMA-*grad*-MAT) – 18 kDa, and (e) PNIPAAm-b-P(DMA-*grad*-MAT) – 48 kDa as the polymer excipients at 25 weight percent of drug loading. The scale bars indicate 1 μm. 61

Figure 3.1. Hydrodynamic radii of PS-PAA block copolymers in methanol (selective solvent) or in methanol-THF mixture (1:1, v/v, nonselective solvent. All solutions were composed of 1 wt % polymer in solvent. Hydrodynamic radii were calculated by fitting the correlation functions using either cumulant or double exponential expansions. Linear regressions of Γ vs q^2 were performed for five angles (30°, 45°, 60°, 75°, 90°). Hashed colored bars represent the major contributing (larger particle concentration) hydrodynamic radius in the sample, and solid colored bars represent the lesser contributing second mode. * – poor solubility of this sample did not allow for the determination of a high quality correlation function. Errors bars denote the standard deviation of the linear regression (3 replicates). 76

Figure 3.2. (a) Image of a 1 wt % solution of PS₃₈-*b*-PAA₃₂₀ polymer in a methanol-THF mixture (1:1, v/v) showing no laser light scattering indicating a homogeneous solution. The cartoon represents soluble unimers in solution. (b) Image of a 1 wt % solution of PS₃₈-*b*-

PAA₃₂₀ polymer in methanol showing scattering of laser light denoting the aggregates. The cartoon represents the aggregation of the polymer chains into micelle-like structures, which leads to close packing of hydrophilic tails and provides a reservoir of binding sites for the drug molecule to promote solubility. 77

Figure 3.3. PXRD patterns (A) for SDDs with probucol loading of 25 wt % comparing (i) crystalline probucol, (ii) PS₉₀-*b*-PAA₈₀ spray dried from methanol, (iii) PS₉₀-*b*-PAA₈₀ spray dried from THF/MeOH (1:1, v/v), (iv) PS₃₈-*b*-PAA₂₂₀ spray dried from methanol, (v) PS₃₈-*b*-PAA₂₂₀ spray dried from THF/MeOH (1:1, v/v), (vi) PS₃₈-*b*-PAA₃₂₀ spray dried from methanol, (vii) PS₃₈-*b*-PAA₃₂₀ spray dried from THF/MeOH (1:1, v/v) and SEM image (B) of the SDD created by spraying a THF/MeOH (1:1) solution of probucol with PS₃₈-*b*-PAA₃₂₀. 78

Figure 3.4. Dissolution data at pH=6.5 for the SDDs formed with the block polymers and analogous homopolymer excipients formed at 25 wt % probucol. A) PS₃₈-*b*-PAA₃₂₀ and PAA₃₉₀, B) PS₃₈-*b*-PAA₂₂₀ and PAA₂₂₆, C) PS₉₀-*b*-PAA₈₀ and PAA₉₆, D) PS₉₀-*b*-PAA₁₅ and PAA₂₀. Blue lines denote block copolymers spray dried from MeOH, red lines denote block copolymer spray dried from THF/MeOH, and green lines denote homopolymers spray dried from MeOH. Error bars denote the range of the measured data (*n*=2). 81

Figure 3.5. Dissolution data when the pH value of the dissolution media is changed from 1.2 to 7.0 (90 minutes time point) for the SDDs formed with the block polymers and analogous homopolymer excipients formed at 25 wt % probucol. A) PS₃₈-*b*-PAA₃₂₀ and PAA₃₉₀, B) PS₃₈-*b*-PAA₂₂₀ and PAA₂₂₆, C) PS₉₀-*b*-PAA₈₀ and PAA₉₆, D) PS₉₀-*b*-PAA₁₅ and PAA₂₀. Blue lines denote block copolymers spray dried from MeOH, red lines denote

block copolymer spray dried from THF/MeOH, and green lines denote homopolymers spray dried from MeOH. Error bars denote the range of the measured data ($n=2$). 82

Figure 3.6. Polymer solubility data using SDDs with 25 wt % probucol at pH=6.5 and dissolution profiles (inset plots, y-axis is drug concentration, $\mu\text{g/mL}$ and x-axis is time in minutes) for the same samples (see Figures 3.4 and 3.5) to demonstrate correlation between formulation performance and excipient solubility. Blue bars denote SDDs prepared in methanol (nonselective solvent) and red bars denote SDDs prepared in THF/methanol (selective solvent). Error bars denote the range of the measured data ($n=2$). 85

Figure 3.7. NMR spectra of the poly(acrylic acid)-*b*-polystyrene diblock copolymer before (brown) and after (blue) deprotection with trifluoroacetic acid from poly(*tert*-butyl acrylate)-*b*-polystyrene block copolymer. NMR shows complete disappearance of *tert*-butyl protecting group. NMR was recorded in deuterated methanol. 92

Figure 3.8. ^{13}C -NMR spectra of the poly(acrylic acid)-*b*-polystyrene diblock copolymer before (bottom) and after (top) deprotection with trifluoroacetic acid from poly(*tert*-butyl acrylate)-*b*-polystyrene block copolymer. NMR shows complete disappearance of *tert*-butyl protecting group as well as a shift in carbonyl carbon peak from 174 to 178 ppm. NMR spectra were recorded in either deuterated chloroform or deuterated methanol... 93

Figure 3.9. NMR spectra (top) and SEC chromatograms (bottom) of the synthesized diblock copolymers and homopolymers. Both techniques were used to determine molecular weight of the diblock copolymers and were in agreement with each other (no more than 10% difference). 94

Figure 3.10. PXRD patterns for SDDs with probucol loadings of 10 and 25 wt % comparing (a) crystalline probucol, (b) PS_{90} -*b*- PAA_{80} spray dried from methanol, (c) PS_{90} -*b*- PAA_{80}

spray dried from THF/MeOH (1:1, v/v), (d) PS₃₈-*b*-PAA₂₂₀ spray dried from methanol, (e) PS₃₈-*b*-PAA₂₂₀ spray dried from THF/MeOH (1:1, v/v), (f) PS₃₈-*b*-PAA₃₂₀ spray dried from methanol, (g) PS₃₈-*b*-PAA₃₂₀ spray dried from THF/MeOH (1:1, v/v). 97

Figure 3.11. SEM images for 25 wt % probucol sprayed with block copolymers from two different solvent systems: (a) MeOH, and (b) THF/MeOH (1:1, v/v). All scale bars are equal to 5 μm 99

Figure 4.1. Illustration of various types of star polymers classified by (A) composition and sequence distribution of the arm polymer, (B) difference in arm species, (C) core structure, and (D) functional placement. Adapted from reference¹¹ 113

Figure 4.3. ¹H NMR spectrum of the 2-methyl-2-(((propylthio)carbonothioyl)thio)propanoic acid recorded in CDCl₃ 117

Figure 4.4. (A) Monomer conversion as a function of time, recorded using variable temperature NMR. Alpha-vinyl hydrogen on the monomer was used for the concentration determination. (B) Plot of the natural logarithm of the inverse instantaneous monomer concentration as a function of time to confirm the first order kinetics law. Reaction conducted in CD₃CN, 400 MHz. 118

Figure 4.5. ¹H-NMR spectrum of the tri-functional CTA in CDCl₃..... 120

Figure 4.6. Representative NMR spectra (of the three-arm star polymer) before (A) and after (B) tert-butyl group deprotection. Spectrum (A) was recorded in CDCl₃ and (B) was recorded in MeOD. End-group analysis demonstrated that polymer architecture stays intact upon deprotection..... 122

Figure 4.7. Dissolution data of the SDDs prepared at 25 wt % of probucol. The target concentration of probucol was 1000 $\mu\text{g/mL}$ (denoting 100% drug solubility) whereas the aqueous solubility of crystalline probucol (without an excipient) is very poor (0.042 $\mu\text{g/mL}$). Data points denote the mean of three dissolution experiments and error bars denote the standard deviation of the measured data ($N=3$). 125

Figure 4.8. Dissolution data of the SDDs at 50 weight percent of probucol. The target concentration of probucol was 1000 $\mu\text{g/mL}$ (denoting 100% drug solubility) whereas the aqueous solubility of crystalline probucol (without an excipient) is very poor (0.042 $\mu\text{g/mL}$). Data points denote the mean of three dissolution experiments and error bars denote the standard deviation of measured data ($N=3$). 126

Figure 4.9. Area under the curve (AUC) as calculated at 360 min from the dissolution data of SDDs with 10, 25, and 50 weight percent probucol (PRB) loading. The calculated AUC is the average of three trials and error bars denote the standard deviation of measured data ($N=3$). 128

Figure 5.1. (A) Proposed synthesis method for the synthesis of hydantoins (Phenytoin's analogues), (B) Structure of the model drug Phenytoin, and (C) Different substituents that will be used around hydantoin core 146

List of Tables

Table 1.1. The range of pH values across various locations in the gastrointestinal tract. Reproduced from reference ²⁶	6
Table 2.1. Molecular characterization of the homopolymers.....	36
Table 2.2. Characterization of the polymers used in this study.....	41
Table 2.3. Comparison of the weight fraction of monomers and drugs in the SDDs and the percent of probucol crystallinity.....	45
Table 2.4. MDSC analysis of SDDs with probucol.....	45
Table 2.5. Calculated area under the curve (AUC) for solubilization of probucol and all polymer excipient SDD formulations at 10, 25 and 50 weight percent drug loading.	52
Table 3.1. Polymer Characterization Data.	73
Table 3.3. Caco-2 cell permeability assay performed using four samples: (1) PAA ₉₆ spray dried with 25 wt % probucol, (2) PS ₉₀ - <i>b</i> -PAA ₈₀ spray dried from methanol with 25 wt % probucol, (3) PS ₉₀ - <i>b</i> -PAA ₈₀ spray dried from THF/MeOH with 25 wt % probucol, and (4) HPMCAS with 25 wt % probucol.	88
Table 4.1. Molecular weight and dispersity data of the star polymers used in this study.	123
Table 4.3. Percent of probucol crystallinity in SDDs formulated with 50 wt % of the drug (as determined by the DSC) and AUC _{360min} value for each of the formulations.....	129

Chapter 1

General Introduction

1.1 Oral drug delivery

The vast majority of current medicines are administered via oral drug delivery. This route is preferable from the perspective of a patient, and can offer “slow release” of the pharmaceutical, effectively extending the duration of treatment. However, the therapeutic efficacy of an orally administered drug can be hindered by a multitude of factors: slow absorption into the bloodstream and/or a seemingly unpredictable absorption rate that depends on the acid-stability of the drug and its propensity to passively/actively diffuse through the intestinal wall. In contrast, the therapeutic efficacy of drugs dosed by intravenous injection (IV) are not limited by the aforementioned issues. Thus, drugs administered by IV can directly reach systemic circulation immediately and give rapid onset effects.

Unfortunately, around 70% of pipeline drugs fall into two low solubility groups of the Biopharmaceutical Classification System:^{1,2} Classes II and IV (Figure 1.1A). Low solubility of active pharmaceutical ingredients (API) decreases their bioavailability and leads to rejection of approximately two out of every three candidates evaluated during the drug approval process.¹ Thus, there is a large discrepancy between the amount of BCS Class II drugs in the developmental pipeline (~70%) and the amount of Class II drugs available on the market (36%). This significant drawback substantially lengthens the time necessary to develop a novel drug candidate which, in turn, increases the overall cost of research and development (R&D; in 2015 a novel API development took on average 13.5 years at a cost of \$1.8B³). In fact, overall losses in the drug development pipeline due to low solubility are estimated to be around \$8.2B in the pharmaceutical industry (GlobalData⁴). Additionally, as shown in Figure 1.1B, it is evident that there is a trend

toward APIs having poor water solubility properties. Thus, improving the aqueous solubility issue is of primary importance for the development and food and drug administration (FDA) approval of novel APIs.

Drugs that are administered orally are divided into four categories based on their solubility in gastrointestinal media: high solubility, high permeability (I); low solubility, high permeability (II); high solubility, low permeability (III); low solubility, low permeability (IV) (Figure 1.1). Classification is based on *in vivo* permeability experiments of the drug through a jejunal membrane and aqueous drug solubility at pH values ranging from 1 to 8. Class II is the most attractive platform for developing novel excipients because *in vitro/in vivo* correlation (IVIVC) is possible, which allows dissolution testing results to predict the bioavailability of the API. This correlation enables drug solubilities to be analyzed *in vitro* via dissolution tests, without requiring the time- and labor-intensive *in vivo* animal experiments.

Currently, there are several methods being developed to enhance the solubility and bioavailability of poorly water soluble drugs: dissolution with lipophilic excipients (self-emulsifying drug delivery system), media milling with polymeric excipients and surfactants (nanocrystal formulation), hot melt extrusion with polymeric excipients, and dissolution and spray drying with polymeric excipients.⁵⁻¹² Some of these methods are currently being applied for industrial pharmaceutical production. This allows to prolong the availability of a drug in a thermodynamically unstable amorphous state, which has much higher solubility in aqueous media compared to highly-ordered, crystalline state.¹³ Spray drying is of particular interest, as it has been extensively studied as a way to obtain amorphous solid dispersions.^{14,15} Additionally, spray drying is a scalable technique for

future applications in industry since most parameters of the resultant spray dried dispersions, such as composition and morphology, are reproducible and controllable. Moreover, spray drying is directed towards producing a homogeneous polymer/drug mixture, in which the ingredients are stabilized in an amorphous state. Furthermore, in contrast to other techniques, spray drying prevents fast recrystallization of the API in polymer-drug solid dispersions in which of nanocrystallites or certain heterogeneities are present, which can significantly decrease its bioavailability.

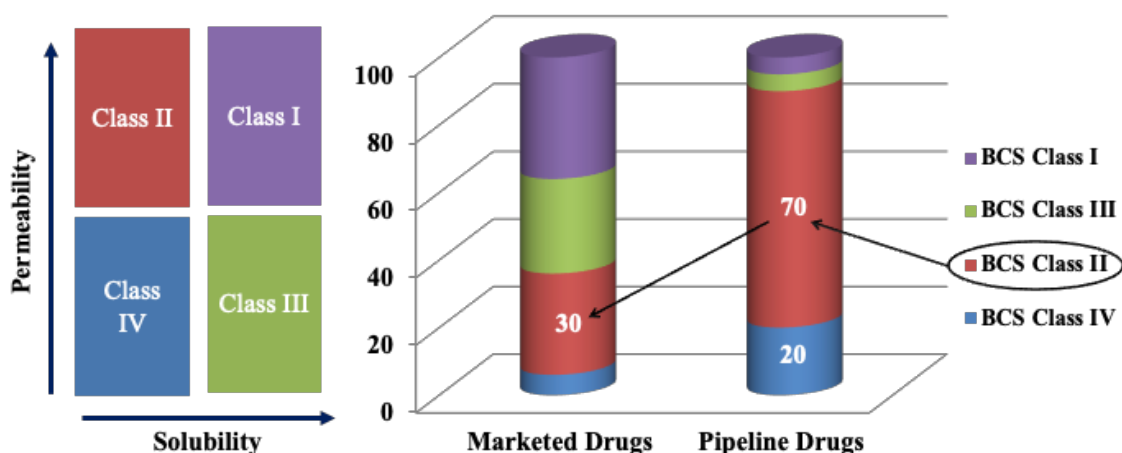


Figure 1.1. Percentages of marketed vs. pipeline drugs: trends towards low solubility. Many pipeline drugs are not brought to the market due to solubility problem. Adapted from reference¹

Polymeric excipients, the key component in preparation of pharmaceutical formulations, require further investigation in terms of structure-property relationships to enable novel medicines. For instance, hydroxypropyl methyl cellulose acetate succinate (HPMCAS), one of the most successful excipient for drug solubility enhancement¹⁶, is lacking in structure-property relationship knowledge. In addition to the chemical functionalities of HPMCAS, its solution state, surface charge, and architecture of also must

be rigorously investigated and understood to inform rational excipient design. Previous research on HPMCAS has shown a dramatic increase in performance due to nanoaggregation in the solution prior to spray drying, demonstrating the value in understanding the solution state properties of polymeric excipients and its correlation to dissolution enhancement.¹⁷⁻¹⁹ Thus, the research described in this dissertation is focused on developing novel polymeric excipients for solubility enhancement of BCS class II drugs based on a systematic evaluation polymer chemical and physical properties in the complex media.

As was mentioned before, many promising medicines belong to class II.²⁰ Unfortunately, the low aqueous solubility of these drugs leads to a limited oral bioavailability because their absorption rates are kinetically limited by low rates of dissolution in addition to thermodynamic limitations. To address this problem, several approaches such as micro emulsions²¹, micronization²², lipid based vehicles²³, self-emulsifying systems²⁴, and solid dispersions²⁵ have been incorporated. Many factors determine the efficacy of these drug delivery systems. First, the pH of the gastrointestinal (GI) tract tends to vary (1.2 – 7.0) and is dependent on multiple factors such as the fed state of the animal, age, health conditions and diet. In Table 1.1 pH values in different locations of gastrointestinal tract are shown depending on a fed state.²⁶ The pH range is important, because the presence of acidic or basic groups in a polymer backbone will cause the whole drug carrier to experience pH-dependent behavior, which in turn may compromise the overall performance of the drug-carrying assembly. It has been shown by Kurkuri and coworkers²⁷ that poly(vinyl alcohol)-based excipients exhibit significant pH-dependence of the diclofenac (model drug for this study) diffusion coefficient in the dissolution media

which in turn can affect the drug's intestinal permeability. Maghsoodi et al. described pH dependence of piroxicam solubility under conditions with different pH values as well. Additionally, interaction of the drug with the polymer matrix plays a major role not only in drug solubility, but in ability of the drug to maintain a high enough concentration to permeate across the tissues and get into the blood stream. Because amorphous pharmaceuticals tend to be more soluble than crystalline ones due to the absence of penalty imposed by crystallization enthalpy, it is important to prevent drug crystallization and allow it to be absorbed through the intestinal membrane.

Table 1.1. The range of pH values across various locations in the gastrointestinal tract. Reproduced from reference²⁶

State	Fed	Unfed
Location	Average pH	Average pH
Stomach	4.9	1.2
Duodenum	5.4	6.5
Jejunum	5.2 – 6.0	6.6
Ileum	7.5	7.4

1.2 Reversible addition-fragmentation chain transfer polymerization

(RAFT)

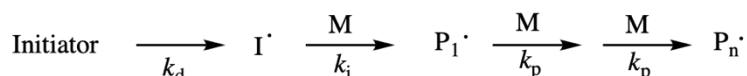
Controlled polymerization, where the ability of a growing polymer chain to transfer or terminate its reactivity has been removed or suppressed, is important for excipient development with the well-defined structures. In most cases, the rate of chain initiation is much higher compared with the rate of chain propagation and thus, it results in a constant number of kinetic chain-carriers throughout the polymerization process.²⁸ Living

polymerization was first discovered by Michael Szwarc in 1956 with the anionic polymerization of styrene.²⁹ Living polymerization is widely used throughout polymer chemistry in both research labs and in industry as it provides facile control over polymer chemical composition and thus, mechanical, structural, and electronic properties of the material. The most common types of living polymerization are atom transfer radical polymerization (ATRP), anionic polymerization, and reversible addition-fragmentation chain transfer polymerization (RAFT).³⁰ The main difference between anionic polymerization and RAFT or ATRP is that both RAFT and ATRP proceed via a degenerative chain transfer process, where propagating species are deactivated (in a dormant state). All of the above-mentioned types of polymerization provide control over molecular weight distribution and are appropriate for synthesis of block copolymers. RAFT polymerization has major advantages in comparison with anionic or ATRP. It does not require work with flammable initiators or with inorganic salts, which are difficult to remove from the final product. Moreover, RAFT polymerization requires only degassing of the solvent as oxygen can terminate chain propagation. However, for anionic polymerization, vigorous purification of reactants should be conducted due to the inherent reactivity of the initiators. Therefore, preparation of all reagents requires a significant amount of time. Also, RAFT polymerization is appropriate for polymerization of most monomers that undergo radical-mediated polymerization reactions, and it is compatible with a wide variety of reaction media and polymerization types such as aqueous solutions³¹, emulsion polymerization³², and organic solutions³³.

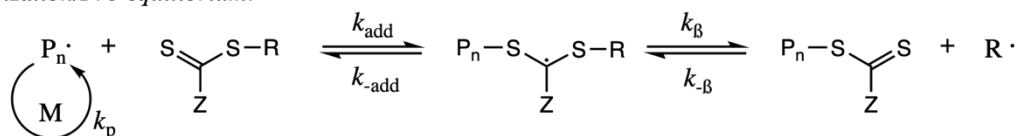
Degenerative chain transfer in RAFT polymerization is facilitated by a thiocarbonylthio group at the chain transfer agent (CTA, or RAFT agent). Figure 1.3

depicts the mechanism of RAFT polymerization. The mechanism of this polymerization begins with an initiation step via decomposition of an initiator resulting in a radical specie that can react with monomers (M) to start the polymerization. This will consequently afford a polymeric radical (P_n). Next, reaction of the polymeric radical with the CTA produces a macro-CTA and RAFT agent-derived radical (R). The R group reinitiates the polymerization, creating another polymeric radical (P_m), which reacts with macro-CTA and produces a system with reactive and dormant species, which are shown in the main equilibrium. At this step, monomers are added to the growing polymer chains in a controlled fashion. The only possibility for a reaction to terminate is when two radicals in the reactive state interact with each other; this allows the polymerization to stop before 90 % conversion and avoid relatively probably coupling of two growing polymer chains. It is also important to choose a RAFT agent that is compatible with the monomer of choice. Some of the manufacturers of CTA agents have guidelines on how to choose correct agent for successful polymerization (*e.g.*, Sigma-Aldrich³⁴).

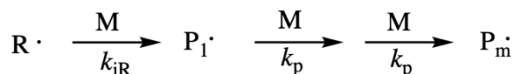
Initiation:



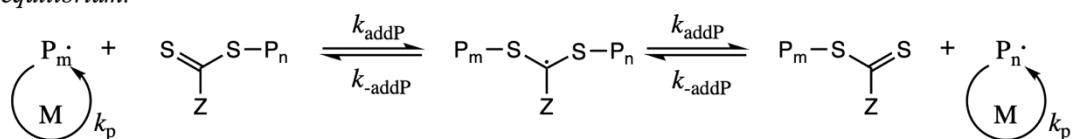
Initialization/Pre-equilibrium:



Reinitiation:



Main equilibrium:



Termination:

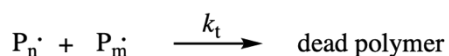


Figure 1.2. Equilibria of reversible-addition fragmentation chain transfer (RAFT) polymerization. I stands for the initiator, P – for the polymeric radical, M – monomer, R – RAFT agent derived radical. The Z group of the RAFT agent affects the stability of C=S bond and the stability of the adduct radical (3) where the R group must be able to produce a stable enough radical such that will favor the formation of the growing polymer chain P_n , but unstable enough to reinitiate growth of a new polymer chain P_m . Adapted from reference³³

When a polymer is synthesized via RAFT polymerization, it contains a thiocarbonylthio functionality, which can be utilized to further promote synthesis of block copolymers. For the synthesis of block copolymers, it is important to consider two main factors: 1) compatibility of the RAFT agent with both monomers, and 2) the order of the monomers, so that the macro-CTA will be able to facilitate polymerization of the second monomer. Figure 1.4 summarizes the order that should be used for monomer selection,

considering the first block after polymerization will play a role of R group for polymerization of the second block.

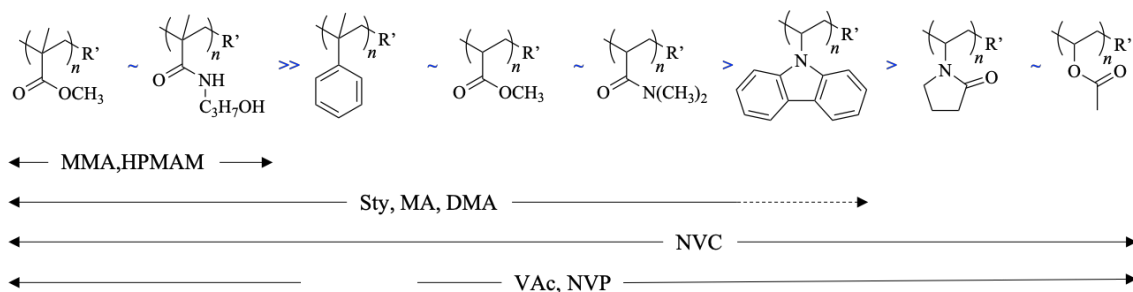


Figure 1.3. Guidelines for selection of the macro-R group for the preparation of block copolymers. Dashed lines indicate poor control over polymerization (high dispersity due to inferior hemolytic group ability or retardation due to slow re-initiation of polymerization). Abbreviations: MMA – methyl methacrylate, HPMAM – N-(2-hydroxypropyl) methacrylamide, St – styrene, DMAM – N,N-dimethylacrylamide, NVC – N-vinylcarbazole, VAc – vinyl acetate, NVP – N-vinylpyrrolidone. Adapted from reference³³

Thus, considering all listed advantage of RAFT polymerization, this technique was used in the synthesis of most targeted compounds described and studied in this dissertation research.

1.3 Block copolymer applications in oral drug delivery

Block copolymers, which consist of segments with discrete monomer compositions, have variable solubility in certain solvents (i.e., amphiphilic block copolymers) and can thus form self-assembled nanostructures in solutions. Depending on the composition of the block copolymers, a myriad of micellar morphologies can arise (Figure 1.4). This self-aggregation of block copolymers is a spontaneous process, due to the negative free energy change and entropic gain associate with solvation of the soluble

constituents and exclusion of insoluble components from a given solvent media upon self-assembling.³⁵ During this process, the block copolymer adopts a structure with a core and corona. The assembly of block copolymers into micellar structures is influenced by factors such as: i) the choice of a solvent, ii) type of a copolymer and its composition, iii) temperature, iv) ionic strength, v) pH. Furthermore, the process of micelle preparation can affect the geometrical parameters, namely size, aggregation number, and dispersity. For instance, direct dissolution or slow solvent substitution can lead to formation of micelles with different architectures.³⁶ Of all the factors that influence aggregate architecture, molecular weight, polymer concentration, and polymer composition have the most dominant effects on architecture and are easiest to modify experimentally.

Polymeric micelles (PM) and other higher-order self-assembled structures have gained attention in the drug delivery field because they can easily be tuned to promote higher drug loading, inhibit drug crystallization, and allow stimuli responsiveness.²⁶ Additionally, the tunability of the micellar structures can enhance stability of the drug delivery vehicle in different media, including disparate parts of the GI tract such as the intestine and stomach.³⁷ Although traditionally, the hydrophobic drug is loaded into the core of the aggregate³⁸, recent studies in oral drug delivery have encapsulated the drug in the corona of the aggregate so that no further stimulus is required to release the pharmaceutical cargo.

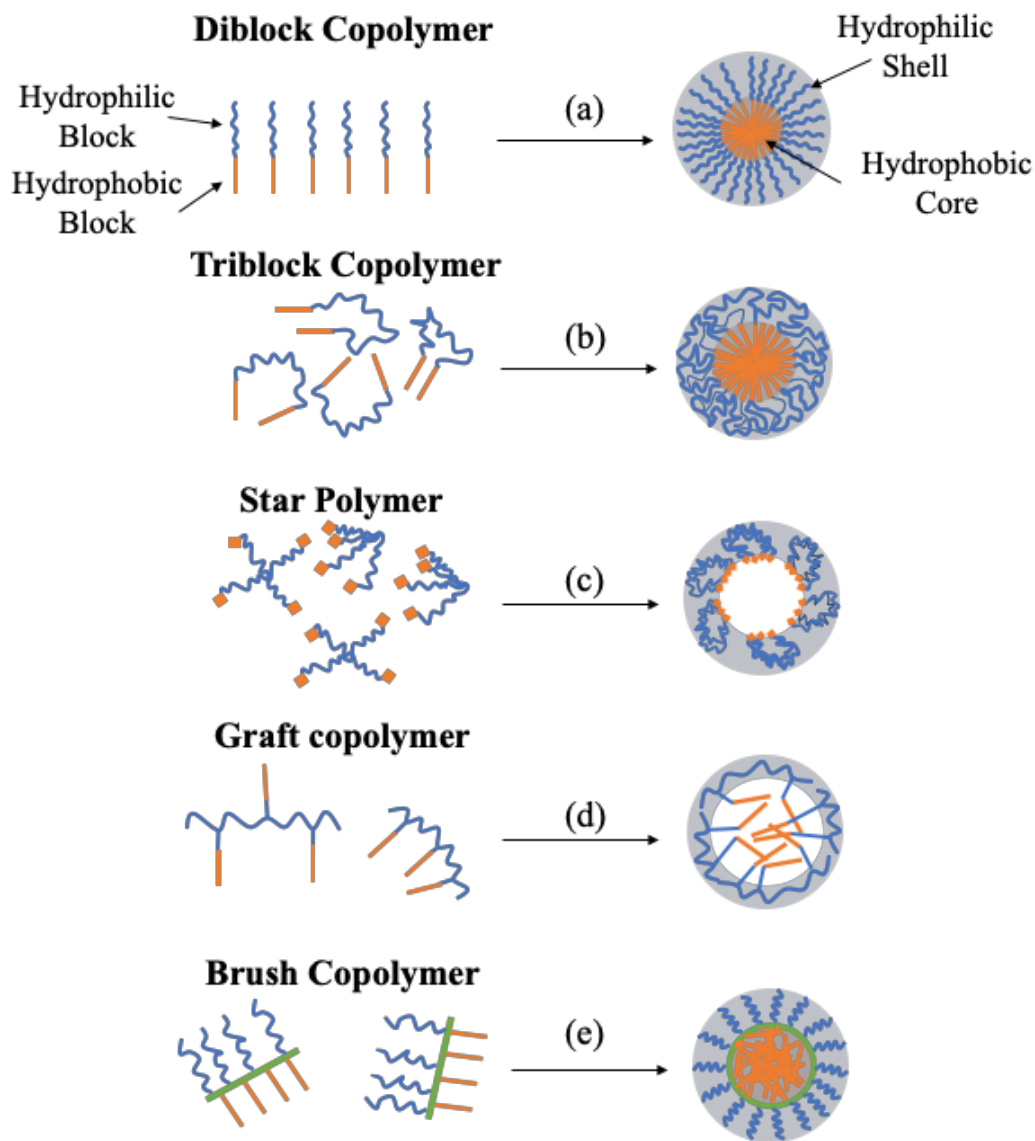


Figure 1.4. Different amphiphilic copolymer architectures lead to different micelle structures by self-assembly. Initial structure of a block copolymer determines the morphology of a micelle. Adapted from reference³⁹

Recent work has shown that hydrophobic drugs can be partitioned in the hydrophilic corona of the aggregate for enhanced solubility and supersaturation maintenance.^{17,40} In one example, Dalsin et al. showed that by aggregating poly(ethylene-*co*-propylene)-*b*-poly(dimethylacrylamide) (PEP-*b*-PDMA) amphiphilic block copolymer

into micelles, significant increase in dissolution performance of probucol, a Class II pharmaceutical, can be observed. This was achieved because forced aggregation of PDMA through the block copolymer micellization sustained drug-polymer interactions even when the formulation was exposed to the aqueous dissolution media. Compared to formulations prepared with non-aggregated PEP-*b*-PDMA, the micellized excipient showed almost complete burst release of the drug and sustained supersaturation for six hours during the dissolution test at different drug loadings (10, 25, and 50 wt %).

Later, Johnson and coworkers⁴⁰ studied the effect of the polymer hydrophobic end-group on the phenytoin solubility enhancement using RAFT-polymerized N-isopropylacrylamide (NIPAm) excipients. Specifically, this study revealed that the highest concentration of phenytoin is achieved at 10 wt % loading only when the excipient has long enough hydrophobic end-group to form micelles in the aqueous media. Later, work by Ting et al.⁴¹ utilized high-throughput screening to identify the ‘ideal’ monomer selection and copolymer composition to sustain phenytoin supersaturation at 1 mg/mL. This work applied 2D Nuclear Overhauser Correlation Spectroscopy (NOE) to elucidate specific polymer-drug interactions between cyclic urea-imide on the drug and the PNIPAm isopropyl groups of the polymer. Li et al.¹⁸ then used these results as a starting point to systematically study the effect of micelle corona density of PNIPAm-*co*-DMA-*b*-PS on the drug solubility maintenance. The authors demonstrated that when the PNIPAm-*co*-DMA copolymer control excipient did not form micelles due to absence of the polystyrene block poor drug solubility was achieved as a result of absence of nanoaggregates. However, when polystyrene of various lengths was incorporated into the polymers, 1 mg/mL drug concentration was sustained at 10 wt % loading, due to the formation of micellar structures.

Interestingly, NOE and diffusion-ordered spectroscopy (DOSY) confirmed that the drug is partitioned into a micelle corona. These findings establish a precedent for enhancing drug solubility without the risk of sacrificing drug bioavailability, as is often the case with the triggered release associated with micelle core-loaded delivery vehicles.

Prior research has also demonstrated that non-pH-sensitive micelles may enhance drug solubilization but not necessarily drug absorption.⁴² As such, when studying transit times of a radio-labeled marker, Camileri et al. found that stomach emptying time is about 180 minutes and small bowel transit time is about 160 minutes.⁴³ Thus, the drug sequestered in the PMs, may not be released close to its absorption window in the GI tract. Several excipients that have been designed to increase the oral bioavailability of hydrophobic compounds exhibit release times that exceed the transit time in the small intestine.^{44,45} This is also true for surfactant micelles, which have been found to impede the absorption of hydrophobic drugs due to excessive retention in the micellar phase.⁴⁶ Pierri and coworkers⁴⁵ studied poly(lactide)-*b*-poly(ethylene glycol) (PLA-PEG) micelles for griseofulvin solubility enhancement and noted that stable micelles formation (with 50-70 molar percent of PEG) is important for prolonged drug solubility maintenance; however, their system did not allow high drug loading and burst release of the cargo. Therefore, adequately controlling drug release rate can avoid either drug crystallization and phase separation from the solution or incomplete absorption in the small intestine.

Kim and coworkers⁴⁷ hypothesized that the physical stability of PMs containing methacrylic acid moieties may decrease in the intestine, allowing the drug to cross the intestinal barrier. Correspondingly, loaded drugs may be released faster in the intestine

rather than in the stomach. Specifically, paclitaxel (PTX) was used as a model drug with a hydrotropic polymer, PEG-*b*-(4-(2-vinylbenzyloxy)-N,N-(diethylnicotinamide)) (PEG-*b*-VBODENA), doped with the methacrylic acid units to add pH sensitivity to the excipient. Loading/release profiles were also studied by changing the pH conditions at which the analyses were conducted. High loading efficiency of PTX was observed at pH < 4 and the polymer-drug complex rapidly dissociated at pH above the pK_a of the poly(methacrylic acid). Authors determined that self-association into well-defined micelles is facilitated by hydrophobic groups, whereas pH sensitivity is governed by carboxylic groups of the MAA moieties.

In an earlier report, Sant et al.⁴⁸ used amphiphilic pH-sensitive block copolymers composed of PEG (hydrophilic component) and poly(methyl methacrylate)-*co*-poly(methacrylic acid) (PMMPMA – hydrophobic, pH responsive component) for solubility enhancement of indomethacin and fenofibrate (BCS Class II drugs). PMs were formed at pH values below 4.7, and drugs were incorporated into the assemblies. After the pH-responsive drug release was confirmed in their *in vitro* study, the authors conducted *in vivo* experiments using fenofibrate-loaded nanoparticles by oral dosing of male Sprague-Dawley rats. The oral bioavailability of fenofibrate using the PEG-*b*-PMMPMA excipient self-assembled into micelles showed a 156% increase versus crystalline drug and 15% increase compared to commercially available formulation Lipidil MicroR. The results suggest that these pH-sensitive PMs could efficiently improve the bioavailability of poorly water-soluble drugs.

Finally, to further enhance bioavailability of orally delivered pharmaceuticals, nanocarriers often possess mucoadhesive properties. Mucoadhesion is a complex phenomenon and can be obtained by building of nonspecific interactions with the intestinal mucus (ionic, hydrogen bonding, van der Waals^{49,50}) or specific interactions by using functionalized polymers with either targeting ligands (lectins) or reactive moieties such as thiols.^{51,52} For instance, Bromberg et al.⁵³ studied bioadhesive properties of commercial Pluronic polymers which were grafted onto poly(acrylic acid). The authors then studied different molecular weights of Pluronic copolymers with various ratios of PPO/PEO (copolymer of polypropylene oxide and polyethylene oxide). It was revealed that the highest molecular weight Pluronic copolymer grafted to PAA resulted in gels with strongest mucoadhesive properties, which make Pluronic-PAA gels a feasible vehicle for oral drug delivery.

This Chapter has served to introduce research aimed at investigating the use of self-assembled nanocarriers in the field of oral drug delivery. Because of the large number of variables, establishing structure-property relationships within each step of drug administration remains an urgent problem in this area. Figure 1.5 summarizes current problems that will be addressed in the Thesis using self-assembling block copolymers.

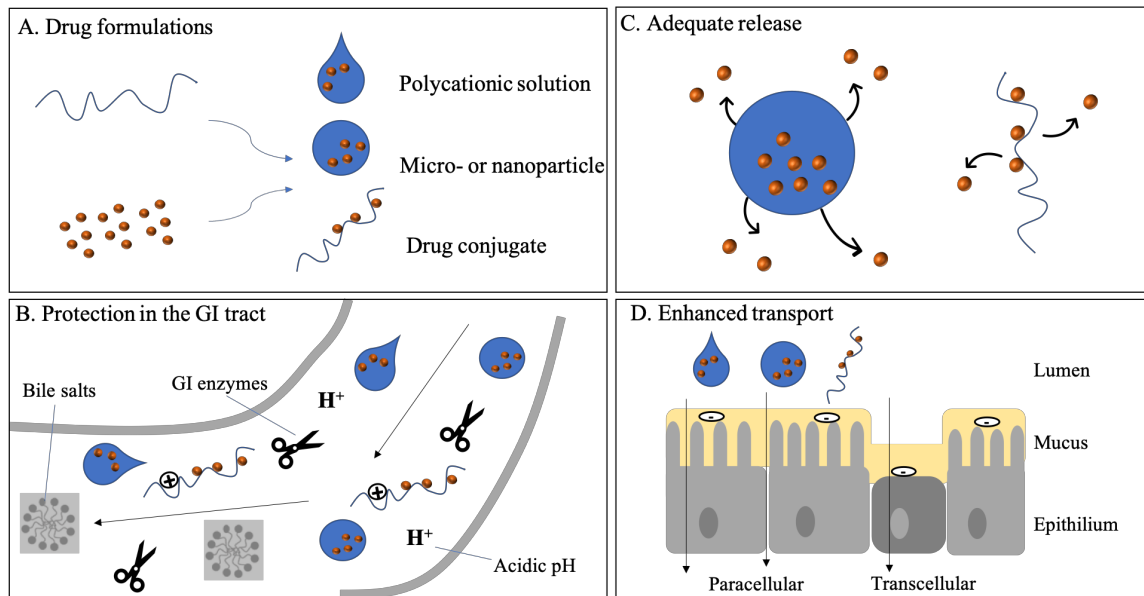


Figure 1.5. Drug–polymer formulations and their advantages. A: Drug formulations prepared with polymeric excipients by either simple mixing to obtain a polymer–drug solution, encapsulating the drug in micro- or nanoparticles, or by synthesizing a covalent drug–conjugate. B: The different formulations should enhance drug stability in the GI tract and shield the drug from the acidic pH, GI enzymes, and bile salts. C: Adequate drug release is required at the targeted site. D: Transport across the intestinal membrane can occur via the paracellular and/or transcellular pathway through epithelial or M cells. Adapted from reference⁵⁴

1.4 Applications and limitations of the Caco-2 cell permeability assay

The Caco-2 cell permeability assay utilizes a cell monolayer of the human adenocarcinoma cell line and is mainly used for high-throughput screening in drug and excipient discovery programs. These cells, when cultured on a porous membrane, differentiate to form a confluent monolayer consisting of polarized cells that express microvilli on the apical side and form tight junctions between neighboring cells.⁵⁵ It has

been shown that there is a good correlation between drug absorption in human jejunum and Caco-2 cells, especially for BCS class II drugs.^{56,57} Additionally, having reliable *in vitro* test method can save time and cost for pharmaceutical development due to the potential of the Caco-2 cell assay to enable high-throughput capability⁵⁸ and general trend towards stricter regulations of animal testing in preclinical trials.⁵⁹

In drug discovery, evaluating the permeability of drug candidates is a crucial step before proceeding to clinical trials. The most common methods to assess permeability include: *in-silico* computation methods, the parallel artificial membrane permeability assay, cell-based systems, Ussing chamber, and *in-situ* perfused intestine preparations.^{44,60–62} Caco-2 cell monolayers resemble the epithelial membrane of a human GI tract, in terms of both polarity and presence of enzymes, which explains its popularity in routine prediction of drug permeability and the fraction of the absorbed dose (f_a). The protocol for the assay has been rigorously described previously.⁶³

Previous work established the utility of the Caco-2 cell permeability assay in the drug-excipient discovery process after initial formulation and prior to animal testing. Joshi and coworkers⁶⁴ used the permeability cell assay to formulate liponavir-loaded (leading component in combined chemotherapy) PLGA nanoparticles to enhance drug permeability. They found that spherical structures of 142 nm in diameter with liponavir entrapment of 93 % lead to 3.0-fold cell permeability increase relative to just pure drug. After the *in vivo* rat studies, they confirmed that their leading formulation leads to 13.9-fold bioavailability enhancement. The authors concluded that the Caco-2 permeability assay is a useful tool to scan through multiple formulations in a fast and reproducible manner.

Li et al.⁶⁵ studied insulin transport across the cellular membrane using the Caco-2 cell assay. The authors established specific lipids (medium chain triglycerides) MCT1 and MCT2 (Miglyol 812N) that increased trans-epithelial permeability of insulin by enhancing the paracellular transport. Moreover, their work demonstrated that long-chain triglycerides do not influence the permeability of insulin, despite the high cellular uptake of the nanoemulsions. This work demonstrated understanding of what transport mechanisms influence drug bioavailability, which in turn, allows intelligent excipient design.

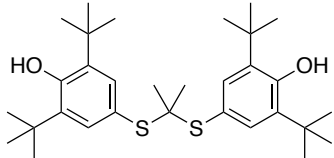
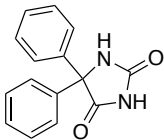
Obringer et al.⁶⁶ studied the suitability of Caco-2 cell assay to predict the oral absorption of aromatic amine molecules. They studied 14 different molecules for which *in vivo* permeability studies were available previously. The authors concluded that their study confirms that non-animal models can be used as alternatives to the *in vivo* toxicokinetic studies as part of the safety assessment of novel pharmaceutical ingredients. This work allowed drug molecules classification based on their intestinal permeability and can potentially predict their bioavailability.

The Caco-2 cell assay is a useful tool in evaluating drug permeability and proper data interpretation can support further more extensive *in-vivo* investigation. The translation of information that can be obtained from the Caco-2 cell assay to *in vivo* necessitates sophisticated data processing with some modeling approaches in order to avoid over-simplified data interpretation. The next steps would be to gain more insight on the *in vivo* – *in vitro* correlation of the Caco-2 cell assay in order to speed up drug discovery and novel API approval in the long run.

1.5 Thesis outline

Considering the imperative role of excipient development, a novel class of self-assembling, stimuli-responsive polymers for oral drug delivery was developed. In pharmaceutical industry, the drug approval process takes longer and costs more, but the structure-property relationship between polymer-drug interactions that allows drug solubility enhancement yet to be established. Chapter 2 describes the development of sugar-derived di-block copolymers that utilize a trehalose H-bonding ability in order to solubilize BCS Class II drug probucol (Table 1.2). By utilizing either hydrophobic, pH-responsive, or thermo-responsive blocks in conjunction with trehalose-containing blocks, the roles of the pH of the dissolution media, solution-state morphology, and the amount of the H-bonding sites were established. Chapter 3 describes a fundamental investigation of how solution state assembly of pH-responsive excipients can alter and enhance drug solubility and in turn, help achieve higher bioavailability. Finally, Chapter 4 extends the work in Chapter 3 and investigates star polymer excipients and their role in drug solubility enhancement. This work provides some fundamental knowledge that can be applied to newly-developed drugs in order to achieve easily administrable dosage and develop more efficient treatments.

Table 1.2. Properties of the model drugs discussed in this dissertation.

	Probucol	Phenytoin
Structure		
T_m (°C)	125, 116	286 (degrades)
$\log P$	8.9	2.2
water solubility (mg/mL)	$4.18 \cdot 10^{-5}$	0.032
pK_a	10.29	8.33

1.6 References

- (1) Lipp, R. Major Advances in Oral Drug Delivery over the Past 15 Years. *American Pharmaceutical Review*. 2013.
- (2) FDA. The Biopharmaceutics Classification System (BCS) Guidance <http://www.fda.gov/AboutFDA/CentersOffices/OfficeofMedicalProductsandTobacco/CDER/ucm128219.htm>.
- (3) Morgan, S.; Grootendorst, P.; Lexchin, J.; Cunningham, C.; Greyson, D. The Cost of Drug Development: A Systematic Review. *Health Policy* **2011**, *100* (1), 4–17. <https://doi.org/10.1016/j.healthpol.2010.12.002>.
- (4) Lipp, R. The Innovator Pipeline: Bioavailability Challenges and Advanced Oral Drug Delivery Opportunities <http://www.americanpharmaceuticalreview.com/Featured-Articles/135982-The-Innovator-Pipeline-Bioavailability-Challenges-and-Advanced-Oral-Drug-Delivery-Opportunities/>.
- (5) Tale, S.; Purchel, A. A.; Dalsin, M. C.; Reineke, T. M. Diblock Terpolymers Are Tunable and PH Responsive Vehicles To Increase Hydrophobic Drug Solubility for Oral Administration. *Mol. Pharm.* **2017**, *14* (11), 4121–4127. <https://doi.org/10.1021/acs.molpharmaceut.7b00458>.
- (6) Onoue, S.; Kojo, Y.; Suzuki, H.; Yuminoki, K.; Kou, K.; Kawabata, Y.; Yamauchi, Y.; Hashimoto, N.; Yamada, S. Development of Novel Solid Dispersion of Tranilast Using Amphiphilic Block Copolymer for Improved Oral Bioavailability. *Int. J. Pharm.* **2013**, *452* (1–2), 220–226. <https://doi.org/10.1016/j.ijpharm.2013.05.022>.
- (7) Choudhary, S.; Gupta, L.; Rani, S.; Dave, K.; Gupta, U. Impact of Dendrimers on

- Solubility of Hydrophobic Drug Molecules. *Front. Pharmacol.* **2017**, *8* (MAY), 1–23. <https://doi.org/10.3389/fphar.2017.00261>.
- (8) Babu, N. J.; Nangia, A. Solubility Advantage of Amorphous Drugs and Pharmaceutical Cocrystals. *Cryst. Growth Des.* **2011**, *11* (7), 2662–2679. <https://doi.org/10.1021/cg200492w>.
- (9) Shimpi, S.; Chauhan, B.; Shimpi, P. Cyclodextrins: Application in Different Routes of Drug Administration. *Acta Pharm.* **2005**, *55* (2), 139–156.
- (10) Khadka, P.; Ro, J.; Kim, H.; Kim, I.; Kim, J. T.; Kim, H.; Cho, J. M.; Yun, G.; Lee, J. Pharmaceutical Particle Technologies: An Approach to Improve Drug Solubility, Dissolution and Bioavailability. *Asian J. Pharm. Sci.* **2014**, *9* (6), 304–316. <https://doi.org/10.1016/j.ajps.2014.05.005>.
- (11) Miller, J. M.; Beig, A.; Carr, R. A.; Spence, J. K.; Dahan, A. A Win – Win Solution in Oral Delivery of Lipophilic Drugs: Supersaturation via Amorphous Solid Dispersions Increases Apparent Solubility without Sacrifice of Intestinal Membrane Permeability. **2012**.
- (12) Censi, R.; Di Martino, P. Polymorph Impact on the Bioavailability and Stability of Poorly Soluble Drugs. *Molecules* **2015**, *20* (10), 18759–18776. <https://doi.org/10.3390/molecules201018759>.
- (13) Hancock, B. C.; Parks, M. What Is the True Solubility Advantage for Amorphous Pharmaceuticals? *Pharm. Res.* **2000**, *17* (4), 397–404.
- (14) Guterres, S. S. Spray-Drying Technique to Prepare Innovative Nanoparticulated Formulations for Drug Administration : A Brief Overview. *Brazilian J. Phys.* **2009**, *39* (1A), 205–209.

- (15) Broadhead, J.; Edmond Rouan, S. K.; Rhodes, C. T. The Spray Drying of Pharmaceuticals. *Drug Dev. Ind. Pharm.* **1992**, *18* (11–12), 1169–1206. <https://doi.org/10.3109/03639049209046327>.
- (16) Curatolo, W.; Nightingale, J. a; Herbig, S. M. Utility of Hydroxypropylmethylcellulose Acetate Succinate (HPMCAS) for Initiation and Maintenance of Drug Supersaturation in the GI Milieu. *Pharm. Res.* **2009**, *26* (6), 1419–1431. <https://doi.org/10.1007/s11095-009-9852-z>.
- (17) Dalsin, M. C.; Tale, S.; Reineke, T. M. Solution-State Polymer Assemblies Influence BCS Class II Drug Dissolution and Supersaturation Maintenance. *Biomacromolecules* **2014**, *15* (2), 500–511. <https://doi.org/10.1021/bm401431t>.
- (18) Li, Z.; Lenk, T. I.; Yao, L. J.; Bates, F. S.; Lodge, T. P. Maintaining Hydrophobic Drug Supersaturation in a Micelle Corona Reservoir. *Macromolecules* **2018**, *51* (2), 540–551. <https://doi.org/10.1021/acs.macromol.7b02297>.
- (19) Johnson, L. M.; Li, Z.; LaBelle, A. J.; Bates, F. S.; Lodge, T. P.; Hillmyer, M. A. Impact of Polymer Excipient Molar Mass and End Groups on Hydrophobic Drug Solubility Enhancement. *Macromolecules* **2017**, *50* (3), 1102–1112. <https://doi.org/10.1021/acs.macromol.6b02474>.
- (20) Van Den Abeele, J.; Brouwers, J.; Mattheus, R.; Tack, J.; Augustijns, P. Gastrointestinal Behavior of Weakly Acidic BCS Class II Drugs in Man - Case Study Diclofenac Potassium. *J. Pharm. Sci.* **2015**, 1–11. <https://doi.org/10.1002/jps.24647>.
- (21) Kawakami, K.; Yoshikawa, T.; Hayashi, T.; Nishihara, Y.; Masuda, K. Microemulsion Formulation for Enhanced Absorption of Poorly Soluble Drugs. II.

- In Vivo Study. *J. Control. Release* **2002**, *81* (1–2), 75–82.
- (22) Guay, D. R. Micronized Fenofibrate: A New Fibric Acid Hypolipidemic Agent. *Ann. Pharmacother.* **1999**, *33* (10), 1083–1103.
- (23) Kalepu, S.; Manthina, M.; Padavala, V. Oral Lipid-Based Drug Delivery Systems – an Overview. *Acta Pharm. Sin. B* **2013**, *3* (6), 361–372. <https://doi.org/10.1016/j.apsb.2013.10.001>.
- (24) Subudhi, B. B.; Mandal, S. Self-Microemulsifying Drug Delivery System: Formulation and Study Intestinal Permeability of Ibuprofen in Rats. *J. Pharm.* **2013**, *2013*, 1–6. <https://doi.org/10.1155/2013/328769>.
- (25) Kushida, I.; Ichikawa, M.; Asakawa, N. Improvement of Dissolution and Oral Absorption of ER-34122, a Poorly Water-Soluble Dual 5-Lipoxygenase/Cyclooxygenase Inhibitor with Anti-Inflammatory Activity by Preparing Solid Dispersion. *J. Pharm. Sci.* **2002**, *91* (1), 258–266.
- (26) Godfroy, I. Polymeric Micelles – The Future of Oral Drug Delivery. *J. Biomater. Appl. Rev.* **2009**, *3*, 216–232.
- (27) Kurkuri, M. D.; Aminabhavi, T. M. Poly(Vinyl Alcohol) and Poly(Acrylic Acid) Sequential Interpenetrating Network PH-Sensitive Microspheres for the Delivery of Diclofenac Sodium to the Intestine. *J. Control. Release* **2004**, *96* (1), 9–20. <https://doi.org/10.1016/j.jconrel.2003.12.025>.
- (28) Jenkins, A. D.; Kratochvíl, P.; Stepto, R. F. T.; Suter, U. W. Glossary of Basic Terms in Polymer Science (IUPAC Recommendations 1996). *Pure Appl. Chem.* **1996**, *68* (12). <https://doi.org/10.1351/pac199668122287>.
- (29) Szwarc, M. ‘Living’ Polymers. *Nature* **1956**, *178* (4543), 1168–1169.

<https://doi.org/10.1038/1781168a0>.

- (30) Braunecker, W. a.; Matyjaszewski, K. Controlled/Living Radical Polymerization: Features, Developments, and Perspectives. *Prog. Polym. Sci.* **2007**, *32* (1), 93–146. <https://doi.org/10.1016/j.progpolymsci.2006.11.002>.
- (31) Lowe, A. B.; McCormick, C. L. Reversible Addition–Fragmentation Chain Transfer (RAFT) Radical Polymerization and the Synthesis of Water-Soluble (Co)Polymers under Homogeneous Conditions in Organic and Aqueous Media. *Prog. Polym. Sci.* **2007**, *32* (3), 283–351. <https://doi.org/10.1016/j.progpolymsci.2006.11.003>.
- (32) Zetterlund, P. B.; Kagawa, Y.; Okubo, M. Controlled/Living Radical Polymerization in Dispersed Systems. *Chem. Rev.* **2008**, *108* (9), 3747–3794. <https://doi.org/10.1021/cr800242x>.
- (33) Keddie, D. J. A Guide to the Synthesis of Block Copolymers Using Reversible-Addition Fragmentation Chain Transfer (RAFT) Polymerization. *Chem. Soc. Rev.* **2014**, *43* (2), 496–505. <https://doi.org/10.1039/c3cs60290g>.
- (34) Science, C. M. RAFT – Choosing the Right Agent. **2005**, 1–19.
- (35) Bromberg, L. Polymeric Micelles in Oral Chemotherapy. *J. Control. Release* **2008**, *128* (2), 99–112. <https://doi.org/10.1016/j.jconrel.2008.01.018>.
- (36) Tale, S. R.; Yin, L.; Reineke, T. M. Trehalose-Functionalized Block Copolymers Form Serum-Stable Micelles. *Polym. Chem.* **2014**, *5* (17), 5160. <https://doi.org/10.1039/C4PY00399C>.
- (37) Torchilin, V. P. Micellar Nanocarriers: Pharmaceutical Perspectives. *Pharm. Res.* **2007**, *24* (1), 1–16. <https://doi.org/10.1007/s11095-006-9132-0>.
- (38) Gil, E.; Hudson, S. Stimuli-Responsive Polymers and Their Bioconjugates. *Prog.*

Polym. Sci. **2004**, *29* (12), 1173–1222.
<https://doi.org/10.1016/j.progpolymsci.2004.08.003>.

- (39) Mondon, K.; Gurny, R.; Möller, M. Colloidal Drug Delivery Systems – Recent Advances With Polymeric Micelles. *Chim. Int. J. Chem.* **2008**, *62* (10), 832–840.
<https://doi.org/10.2533/chimia.2008.832>.
- (40) Johnson, L. M.; Li, Z.; LaBelle, A. J.; Bates, F. S.; Lodge, T. P.; Hillmyer, M. A. Impact of Polymer Excipient Molar Mass and End Groups on Hydrophobic Drug Solubility Enhancement. *Macromolecules* **2017**, *50* (3), 1102–1112.
<https://doi.org/10.1021/acs.macromol.6b02474>.
- (41) Ting, J. M.; Tale, S.; Purchel, A. A.; Jones, S. D.; Widanapathirana, L.; Tolstyka, Z. P.; Guo, L.; Guillaudeu, S. J.; Bates, F. S.; Reineke, T. M. High-Throughput Excipient Discovery Enables Oral Delivery of Poorly Soluble Pharmaceuticals. *ACS Cent. Sci.* **2016**, *2* (10), 748–755. <https://doi.org/10.1021/acscentsci.6b00268>.
- (42) Lu, Y.; Park, K. Polymeric Micelles and Alternative Nanonized Delivery Vehicles for Poorly Soluble Drugs. *Int. J. Pharm.* **2013**, *453* (1), 198–214.
<https://doi.org/10.1016/j.ijpharm.2012.08.042>.
- (43) Camilleri, M.; Colemont, L. J.; Phillips, S. F.; Brown, M. L.; Thomforde, G. M.; Chapman, N.; Zinsmeister, A. R. Human Gastric Emptying and Colonic Filling of Solids Characterized by a New Method. *Am. J. Physiol. Liver Physiol.* **1989**, *257* (2), G284–G290. <https://doi.org/10.1152/ajpgi.1989.257.2.G284>.
- (44) Ould-Ouali, L.; Noppe, M.; Langlois, X.; Willems, B.; Te Riele, P.; Timmerman, P.; Brewster, M. E.; Ariën, A.; Pr at, V. Self-Assembling PEG-p(CL-Co-TMC) Copolymers for Oral Delivery of Poorly Water-Soluble Drugs: A Case Study with

- Risperidone. *J. Control. Release* **2005**, *102* (3), 657–668.
<https://doi.org/10.1016/j.jconrel.2004.10.022>.
- (45) Pierri, E.; Avgoustakis, K. Poly(Lactide)-Poly(Ethylene Glycol) Micelles as a Carrier for Griseofulvin. *J. Biomed. Mater. Res. Part A* **2005**, *75A* (3), 639–647.
<https://doi.org/10.1002/jbm.a.30490>.
- (46) Chen, W.; Zhong, P.; Meng, F.; Cheng, R.; Deng, C.; Feijen, J.; Zhong, Z. Redox and PH-Responsive Degradable Micelles for Dually Activated Intracellular Anticancer Drug Release. *J. Control. Release* **2013**, *169* (3), 171–179.
<https://doi.org/10.1016/j.jconrel.2013.01.001>.
- (47) Kim, S.; Kim, J. Y.; Huh, K. M.; Acharya, G.; Park, K. Hydrotropic Polymer Micelles Containing Acrylic Acid Moieties for Oral Delivery of Paclitaxel. *J. Control. Release* **2008**, *132* (3), 222–229.
<https://doi.org/10.1016/j.jconrel.2008.07.004>.
- (48) Sant, V. P.; Smith, D.; Leroux, J.-C. Novel PH-Sensitive Supramolecular Assemblies for Oral Delivery of Poorly Water Soluble Drugs: Preparation and Characterization. *J. Control. Release* **2004**, *97* (2), 301–312.
<https://doi.org/10.1016/j.jconrel.2004.03.026>.
- (49) Choonara, B. F.; Choonara, Y. E.; Kumar, P.; Bijukumar, D.; du Toit, L. C.; Pillay, V. A Review of Advanced Oral Drug Delivery Technologies Facilitating the Protection and Absorption of Protein and Peptide Molecules. *Biotechnol. Adv.* **2014**, *32* (7), 1269–1282. <https://doi.org/10.1016/j.biotechadv.2014.07.006>.
- (50) Park, K.; Kwon, I. C.; Park, K. Oral Protein Delivery: Current Status and Future Prospect. *React. Funct. Polym.* **2011**, *71* (3), 280–287.

<https://doi.org/10.1016/j.reactfunctpolym.2010.10.002>.

- (51) DEACON, M. P.; McGURK, S.; ROBERTS, C. J.; WILLIAMS, P. M.; TENDLER, S. J. B.; DAVIES, M. C.; DAVIS, S. S. (Bob); HARDING, S. E. Atomic Force Microscopy of Gastric Mucin and Chitosan Mucoadhesive Systems. *Biochem. J.* **2000**, *348* (3), 557–563. <https://doi.org/10.1042/bj3480557>.
- (52) Lehr, C. M.; Bouwstra, J. A.; Schacht, E. H.; Junginger, H. E. In Vitro Evaluation of Mucoadhesive Properties of Chitosan and Some Other Natural Polymers. *Int. J. Pharm.* **1992**, *78* (1–3), 43–48. [https://doi.org/10.1016/0378-5173\(92\)90353-4](https://doi.org/10.1016/0378-5173(92)90353-4).
- (53) Bromberg, L.; Temchenko, M.; Alakhov, V.; Hatton, T. A. Bioadhesive Properties and Rheology of Polyether-Modified Poly(Acrylic Acid) Hydrogels. *Int. J. Pharm.* **2004**, *282* (1–2), 45–60. <https://doi.org/10.1016/j.ijpharm.2004.05.030>.
- (54) Schulz, J. D.; Gauthier, M. A.; Leroux, J.-C. Improving Oral Drug Bioavailability with Polycations? *Eur. J. Pharm. Biopharm.* **2015**, *97*, 427–437. <https://doi.org/10.1016/j.ejpb.2015.04.025>.
- (55) Hidalgo, I. J.; Raub, T. J.; Borchardt, R. T. Characterization of the Human Colon Carcinoma Cell Line (Caco-2) as a Model System for Intestinal Epithelial Permeability. *Gastroenterology* **1989**, *96* (3), 736–749. [https://doi.org/10.1016/0016-5085\(89\)90897-4](https://doi.org/10.1016/0016-5085(89)90897-4).
- (56) Juergenliemk, G.; Boje, K.; Huewel, S.; Lohmann, C.; Galla, H. J.; Nahrstedt, A. In Vitro Studies Indicate That Miquelianin (Quercetin 3-O-??-D-Glucuronopyranoside) Is Able to Reach the CNS from the Small Intestine. *Planta Med.* **2003**, *69* (11), 1013–1017. <https://doi.org/10.1055/s-2003-45148>.
- (57) Fagerholm, U. Prediction of Human Pharmacokinetics -Gastrointestinal Absorption.

- J. Pharm. Pharmacol.* **2007**, *59* (7), 905–916. <https://doi.org/10.1211/jpp.59.7.0001>.
- (58) Li, C.; Wainhaus, S.; Uss, A. S.; Cheng, K.-C. High-Throughput Screening Using Caco-2 Cell and PAMPA Systems. In *Drug Absorption Studies*; Springer US: Boston, MA; pp 418–429. https://doi.org/10.1007/978-0-387-74901-3_18.
- (59) Schumann, R. The Seventh Amendment to the Cosmetics Directive: What Does DG Enterprise Want from ECVAM? *Altern. Lab. Anim.* **2002**, *30 Suppl 2*, 213–214.
- (60) Hubbard, D.; Bond, T.; Ghandehari, H. Regional Morphology and Transport of PAMAM Dendrimers Across Isolated Rat Intestinal Tissue. *Macromol. Biosci.* **2015**, 1–9. <https://doi.org/10.1002/mabi.201500225>.
- (61) Uchiyama, H.; Tozuka, Y.; Imono, M.; Takeuchi, H. Transglycosylated Stevia and Hesperidin as Pharmaceutical Excipients: Dramatic Improvement in Drug Dissolution and Bioavailability. *Eur. J. Pharm. Biopharm.* **2010**, *76* (2), 238–244. <https://doi.org/10.1016/j.ejpb.2010.07.006>.
- (62) Li, A. In Vitro Approaches to Evaluate ADMET Drug Properties. *Curr. Top. Med. Chem.* **2004**, *4* (7), 701–706. <https://doi.org/10.2174/1568026043451050>.
- (63) Hubatsch, I.; Ragnarsson, E. G. E.; Artursson, P. Determination of Drug Permeability and Prediction of Drug Absorption in Caco-2 Monolayers. *Nat. Protoc.* **2007**, *2* (9), 2111–2119. <https://doi.org/10.1038/nprot.2007.303>.
- (64) Joshi, G.; Kumar, A.; Sawant, K. Bioavailability Enhancement, Caco-2 Cells Uptake and Intestinal Transport of Orally Administered Lopinavir-Loaded PLGA Nanoparticles. *Drug Deliv.* **2016**, *23* (9), 3492–3504. <https://doi.org/10.1080/10717544.2016.1199605>.
- (65) Li, P.; Nielsen, H. M.; Müllertz, A. Impact of Lipid-Based Drug Delivery Systems

on the Transport and Uptake of Insulin Across Caco-2 Cell Monolayers. *J. Pharm. Sci.* **2016**, *105* (9), 2743–2751. <https://doi.org/10.1016/j.xphs.2016.01.006>.

- (66) Obringer, C.; Manwaring, J.; Goebel, C.; Hewitt, N. J.; Rothe, H. Suitability of the in Vitro Caco-2 Assay to Predict the Oral Absorption of Aromatic Amine Hair Dyes. *Toxicol. Vitro.* **2016**, *32*, 1–7. <https://doi.org/10.1016/j.tiv.2015.11.007>.

Chapter 2

Diblock Terpolymers are Tunable and pH Responsive Vehicles to Increase Hydrophobic Drug Solubility for Oral Administration *

*Reproduced in part with permission from Tale, S.; Purchel, A.; Dalsin, M.; Reineke, T.M.
Mol. Pharm., **2017**, *14*(11), 4121-4127. DOI: 10.1021/acs.molpharmaceut.7b00458

2.1 Introduction

Oral delivery is the most utilized and convenient method for routine administration of active pharmaceutical ingredients (APIs) in the solid dose form.⁶⁷⁻⁶⁹ This preferred administration route promotes increased patient compliance and lower costs as systemic injection routes are avoided. Approximately 40-60% of new drug candidates in the pharmaceutical pipeline suffer from poor aqueous solubility in the gastrointestinal track (GI), resulting in reduced bioavailability and low therapeutic effect.^{70,71} Also, about 70% of pipeline drug candidates are Biopharmaceutics Classification System (BCS) Class II compounds, which denote compounds with low aqueous solubility and high permeability across the GI tract.⁷⁰ Synthetic and natural polymers have shown great potential to improve bioavailability, shelf life, and therapeutic efficacy of BCS class II drugs for oral administration.⁷² Various methods exist to disperse APIs in a polymer matrix to form drug-polymer solid dispersions (*e.g.*, spray drying, hot melt extrusion).^{17,73-76} Spray drying has emerged as a convenient technology for the formulation of amorphous solid dispersions, which are then physically pressed into a tablet for ease in packaging and dosing.⁷⁴ This formulation technology is readily scalable and has been utilized commercially in developing new formulations with various drugs, such as ivacaftor, a drug with a high tendency to crystallize (melting point 291°C), which can be dispersed in hydroxypropyl methyl cellulose acetate succinate (HPMCAS).⁷⁷ Indeed, polymer-drug interactions play a critical role in dictating dissolution performance of spray dried dispersions (SDDs).⁷⁸ Therefore, to fully employ the promise of polymer excipients, it is vital to understand the fundamental structure-property relationships of drug dissolution with polymer excipients to fine-tune design parameters for optimizing SDD performance.⁷⁹

To date, hydroxypropyl methylcellulose acetate succinate (HPMCAS) is one of the top performing polymer excipients on the market that effectively inhibits API nucleation, crystal growth, and maintains high levels of drug supersaturation, which leads to an increase in drug absorption in the GI track.^{15,16} HPMCAS solid dispersion formulations are components of FDA-approved formulations currently on the market. These formulations include telaprevir (Hepatitis C), vemurafenib (late stage melanoma), and ivacaftor (cystic fibrosis).⁷⁷ The use of HPMCAS enhances aqueous drug solubility, improves bioavailability, and increases therapeutic effect for these drugs.

Understanding the structure-property relationships of API interactions with excipients is a challenge within this field. For example, the high dispersity (in terms of both length and chemical substitution) of industrially manufactured HPMCAS offers difficulties in characterizing its physiochemical properties; thus, examining structure-property relationships using model polymer systems has allowed understanding of the design parameters required to create improved formulations.⁷ For example, Dalsin et al. demonstrated that micelle structures in excipient formulations improve drug dissolution and supersaturation maintenance when compared to polymer formulations with the same composition that were not preassembled into micelles.¹⁷ Mundargi et al. showed that a diblock copolymer composed of polylactic acid (PLA) and polyethylene glycol (PEG) (PLA-PEG) can control the release of zidovudine (AZT).⁸⁰ Ting et al. revealed that polymers created by chain-growth methods containing pendant chemistries that model HPMCAS can be tuned to yield outstanding probucol solubility profiles.⁸¹ That study demonstrated that API solubility and super saturation maintenance could be achieved due to their increased intermolecular hydrogen bonding interactions between the polymers and API. Interactions

could be fine-tuned via increasing composition of hydroxy propyl, glucose, and carboxylic acid functional groups that promoted API H-bonding to the polymer.⁸¹ Also, recently published data by Ting et al. indicates that matching polymer backbone chemical structure and composition to that found on drugs can dramatically increase drug solubility.⁷⁸ This promotes the polymer-drug interactions, crystallization inhibition, high supersaturation maintenance, and effective oral bioavailability/pharmacokinetics in rat models orally dosed with phenytoin, a common anticonvulsant.⁷⁸

Herein, five well-defined block copolymers have been designed and synthesized to evaluate the effects of block chemistry and length toward promoting SDD formation and drug solubility in oral delivery conditions. To examine the how the polymer chemistry affects drug interactions and supersaturation maintenance, blocks of PEP (hydrophobic), PNIPAm (exhibits both hydrophilic and hydrophobic character depending on temperature⁷⁸), or PDEAEMA (hydrophilic and pH responsive H-bonding) were each copolymerized with consistent lengths/composition of a second block (*DMA-grad-MAT*). Three polymer variants were created of similar molecular weight (between 28-32 kDa): PEP-*b*-P(*DMA-grad-MAT*), PNIPAm-*b*-P(*DMA-grad-MAT*), and PDEAEMA-*b*-P(*DMA-grad-MAT*). To explore molecular weight effects of the hydrophilic block, two other PNIPAm-*b*-P(*DMA-grad-MAT*) variants were created (18, 32, and 48 kDa) with varying lengths of *DMA-grad-MAT* block (while maintaining similar composition) for the purpose of evaluating the effects of H-bonding between the sugar units and a model drug. A homopolymer of poly(N,N'-dimethylacrylamide) (PDMA) was also prepared as a sixth polymer (control) variant for drug solubility studies. With these polymers, SDDs were created to encapsulate probucol, an off-market anti-hyperlipidemic drug, which was

examined as a model BCS Class II API due to its very low aqueous solubility of 0.042 $\mu\text{g/mL}$.⁸² Herein, we demonstrate that the functionality of block polymer excipients can be tuned to solubilize and maintain supersaturation of probucol at different pH profiles, offering new design parameters for future excipient design to solubilize drugs in differing GI tract environments.

2.2 Results and Discussion

2.2.1 Synthesis of the diblock terpolymers

Synthesis of trimethylsilyl protected 2-methacrylamidotrehalose (TMS-MAT) (2) was achieved in six steps according to previously published procedure.⁸³ The macromolecular chain transfer agent (CTA), PEP-CTA (1a), was synthesized according to a published procedure by Yin et.al.⁷⁹ The M_n of this macromolecule was determined to be 3.6 kg mol^{-1} by end group analysis using ^1H NMR spectroscopy, with a dispersity (\mathcal{D}) of 1.06 as measured by size exclusion chromatography using chloroform as the eluent (calibration with PS standards). The two other macromolecular CTAs, PNIPAm-CTA (1b) and PDEAEMA-CTA (1c), were synthesized by reversible addition-fragmentation chain transfer (RAFT) polymerization using 4-Cyano-4-(propylsulfanylthiocarbonyl)sulfanylpentanoic acid (CPP)⁸⁴ as the CTA. The M_n of PNIPAAm-CTA and PDEAEMA-CTA (^1H NMR spectroscopy) were determined to be 5.6 kg mol^{-1} and 8.0 kg mol^{-1} respectively. Further details of the synthesis and characterization of these systems are given in the Table 2.1, Figures 2.1, and 2.2.

Table 2.1. Molecular characterization of the homopolymers

Sample	[AIBN] : [CTA] : [Monomer]	[M ₀]	Time (h)	Conv. of monomer	M _n , kg/mol ^a	D ^b
PNIPAm-CTA	0.05 : 1 : 50	1.69	6	99%	5.6	1.07
PDEAEMA-CTA	0.05 : 1 : 50	1.69	8	87%	8.0	1.15
PDMA	0.05 : 1 : 250	1.80	6	93%	23	1.17

^aThe number average molecular weight of the poly (CTA) as determined by ¹H NMR spectroscopy. ^bThe dispersities of poly (CTA) as determined by SEC using THF as a mobile phase.

Note: CTA used: 2-(dodecylthiocarbonothioylthio)-2-methylpropionic acid.

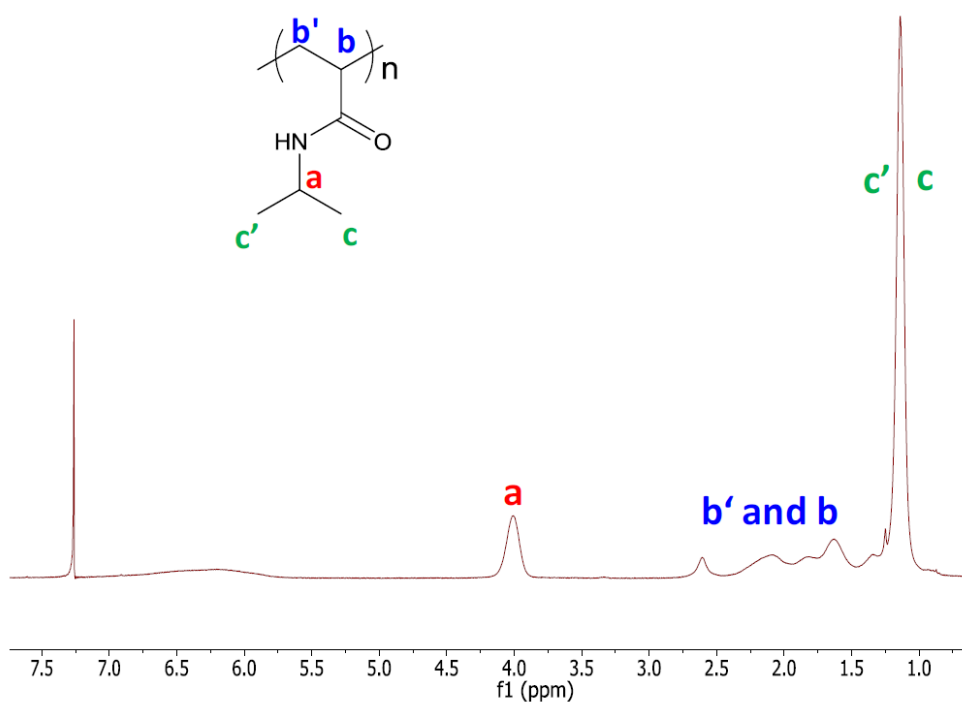


Figure 2.1. ¹H NMR spectrum recorded for PNIPAAm-CTA in CDCl₃. Copyright © 2017 American Chemical Society.

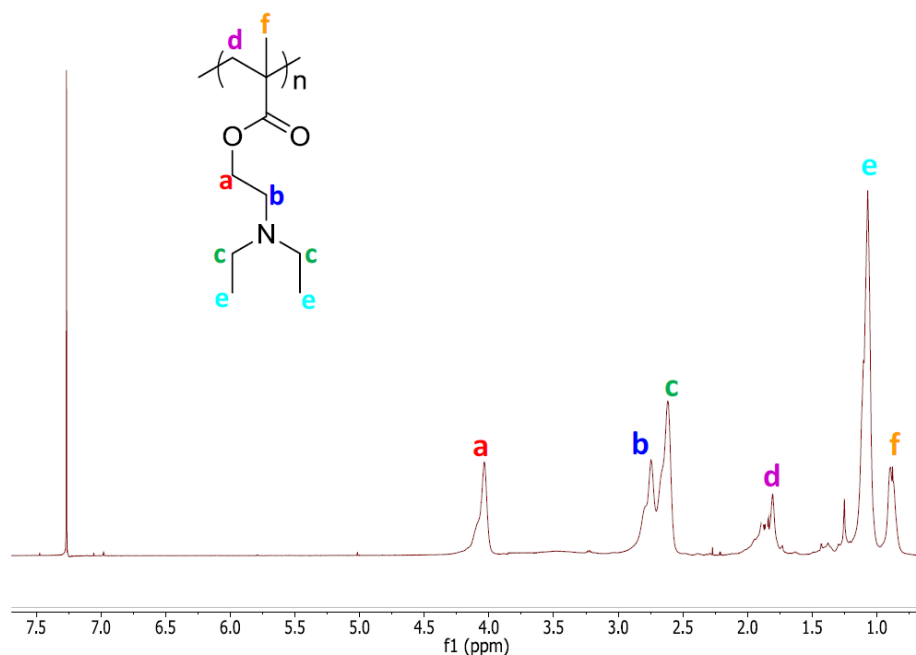


Figure 2.2. ¹H NMR spectrum recorded for PDEAEMA-CTA in CDCl₃. Copyright © 2017 American Chemical Society

Five diblock terpolymers, PEP-*b*-P(DMA-*grad*-MAT) (28 kDa), PNIPAm-*b*-P(DMA-*grad*-MAT) (18, 32, and 48 kDa), and PDEAEMA-*b*-P(DMA-*grad*-MAT) (31 kDa), were prepared by copolymerizing the macromolecular-CTA (1a, 1b, 1c) with DMA and TMS-MAT in toluene at 70 °C using AIBN as the initiator. The reported literature values for the reactivity ratios of TMS-MAT and DMA are $r_1 = 0.09$ and $r_2 = 1.62$.⁸⁵ These reactivity ratios indicate that the copolymer had a gradient structure, which consisted of an initial higher DMA ratio (close to PEP block) that was terminated with a higher content of MAT. The three variants of PNIPAm-*b*-P(DMA-*grad*-MAT) (18, 32, and 48 kDa) were synthesized to have a consistent molar composition of both the DMA and MAT monomers (72% DMA and 28% MAT) such that the role of the hydrophilic block length only was studied. The TMS groups were then deprotected by using HCl in methanol to yield the

diblock terpolymers. All polymers were purified by precipitation in ether and vacuum dried at 40 °C for 10 h. Table 1 contains characterization details of the diblock terpolymers and Figures 2.3 and 2.4 include the ^1H NMR spectra of purified PNIPAm-*b*-P(DMA-*grad*-MAT) and PDEAEMA-*b*-P(DMA-*grad*-MAT) polymers. The PEP derivative was previously made, characterized, and published by our lab.⁸⁵

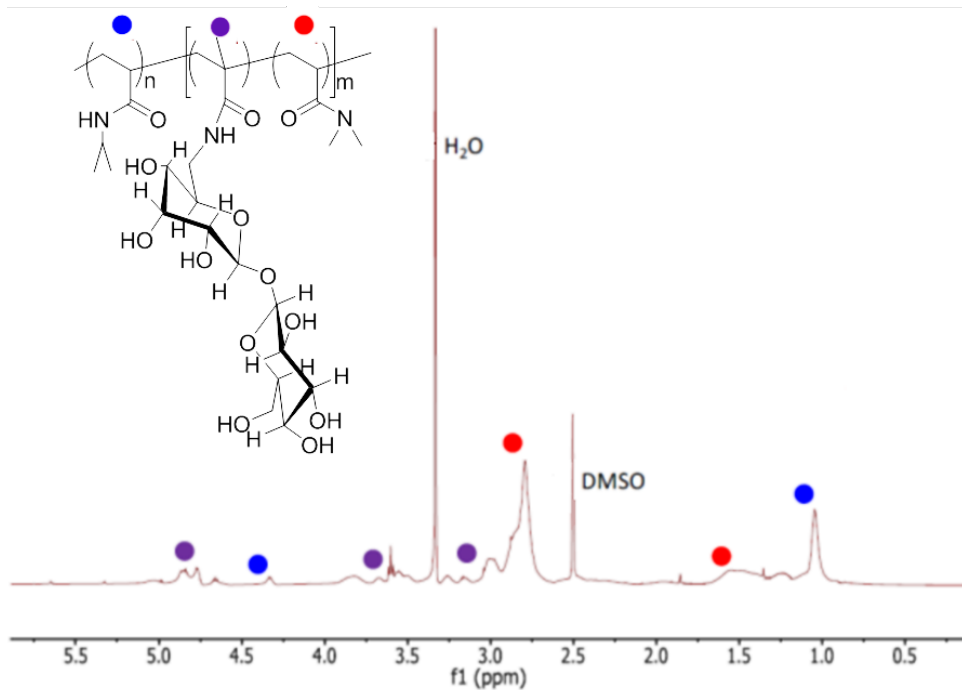


Figure 2.3. ^1H NMR spectrum recorded for PNIPAm-*b*-P(DMA-*grad*-MAT) in d_6 -DMSO. Copyright © 2017 American Chemical Society.

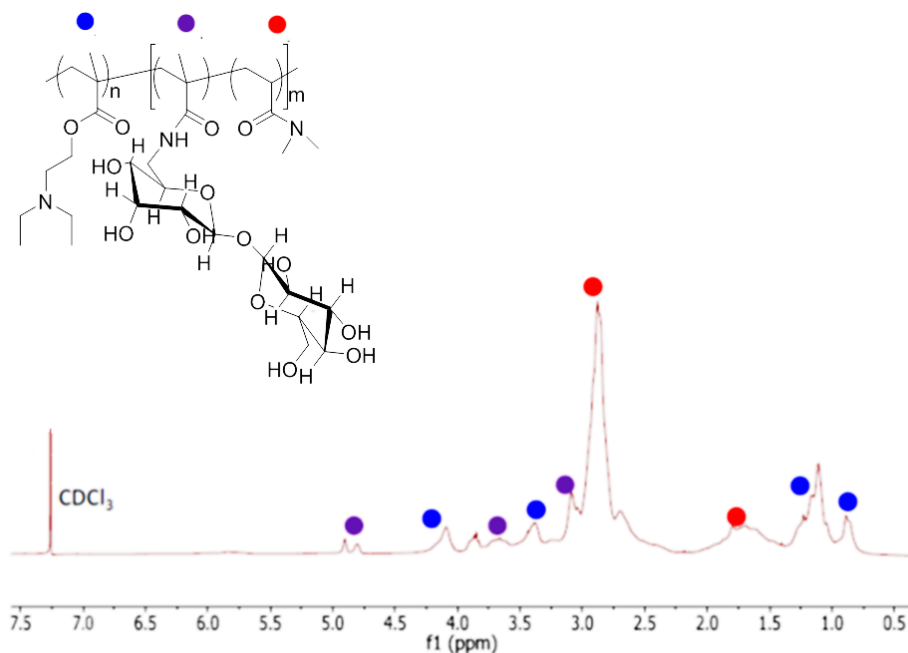


Figure 2.4. ^1H NMR spectrum recorded for PDEAEMA-*b*-P(DMA-*grad*-MAT) in CDCl_3 .
Copyright © 2017 American Chemical Society.

2.2.2 Synthesis of the PDMA homopolymer

Synthesis of the PDMA was achieved using a procedure from a previously published study.¹⁷ Commercially available N,N' -dimethylacrylamide was used as a monomer, 4-Cyano-4-(dodecylsulfanylthiocarbonyl) sulfanylpentanoic acid as a chain transfer reagent, and AIBN as an initiator. The M_n of the PDMA was determined to be 23.0 kDa according to THF-SEC characterization.

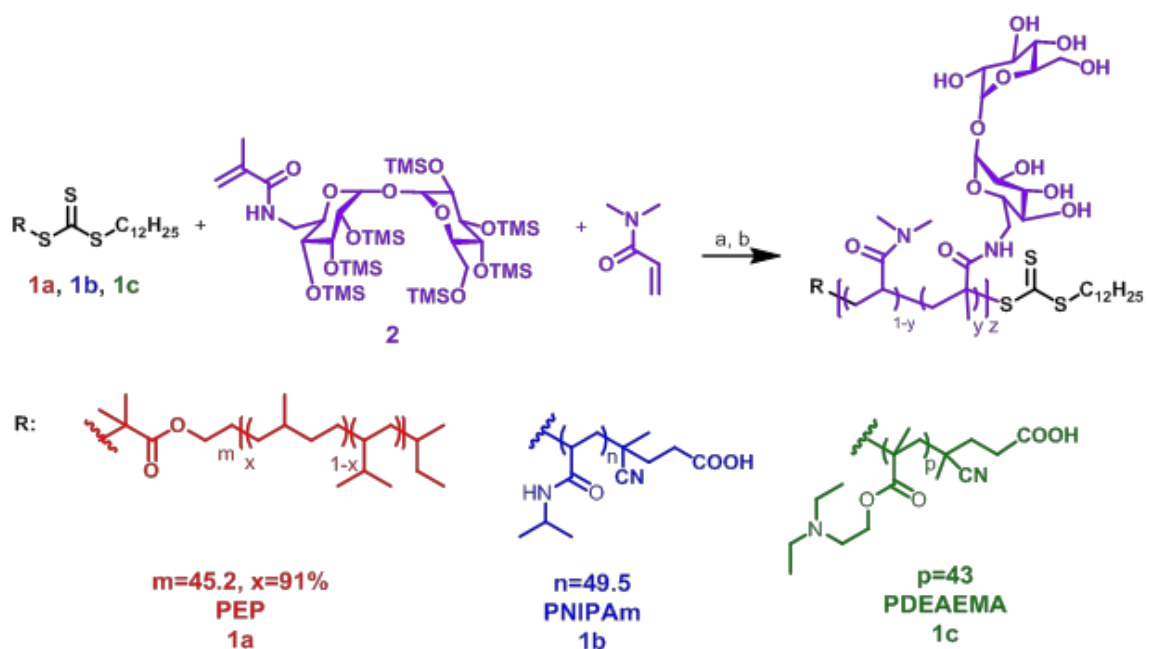


Figure 2.5. Synthesis of the diblock terpolymers. Reagents and Conditions: a) AIBN, 70 °C, Toluene b) 1.25M HCl in methanol.

Table 2.2. Characterization of the polymers used in this study.

Sample ^a	[AIBN] : [Poly-CTA] : [DMA] : [TMS-TMAT] ^b	[M ₀]	Time (h)	Conv. of DMA ^c	Conv. of TMS-MAT ^c	M _n kg/mol ^d	D ^e	T _g ^f
PEP- <i>b</i> -P(DMA- <i>grad</i> -MAT) (3.6-24.5-0.1)	0.05 : 1 : 180 : 20	1.69	10	99%	92%	28	1.23	14
EAEMA- <i>b</i> -P(DMA- <i>grad</i> -MAT) (8-23-0.1)	0.05 : 1 : 180 : 20	1.69	19	89%	85%	31	1.33	12
NIPAm- <i>b</i> -P(DMA- <i>grad</i> -MAT) (6.1-12.4-0.28)	0.05 : 1 : 130 : 10	1.69	6	95%	85%	18	1.16	12
NIPAm- <i>b</i> -P(DMA- <i>grad</i> -MAT) (5.6-26.4-0.31)	0.05 : 1 : 180 : 20	1.69	12	99%	99%	32	1.21	15
NIPAm- <i>b</i> -P(DMA- <i>grad</i> -MAT) (6.1-42.1-0.28)	0.05 : 1 : 420 : 35	1.69	20	98%	85%	48	1.22	16
PDMA (23.0 kDa)	0.05 : 1 : 250	1.80	6	93 %	N/A	23	1.17	11

^aThe first value in parentheses indicates the number average molecular weight of either PEP, PNIPAm, or PDEAEMA in kg/mole and the second number indicates the number average molecular weight of the PDMA/PMAT block in kg/mole. The third number indicates the molar fractions of MAT (trehalose) in the block of the terpolymers. ^bInitial composition of the AIBN (initiator), poly(CTA), and monomers in the feed. ^cConversion of DMA and TMS-MAT as monitored by ¹H NMR spectroscopy. ^dNumber average molecular weight of the diblock terpolymers after deprotection of the TMS groups. ^ePolydispersity of the diblock terpolymers before the removal of the trimethylsilyl protecting groups. ^fGlass transition temperature of polymers reported as the second heating with a 5 °C/min heating rate.

2.2.3 Solid dispersions preparation and solid-state characterization

All samples were spray dried using a Bend Research lab scale Mini Spray Drier from THF : MeOH (15:2, v/v). Because this study was completed using block copolymers, it was important to increase the polymer solubility and decrease the formation of large aggregates, since aggregation has previously demonstrated to affect dissolution profiles.⁷⁵ Dynamic light scattering characterization for all systems prior to spray drying is shown in Figure 2.10. All polymer samples show some degree of aggregation, which changes depending on the hydrophobicity of the PNIPAm, PDEAEMA, or PEP blocks. The effect of the aggregation of analogous polymers was evaluated in a previous study¹⁷ and it was shown that preformed micelles increase dissolution performance due to sustained drug-polymer interactions when exposed to the dissolution media. In general, the physical stability of the SDDs is a critical component for thermodynamic stability of the drug molecules.⁸⁶ The drug should be molecularly dispersed in the polymer matrix yielding an amorphous mixture. A physically-stable and amorphous SDD formulation leads to increased aqueous solubility of the drug, improved bioavailability (potentially leading to decreased costs and side effects).⁸⁶ Scanning electron microscopy (SEM), powder X-ray diffraction (PXRD), and modulated differential scanning calorimetry (MDSC) were used for solid-state characterization of the obtained spray dried dispersions. Selected data is presented in Figures 2.6 and 2.7 and Tables 2.3 and 2.4. Based on the experimental results, at least 95 wt % of probucol is in an amorphous state in all spray dried dispersions. Probucol-polymer interactions appear to increase with the increased amount of H-bonding sites in the polymer, and from these characterization data the drug is molecularly dispersed in the polymer matrix.

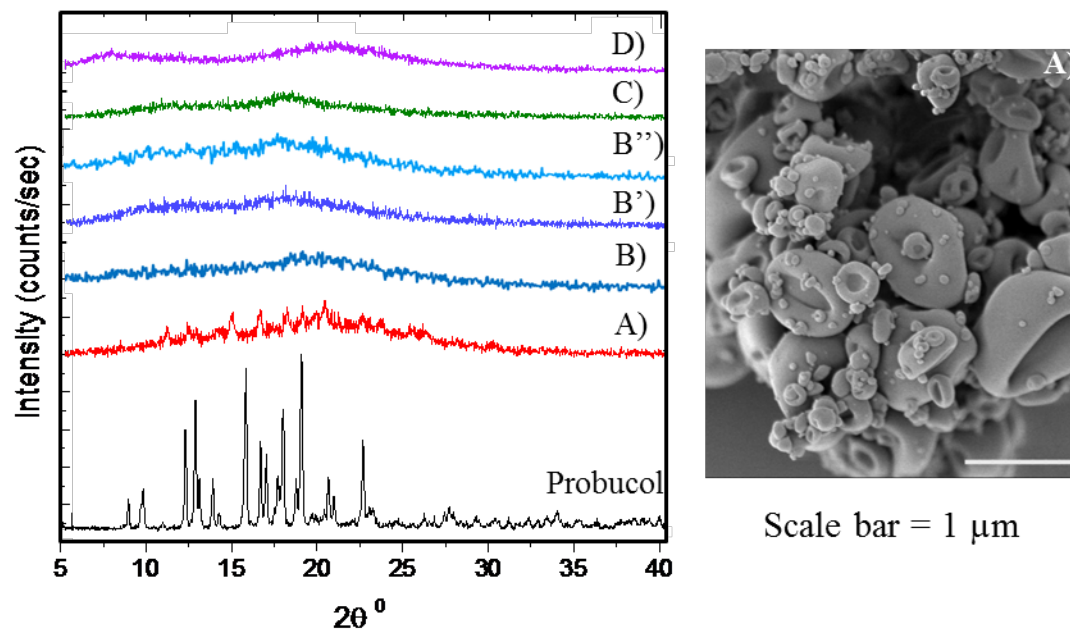


Figure 2.6. Powder XRD patterns of crystalline probucol comparing SDDs with A) PEP-*b*-P(DMA-*grad*-MAT), B), B'), B'') PNIPAm-*b*-P(DMA-*grad*-MAT) (18, 32, 48 kDa, respectively), C) PDEAEMA-*b*-P(DMA-*grad*-MAT), and D) PDMA as the matrices at 25 weight percent. SEM image is of the SDD created by spraying a THF:MeOH (15:2) solution of probucol with PEP-*b*-P(DMA-*grad*-MAT). Copyright © 2017 American Chemical Society.

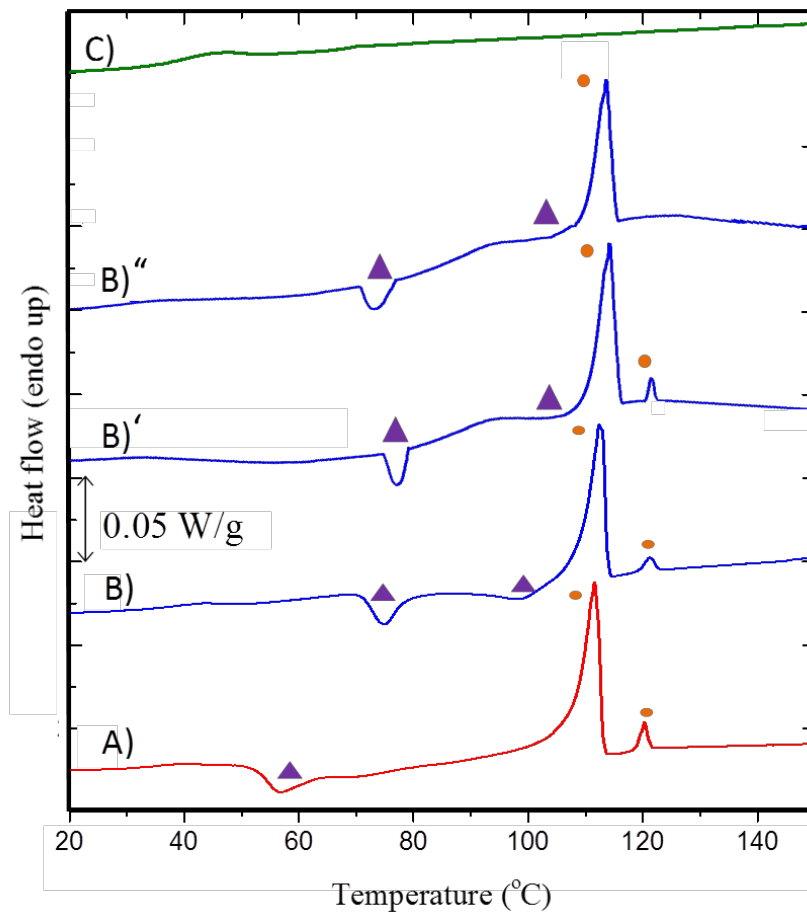


Figure 2.7. MDSC thermograms of total heat flow from SDDs containing 50 weight percent of probucol A) PEP-*b*-P(DMA-*grad*-MAT), B) PNIPAm-*b*-P(DMA-*grad*-MAT) – 32 kDa, B)' – PNIPAm-*b*-P(DMA-*grad*-MAT) – 18 kDa, B)'' – PNIPAm-*b*-P(DMA-*grad*-MAT) – 48 kDa, and C) PDEAEMA-*b*-P(DMA-*grad*-MAT). Copyright © 2017 American Chemical Society.

Table 2.3. Comparison of the weight fraction of monomers and drugs in the SDDs and the percent of probucol crystallinity.

Sample	SDD weight fraction					Probucol loading	% PBC Crystallinity
	PEP	PNIPAm	PDEAEMA	PDMA	PMAT		
PEP-b-P(DMA- <i>grad</i> -MAT)	0.06	0	0	0.31	0.13	0.50	42.1
PNIPAm-b-P(DMA- <i>grad</i> -MAT) – 18 kDa	0	0.16	0	0.24	0.10	0.50	25.7
PNIPAm-b-P(DMA- <i>grad</i> -MAT) – 32 kDa	0	0.09	0	0.29	0.12	0.50	35.8
PNIPAm-b-P(DMA- <i>grad</i> -MAT) – 48 kDa	0	0.07	0	0.31	0.12	0.50	34.0
PDEAEMA-b-P(DMA- <i>grad</i> -MAT)	0	0	0.13	0.26	0.11	0.50	0

Table 2.4. MDSC analysis of SDDs with probucol.

Probucol Loading	SDD	T_g (°C)	T_{c1} (°C)	Enthal py (J/g)	T_{c2} (°C)	Enthal py (J/g)	T_{m1} (°C)	Enthal py (J/g)	T_{m2} (°C)	Enthal py (J/g)	% PBC Crystal linity
10 wt %	PEP-b-P(DMA- <i>grad</i> -MAT)	106.4	-	-	-	-	-	-	-	-	-
	PNIPAm-b-P(DMA- <i>grad</i> -MAT) – 18 kDa	104.2	-	-	-	-	-	-	-	-	-
	PNIPAm-b-P(DMA- <i>grad</i> -MAT) – 32 kDa	127.6	-	-	-	-	-	-	-	-	-
	PNIPAm-b-P(DMA- <i>grad</i> -MAT) – 48 kDa	141.1	-	-	-	-	-	-	-	-	-
	PDEAEMA-b-P(DMA- <i>grad</i> -MAT)	150.2	-	-	-	-	-	-	-	-	-
25 wt %	PEP-b-P(DMA- <i>grad</i> -MAT)	105.1	-	-	-	-	107.1	5.2	-	-	14.1
	PNIPAm-b-P(DMA- <i>grad</i> -MAT) – 18 kDa	102.8	74.3	3.8	101.1	2.3	106.3	5.3	-	-	9.3
	PNIPAm-b-P(DMA- <i>grad</i> -MAT) – 32 kDa	116.6	80.2	2.6	-	-	107.6	4.8	-	-	12.9
	PNIPAm-b-P(DMA- <i>grad</i> -MAT) – 48 kDa	118.8	80.4	3.2	-	-	108.1	5.9	-	-	14.2
	PDEAEMA-b-P(DMA- <i>grad</i> -MAT)	126.9	-	-	-	-	-	-	-	-	-
50 wt %	PEP-b-P(DMA- <i>grad</i> -MAT)	104.3	56.8	15.9	-	-	107.9	28.9	120.3	1.46	42.1
	PNIPAm-b-P(DMA- <i>grad</i> -MAT) – 18 kDa	103.7	78.2	3.4	101.3	1.3	114.2	15.3	123.4	2.1	28.4
	PNIPAm-b-P(DMA- <i>grad</i> -MAT) – 32 kDa	105.9	74.9	5.3	98.2	2.1	112.4	18.4	121.1	1.2	35.8
	PNIPAm-b-P(DMA- <i>grad</i> -MAT) – 48 kDa	112.2	73.1	5.7	98.3	2.4	113.2	24.3	-	-	40.2
	PDEAEMA-b-P(DMA- <i>grad</i> -MAT)	111.1	-	-	-	-	-	-	-	-	-

2.2.4 Drug dissolution testing

Next, we studied how well the SDDs achieve and maintain the *in vitro* dissolution performance of probucol. Ideally, a dispersion of the drug and polymer should be able to maintain supersaturation levels of drug and inhibit crystal nucleation in the GI tract. Simulated intestinal fluid was added to the dissolution media to test *in vitro* performance of all the SDDs. Figure 2.8 shows the dissolution profiles of all the SDD formulations and AFFINISOL™ 912G labeled as HPMCAS in Figure 2.8 (positive control) at 10 and 25 weight percent of probucol loading. The SDD with PNIPAm-*b*-P(DMA-*grad*-MAT) (32 kDa) showed an excellent fast release profile with probucol in aqueous solution and maintained drug supersaturation for 360 min (6 h). We attributed the excellent performance of PNIPAm-*b*-P(DMA-*grad*-MAT) (32 kDa) to its ability to dissolve rapidly in aqueous solution, release probucol in the dissolution media, and inhibit crystal nucleation by potentially binding to the drug through both H-bonding and hydrophobic interactions. The PEP-*b*-P(DMA-*grad*-MAT) did not dissolve fully in the dissolution media and resulted in a poor solubilization/release profile of probucol. Due to the insolubility of the polymer matrix, the drug may be trapped and remain undissolved with the polymer in the dissolution media. The PDEAEMA-*b*-P(DMA-*grad*-MAT) polymer also did not fully dissolve during dissolution at pH 6.5 and revealed a poor drug solubilization/release profile at this pH.

DEAEMA is a pH responsive component of this system and it is well documented in the literature that DEAEMA becomes protonated in aqueous solution upon lowering of the pH, which could significantly affect solubility of the SDD. Therefore, we conducted dissolution tests of this SDD at a lower pH of 5.1 and 3.1, respectively, which improves solubility of the excipient. At pH 5.1, this SDD was still insoluble and no significant change

in the dissolution profile was found. Interestingly, at pH 3.1, the SDD formulations with PDEAEMA-*b*-P(DMA-*grad*-MAT) exhibited a timed release of probucol to 1000 µg/mL and maintained full drug supersaturation for 6 h. This result points to the high importance of excipient solubility at differing pH profile to tune/promote drug supersaturation and inhibiting crystal growth.

To understand the effect of the DMA-*grad*-MAT block on drug dissolution profiles, three solid dispersions were created with the PNIPAm-based excipients and compared with AFFINISOL™ 912G as well as with a PDMA control polymer at two different drug loadings of 10 and 25 wt % (Figure 2.9). The difference in the amount of H-bonding units in these block copolymers manifested itself in the amount of the drug available in the dissolution media. At 10 wt % drug loading, all of the excipients yielded immediate probucol release and solubility maintenance between 80-100% drug. The copolymer containing the short DMA-*grad*-MAT block length of 12.4 kDa yielded a slightly lower solubility performance than the analogs with a longer DMA-*grad*-MAT block lengths. This may be attributed to the importance of this hydrophilic block in overall SDD solubility and promoting both H-bonding and with the drug and dissolution media. The PNIPAm polymers containing the longer blocks of (DMA-*grad*-MAT) (26.4 and 41.2 kDa) showed similarly high levels of drug supersaturation (at or close to a 100%). At 25% drug loading, the difference between the analogs was even more dramatic. The polymer containing the shortest DMA-*grad*-MAT block revealed poor performance (~50% of the drug was released) while the longer block lengths facilitated full solubility of probucol in a similar manner to the 10% drug formulations. Therefore, increasing the content of the DMA-*grad*-MAT block in the NIPAm-containing terpolymers appears to impact performance at lower

molecular weights and higher drug loading percentages. This indicates that the neutral hydrophilic block may play a role in both drug binding and aiding drug-polymer SDD solubility in the solution, where further inclusion of an alternative block such as PNIPAm adds additional drug-polymer affinity and solubility maintenance. To further support this concept, a control polymer containing only PDMA was formulated with probucol and examined. Indeed, at low drug loading (10%), the SDD formulation offered a similar performance to the lowest molecular weight of the PNIPAm-*b*-P(DMA-*grad*-MAT) system. However, at 25% probucol loading, the performance was very poor leading to minimal drug solubility. This observation suggests that increasing both the amount of H-bonding sites (to bind the drug) and the overall polymer matrix solubility in the dissolution media (with the addition of trehalose) are both important factors to promote solubility and supersaturation maintenance of drugs.

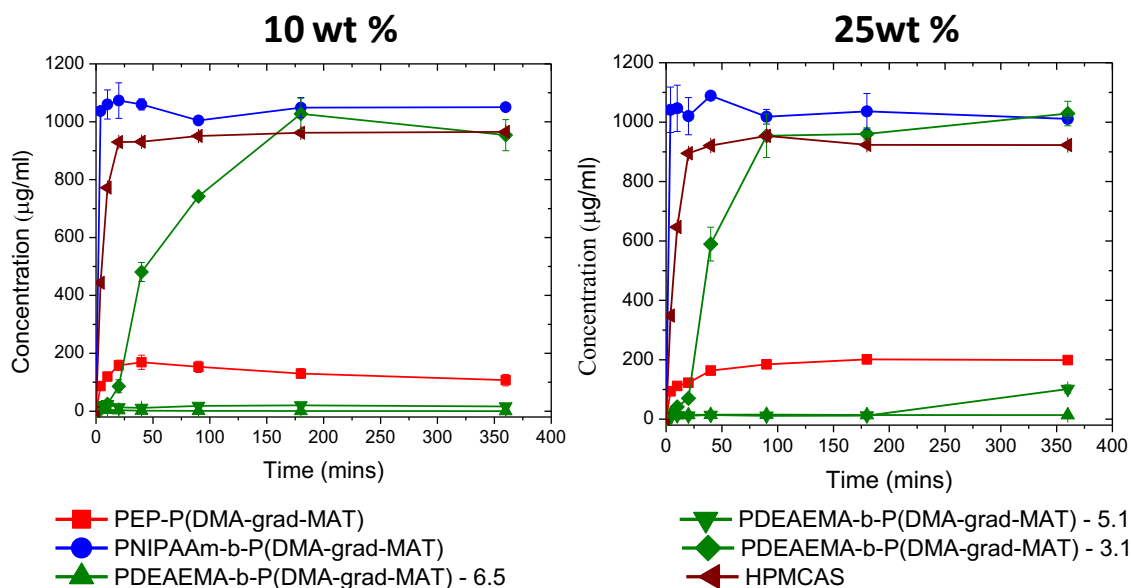


Figure 2.8. Dissolution data of the SDDs with 10 and 25 weight percent of probucol. PNIPAm-*b*-P(DMA-*grad*-MAT) – 32 kDa showed excellent rapid initial dissolution and supersaturation maintenance profile for probucol at pH 6.5. PDEAEMA-*b*-P(DMA-*grad*-

MAT) showed a controlled release profile for probucol at pH 3.1. The target concentration of probucol was 1000 $\mu\text{g/mL}$ (denoting 100% drug solubility) whereas the aqueous solubility of crystalline probucol (without an excipient) is very poor (0.042 $\mu\text{g/mL}$). Data points denote the mean of two dissolution experiments and error bars denote the range of measured data ($N=2$). Copyright © 2017 American Chemical Society.

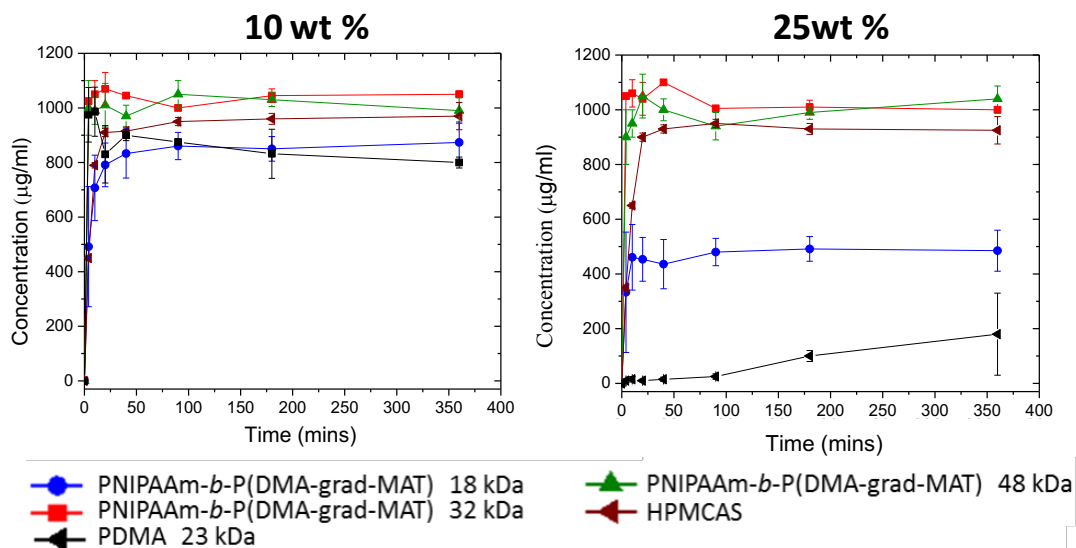


Figure 2.9. Dissolution data of the SDDs with three differing DMA-grad-MAT lengths with 10 and 25 weight percent of probucol and controls. The target concentration of probucol was 1000 $\mu\text{g/mL}$ (denoting 100% drug solubility) whereas the aqueous solubility of crystalline probucol (without an excipient) is very poor (0.042 $\mu\text{g/mL}$). Data points denote the mean of two dissolution experiments and error bars denote the range of measured data ($N=2$). Copyright © 2017 American Chemical Society.

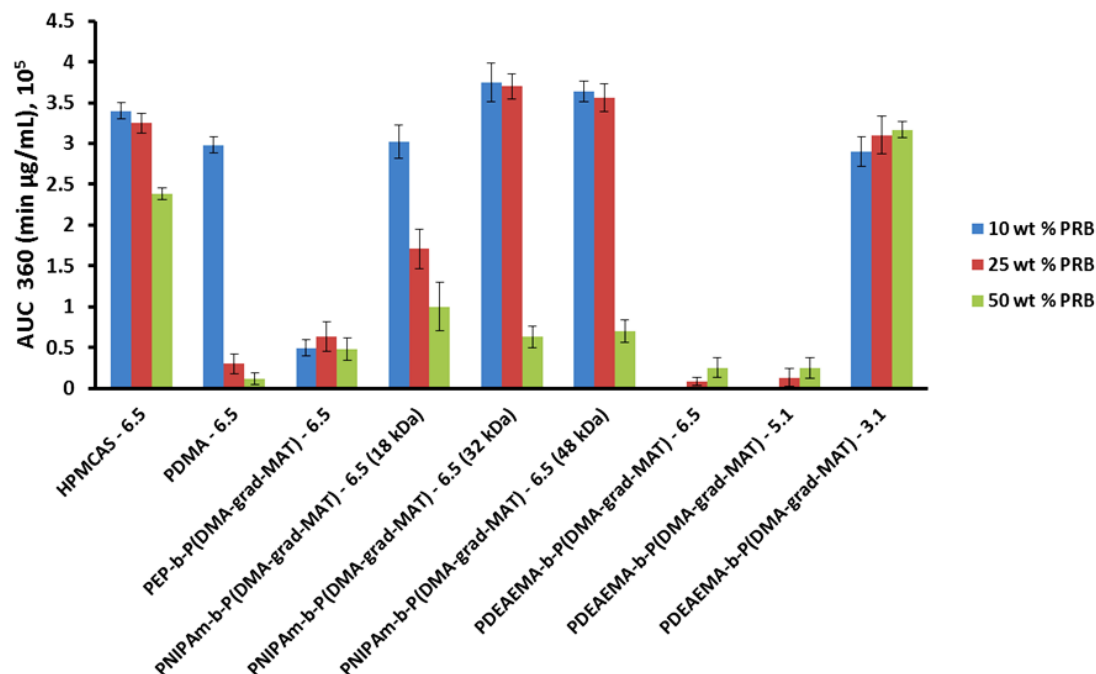


Figure 2.10. Area under the curve (AUC) as calculated at 360 min from the dissolution data of SDDs with 10, 25, and 50 weight percent probucol (PRB) loading. The calculated AUC is the average of two trials and error bars denote the range of measured data ($N=2$). The data for the homopolymer of PDMA with probucol SDD was obtained from previously published work.¹⁷ Copyright © 2017 American Chemical Society.

The area under the curve ($AUC_{360\text{min}}$) is the area under the drug concentration – time profile curves over the period of a 6 h dissolution test and represents the solubility maintenance of the excipient system for a particular drug. The $AUC_{360\text{max}}$ is the theoretical maximum area under the drug concentration time profile over the period of a 6 h dissolution test, where $3.6 \times 10^5 \mu\text{g}\cdot\text{min}/\text{mL}$ denotes 100% drug solubility and supersaturation maintenance over the period of six hours. Incorporating a higher drug loading percentage in a SDD formulation is desirable; however, there is a fine interplay between higher drug loading, and the increased tendency of the drug to crystallize. With HPMCAS, the targeted

probutol solubility concentration was achieved (up to 25 weight percent of drug loading, Figure 2.10 and Table 2.5). At 50 weight percent drug loading, only 64% of the targeted drug concentration was soluble, which was likely due to the lower amount of polymer excipient available to aid solubility (and thus prevent crystallization) of the hydrophobic drug molecules. The SDD of PEP-*b*-P(DMA-*grad*-MAT) exhibited poor solubility enhancement at all drug loading levels. Similar to HPMCAS, the SDDs of PNIPAm-*b*-P(DMA-*grad*-MAT) at higher molecular weights was able to achieve the targeted drug solubility concentration (100% soluble) up to 25 weight percent of drug loading. However, this polymer matrix achieved less than 20% of the targeted drug concentration at 50 weight percent of drug loading. The SDD of the homopolymer PDMA control achieved 83% of targeted drug concentration at 10 weight percent of loading but failed to perform at 25 and 50 weight percent of drug loading. This results indicates the hydrophilic block containing N,N'-dimethylacrylamide may play a lesser role in drug binding and solubility maintenance. These results indicated that the PNIPAm component of PNIPAm-*b*-P(DMA-*grad*-MAT) is the primary contributor to achieving the targeted drug concentrations at 25 weight percent of drug loading. A secondary contributor appears to also involve the hydrophilic P(DMA-*grad*-MAT) block that aids solubility of the whole formulation and also appears to contribute to drug binding. The SDD of PDEAEMA-*b*-P(DMA-*grad*-MAT) failed to show any significant increase in AUC_{360min} at pH 6.5 and 5.1. Interestingly, at a lower pH of 3.1, the SDD formulation was able to achieve almost 90% of the targeted probucol concentration at all drug loadings (10, 25, and 50 weight percent). With this pH-responsive excipient, the AUC_{360min} value gradually increased by decreasing the pH of the dissolution media with 10, 25, and 50 weight percent of drug loading. This is likely due to

a high fraction of amines being protonated along the PDEAEMA backbone, which increases polymer solubility, H-bonding sites for drug binding, and could possibly even facilitate cation- π interaction with the drug.⁸⁷ Therefore, this particular SDD, at a lower pH, outperformed HPMCAS by demonstrating 1.5 times increase in AUC_{360min} value at the highest drug loading percent tested (50 wt. %). This denotes that PDEAEMA structures may be useful motifs for facilitating triggered drug dissolution/solubility maintenance for targeted release in acidic pH environments (stomach) while shielding from drug release at more neutral pH values (intestines).

Table 2.5. Calculated area under the curve (AUC) for solubilization of probucol and all polymer excipient SDD formulations at 10, 25 and 50 weight percent drug loading.

Polymer	10 wt %		25 wt %		50 wt %	
	AUC_{360min} ($\mu\text{g/mL}$)	$AUC_{360min}/$ AUC_{360max} ($\mu\text{g/mL}$)	AUC_{360min} ($\mu\text{g/mL}$)	AUC_{360min} / AUC_{360max} ($\mu\text{g/mL}$)	AUC_{360min} ($\mu\text{g/mL}$)	AUC_{360min} / AUC_{360max} ($\mu\text{g/mL}$)
HPMCAS – 6.5	3.4×10^5	0.97	3.3×10^5	0.92	2.3×10^5	0.64
PEP-b-P(DMA-grad-MAT) – 6.5	4.8×10^4	0.13	6.7×10^4	0.19	4.2×10^4	0.12
PNIPAm-b-P(DMA-grad-MAT) – 6.5 (18 kDa)	3.1×10^5	0.84	1.6×10^5	0.43	9.8×10^4	0.26
PNIPAm-b-P(DMA-grad-MAT) – 6.5 (32 kDa)	3.7×10^5	~1.0	3.7×10^5	~1.0	6.6×10^4	0.18
PNIPAm-b-P(DMA-grad-MAT) – 6.5 (48 kDa)	3.7×10^5	~1.0	3.6×10^5	0.97	7.2×10^4	0.19
PDEAEMA-b-P(DMA-grad-MAT) – 6.5	3.9×10^2	0	5.1×10^3	0.01	2.3×10^4	0.06
PDEAEMA-b-P(DMA-grad-MAT) – 5.1	4.2×10^2	0	1.2×10^4	0.03	2.4×10^4	0.07
PDEAEMA-b-P(DMA-grad-MAT) – 3.1	2.9×10^5	0.81	3.1×10^5	0.86	3.2×10^5	0.89
PDMA – 6.5	3.0×10^6	0.83	2.9×10^4	0.08	1.1×10^4	0.03

2.3 Conclusion

In summary, we have synthesized five well-defined architectures of diblock polymers PEP-*b*-P(DMA-grad-MAT), PNIPAm-*b*-P(DMA-grad-MAT) at three molecular weights, and PDEAEMA-*b*-P(DMA-grad-MAT) and formulated SDDs of these materials with probucol. Our results clearly indicate that the solubility of the polymer

matrices in the dissolution media and an increase in hydrogen bonding sites in the polymer matrices are critical to decrease probucol crystallization, increase drug solubility (i.e., the AUC_{360min} value), and achieve supersaturation concentration of hydrophobic drugs in the dissolution media. Our study gives new insight into the field of excipient design by demonstrating the importance of monomer selection and polymer composition to fine-tune drug release and maintain solubility of a highly hydrophobic API. The development of tunable high performance excipients and efforts to understand the structure-activity relationships may help decrease the current high attrition rate of drugs in the pharmaceutical development pipeline.

2.4 Materials and Methods

2.4.1 Materials

All chemicals were used as received (reagent grade) unless otherwise noted. All solvents utilized were HPLC or analytical grade. Anhydrous D-trehalose (99%, Acros Organics), iodine (Aldrich, >99.8%), triphenylphosphine (Aldrich, 99%), acetic anhydride (99.6%, Fisher), dry pyridine (99.8%, Sigma Aldrich), sodium azide (Aldrich, >99.5%), Pd/C (Aldrich), sodium methoxide (Aldrich, 95%), sodium chloride (Fisher), silica gel (Sorbent technologies, porosity 60Å size 40-60µm), chlorotrimethylsilane TMSCl (Fisher, 98%), triethylamine (TEA) (Acros Organics, 99.7%), and HCl 1.25M in methanol (Fluka), 2,2'-Azobis(2-methylpropionitrile) (AIBN, Aldrich, 98%) were used as received. Freshly distilled methacryloyl chloride (Acros, 95%) was used for synthesis. *N,N*-Dimethylacrylamide (DMA) (Aldrich, 99+%) was purified by passage through activated basic alumina columns to remove trace amounts of inhibitors. The monomers *N*-isopropylacrylamide (NIPAAm) (Aldrich, >99%), 2-(diethylamino)ethylmethacrylate

(DEAEMA) (Aldrich, 99%), and 2-(dodecylthiocarbonothioylthio)-2-methylpropionic acid (Aldrich, 98%) were used as received. *Sec*-butyllithium (1.4 M in cyclohexane, Aldrich), 1,3-isoprene (Aldrich, 99%), and ethylene oxide (Aldrich, 99.5+%) were degassed with three freeze-pump-thaw cycles followed by removing trace amounts of acidic impurities by multiple treatments with *n*-butyllithium (2.5 M in hexanes, Aldrich) for 1 hour each and *n*-butylmagnesium chloride (2.0 M in diethyl ether, Aldrich) for 4 hours each, respectively. Toluene (Sigma-Aldrich, HPLC grade, 99.9+%), and dichloromethane (Sigma-Aldrich, anhydrous, 99.8+%), and tetrahydrofuran (THF, Sigma-Aldrich, HPLC grade, 99.9+%, inhibitor free) were purified via an MBRAUN solvent purification system. Probucol (PBC) was purchased from Sigma-Aldrich (Milwaukee, WI) and used without further purification. HPMCAS (AFFINISOL™ 912G, The Dow Chemical Company) was used as received with degree of substitution (DS) as follows: DS of succinate 0.28, DS of acetate 0.57, DS of methoxy, and 1.94 DS hydroxypropyl 0.25. Fasted simulated intestinal fluid powder (FaSSIF) was purchased from Biorelevant (Surrey, UK). Phosphate buffered saline (PBS) was prepared that consisted of 82 mM sodium chloride (Fisher, $\geq 99.0\%$), 20 mM sodium phosphate dibasic heptahydrate (Fisher, 98%), and 47 mM potassium phosphate monobasic (J.T. Baker, $\geq 99.0\%$).

2.4.2 Polymer synthesis

The synthesis of trimethylsilyl protected 2-methacrylamidotrehalose (TMS-MAT) was synthesized as previously described by our group.^{1,2} The ¹H NMR was in agreement with previously published spectral data.^{1,2} The diblock terpolymer PEP-P(DMA-*grad*-MAT) was synthesized using a combination of anionic and reversible addition fragmentation chain transfer (RAFT) copolymerizations as previously published.² The

PEP-b-P(DMA-*grad*-MAT) was characterized by ^1H NMR and size exclusion chromatography (SEC). The analysis and characterization data were also in agreement with the previously published data.² The synthesis of the diblock terpolymers PNIPAAm-b-P(DMA-*grad*-MAT) (18, 32, and 48 kDa) (Figure 2.3, ^1H NMR) and PDEAEMA-b-P(DMA-*grad*-MAT) (Figure 2.4, ^1H NMR) was achieved via polymerization from of the macromolecular chain transfer agents (CTA), PNIPAAm-CTA and PDEAEMA-CTA, respectively. For example, a 25 mL round conical flask was charged with PNIPAAm-CTA (0.6 g, 0.1 mmol), DMA (1.8 g, 18 mmol), TMS-MAT (1.8 g, 2 mmol), AIBN (0.8 mg, 0.0005 mmol), and 1,4-dioxane (10 mL). The reaction mixture was degassed for 1 h by bubbling nitrogen through the solution and adding the flask to a preheated oil bath at 70 °C for 12 h. Both polymers were purified by precipitation in diethyl ether twice and dried in a vacuum oven for 24 h at 45 °C. Detailed characterization information is reported in Table 2.1 and Figure 2.4, which shows SEC chromatograms for PNIPAAm-b-P(DMA-*grad*-MAT) and PDEAEMA-b-P(DMA-*grad*-MAT). PNIPAAm-CTA (Figure 2.1, ^1H NMR) and PDEAEMA-CTA (Figure 2.2, ^1H NMR) were obtained by RAFT polymerization using a small molecule trithiocarbonate-based CTA, 2-(dodecylthiocarbonothioylthio)-2-methylpropionic acid in 1,4-dioxane using AIBN as an initiator at 70 °C. For example, a 50 mL round conical flask was charged with NIPAAm (5 g, 45 mmol), 357 mg of CTA (357 mg, 0.88 mmol), Azobisisobutyronitrile (AIBN) (7.2 mg, 0.044 mmol), and 1, 4-dioxane (22 mL, 1.69 M). The reaction mixture was degassed for 45 min by bubbling nitrogen through the solution. The reaction flask was then added to a preheated oil bath at 70 °C for 6 h. The PNIPAAm-CTA was isolated by precipitation into pentane and purified by dialysis against water to remove trace amounts of impurities such as monomers and

solvent. PDEAEMA-CTA was purified by precipitation into diethyl ether twice. Detailed characterization information is reported in Table S1. The yields for PNIPAAm-CTA and PDEAEMA-CTA were 87% and 72%, respectively. The macromolecular-CTAs were dried in a vacuum oven for 48 h at 40 °C before utilization to synthesize diblock terpolymers. For PNIPAAm-containing diblock terpolymers, three reactions were setup where feed ratio of monomers to macro-CTA was varied along with the time of the reaction. For instance, for PNIPAAm-b-P(DMA-*grad*-MAT) – 18 kDa synthesis, 250 mg of PNIPAAm macro-CTA (0.0409 mmol), 527 mg of N,N-dimethylacrylamide (5.33 mmol) and 357 mg of TMS-MAT (0.409 mmol) were mixed together in 4 mL of toluene, degassed with nitrogen for 30 minutes and placed in an oil bath at 70 °C for 18 hours. After, polymer was precipitated in 200 mL of diethyl ether, redissolved in methanol and treated with 5 mL of HCl/MeOH solution overnight. Solution was dialyzed in water to obtain pure product (yield was 88%). To obtain two other PNIPAAm-based diblock terpolymers (32 and 48 kDa), a ratio of CTA to monomers was changed to 1 : 180 : 20 (PNIPAAm : DMA : TMS-MAT) and 1: 420 : 35 (PNIPAAm : DMA : TMS-MAT) respectively and reaction time was increased to 32 or 48 hours (yields were 78% and 85% respectively).

Poly(N,N-dimethyl acrylamide) (PDMA) was synthesized using 4-Cyano-4-(dodecylsulfanylthiocarbonyl) sulfanylpentanoic acid as a chain transfer agent. For this synthesis, N,N-dimethylacrylamide (DMA, 2.00 g, 20.2 mmol) was added to 12 mL of 1,4-dioxane in a 25 mL flask with 4-Cyano-4-(dodecylsulfanylthiocarbonyl)sulfanyl pentanoic acid (32.6 mg, 0.0808 mmol) and AIBN (0.663 mg, 0.00404 mmol). The mixture was capped with a septum and degassed with nitrogen flow for 30 minutes while being submerged in water/ice bath. After, the reaction was placed in a preheated block at 70 °C

for 6 hours. When the reaction was completed, the flask was opened to air and cooled using liquid nitrogen. The mixture was precipitated in pentane and polymer was dried in a vacuum overnight (yield was 92%).

2.4.3 Methods

2.4.3.1 Size exclusion chromatography (SEC) method

SEC measurements were carried out on an Agilent 1260 Infinity liquid chromatograph equipped with a Waters Styragel guard column and three Waters Styragel columns (HR6, HR4, and HR1; 100-10,000,000 g/mol) to provide effective separation for molecular weight determination. The detectors used were an Agilent 1260 VWD UV-vis detector, a Wyatt Dawn Heleos II light-scattering detector, and a Wyatt Optilab T-rEX refractive-index detector. Tetrahydrofuran was used as the mobile phase at 1.0 mL/min at 25 °C.

2.4.3.2 Spray drying

Spray drying was performed on a Bend Research Mini Spray Drier under the following conditions: inlet temperature of 68 °C, nitrogen flow rate of 12.8 SLPM, and a 0.65 mL/min syringe flow rate. The SDDs were collected on a 4" Whatman filter. Unless otherwise noted, the total solute content spray dried was always one weight percent. Solutions were sprayed from a THF:MeOH mixture (15:2, v/v). All diblock terpolymers were completely soluble in a THF:MeOH mixture prior to spray drying. The SDD composition is reported as the weight percent (wt %) drug in the dispersion. For example, 30 mg of probucol and 270 mg of polymer were dissolved in 29.7 g of THF:MeOH mixture to make 10 wt% probucol with (PEP-b-P(DMA-*grad*-MAT)). Three different

compositions were used for the polymer/drug dispersions: 10, 25, and 50 wt % probucol relative to polymer.

2.4.3.3 *Dynamic light scattering (DLS)*

A Brookhaven Instrument system was used for DLS measurements. It includes a Mini L-30 laser source ($\lambda = 637$ nm), a BI-APD avalanche photodiode detector, and a BI-9000AT digital correlator, all aligned on a BI-200SM goniometer with a decaline thermo regulating bath. All samples were filtered using 0.45 μm Teflon syringe filters. For measurements, polymers were dissolved in THF: MeOH (15:2, v/v) mixture until a 1 wt % concentration was reached. For each sample, the second-order scattering intensity correlation function ($g_2(t)$) was measured at a 90 degree angle and converted using the regularized positive exponential sum⁴ (REPES) algorithm. The size distribution of aggregates is shown in the Figure 2.11. All polymer samples show some degree of aggregation, which changes depending on the hydrophobicity of the PNIPAm, PDEAEMA, or PEP blocks.

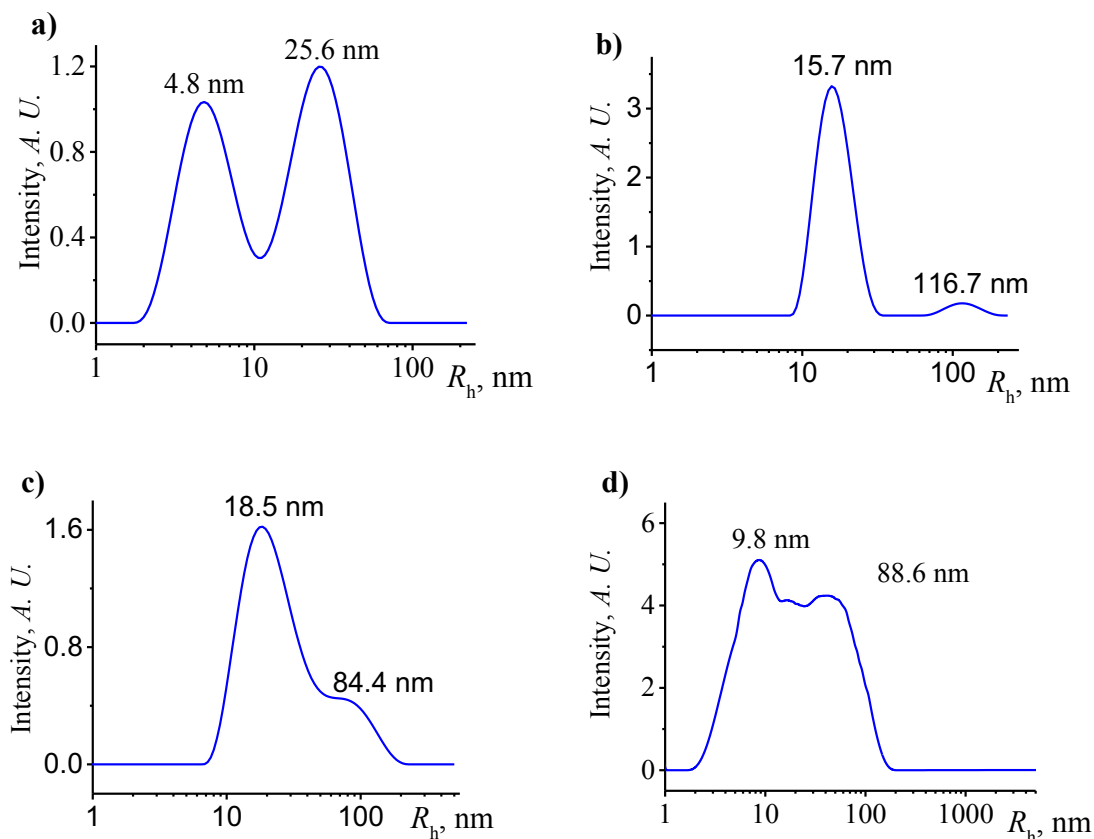


Figure 2.11. REPES analysis of data obtained from intensity correlation function at a 90° angle for the solutions in THF:MeOH (15:2, v/v) of a) PNIPAm-b-P(MAT-grad-DMA) – 32 kDa, b) PDEAEMA-b-P(MAT-grad-DMA), c) PEP-b-P(MAT-co-DMA), and d) PNIPAm-b-P(MAT-grad-DMA) – 18 kDa. Polymer concentration is at 1 wt %. Copyright © 2017 American Chemical Society.

2.4.3.4 Powder X-ray diffraction (PXRD)

PXRD experiments were carried out on a Bruker- AXS (Siemens) D5005 diffractometer. Samples (50 mg) were packed into standard 0.5 mm deep glass holders with zero background. The x-ray source ($\text{KCu}\alpha$, $\lambda = 1.54 \text{ \AA}$) was operated at a voltage of 45 kV and a current of 40 mA. Data for each sample was collected from 5° to 40° on the 2θ scale over approximately 30 minutes at a scan step of 1 seconds and a step size of $0.02^\circ/\text{s}$.

2.4.3.5 Differential scanning calorimetry (DSC)

Modulated differential scanning calorimetry (MDSC) was used to determine the thermal features of the SDDs and was conducted on a TA-Instruments Discovery DSC equipped with an autosampler. Samples from 5–10 mg were placed in T-zero aluminum pans and sealed with a hermetic lid. MDSC analysis was performed with a nitrogen flow rate of 50.00 mL/min and a heating rate of 1 °C/min from 0 to 180 °C. The temperature was modulated at ± 2 °C with a period of 40 s. The first heating scans are reported. For polymer only samples (not spray dried), the temperature was not modulated, but was ramped between -50 °C and 180 °C at a rate of 10 °C/min. The second heating scans are reported for those samples. For all samples, TA TRIOS software version 2.2 was used to analyze T_g values and enthalpic components.

2.4.3.6 Scanning electron microscopy (SEM)

A Hitachi S-900 microscope was used, and samples were sputtered with gold/palladium for 30 s at 40 kV on a Denton DV-502A high vacuum deposition system to provide a conductive coating for analysis. SEM was used to obtain particle size and information about morphology data from the SDDs.

All spray dried dispersions with probucol revealed wrinkled, collapsed sphere morphologies according to SEM, which is indicative of the large surface area of the SDD powders that encapsulate the amorphous drug to aid dissolution and supersaturation maintenance.

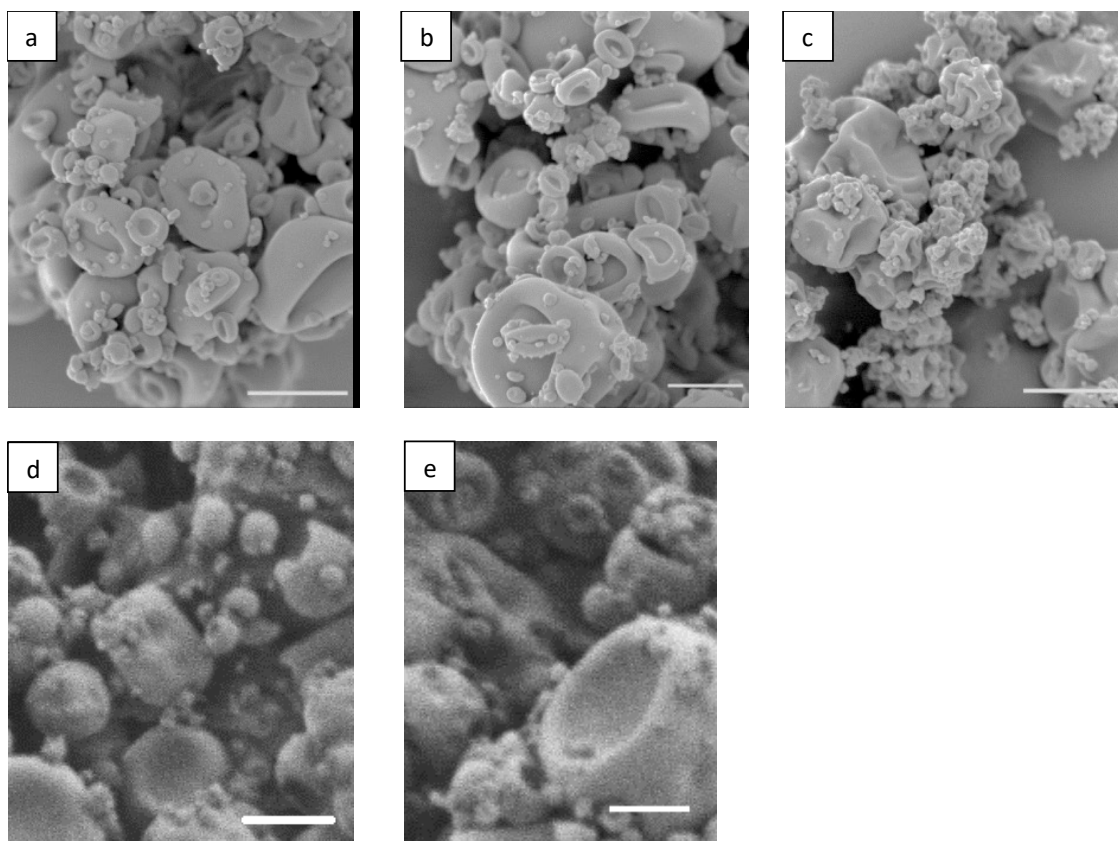


Figure 2.12. SEM images of the SDDs created by spraying a THF:MeOH (15:2) solution of probucol with (a) PEP-b-P(DMA-grad-MAT), (b) PNIPAAm-b-P(DMA-grad-MAT) – 32 kDa, (c) PDEAEMA-b-P(DMA-grad-MAT), (d) PNIPAAm-b-P(DMA-grad-MAT) – 18 kDa, and (e) PNIPAAm-b-P(DMA-grad-MAT) – 48 kDa as the polymer excipients at 25 weight percent of drug loading. The scale bars indicate 1 μm . Copyright © 2017 American Chemical Society.

2.4.3.7 *In-vitro* dissolution test

Dissolution testing was performed on each SDD formulation and the crystalline drug to determine the concentration of drug in the dissolution media and maintenance of supersaturation. The dissolution medium consisted of phosphate buffer saline (82 mM sodium chloride, 20 mM sodium phosphate dibasic, 47 mM potassium phosphate monobasic) supplemented with 0.5 wt% FaSSIF. The medium was adjusted to pH 6.5 with

NaOH. An appropriate amount of SDD or crystalline drug was weighed and added into 2.0 mL microcentrifuge tubes to yield a final total drug concentration of 1000 mg/mL (if all material is fully dissolved). For example: At 10 wt % of drug loading, we took 18.0 mg of SDD consisting of 1.8 mg of drug and 16.2 mg of polymer and diluted the SDD with 1.8 mL of PBS buffer (containing FaSSIF) solution for dissolution testing. All samples were analyzed in duplicate ($n = 2$). The first step in dissolution testing involved vortexing the samples for 1 min in 1.8 mL of PBS+FaSSIF medium and then placing the sample into an isothermal aluminum heating block held at 37°C. At each time point (4, 10, 20, 40, 90, 180, and 360 min), tubes were removed from the heating blocks and centrifuged at 13,000 rpm, 37 °C for 1 min to remove undissolved drug from dissolved drug, and then a 50 μ L aliquot of the supernatant was transferred to an HPLC vial. The samples were again vortexed for 30 s and held at 37 °C until the next time point. The supernatant in the HPLC vials was then diluted with 250 μ L of methanol and analyzed for drug via HPLC.

2.4.3.8 Reverse phase HPLC

Drug concentration in each aliquot was determined by reverse phase HPLC. The HPLC consisted of a reversed-phase EC-C18 column (Poroshell 120, 4.6 \times 50 mm, 2.7 μ m, Agilent, USA). A mobile phase of 96:4 (v/v) acetonitrile:water was used for probucol detection with a flow rate of 1.0 mL/min at 30 °C. A 10 μ L aliquot of sample was injected, and the column effluent was detected at 241 nm with a UV detector (1260 Infinity Multiple Wavelength Detector, Agilent). The probucol concentration in the samples was determined using a calibration curve of 0.1–500 μ g/mL concentrations.

2.5 References

- (67) Gaucher, G.; Satturwar, P.; Jones, M. C.; Furtos, A.; Leroux, J. C. Polymeric Micelles for Oral Drug Delivery. *Eur. J. Pharm. Biopharm.* **2010**, *76* (2), 147–158. <https://doi.org/10.1016/j.ejpb.2010.06.007>.
- (68) Delie, F.; Blanco-Prieto, M. J. Polymeric Particulates to Improve Oral Bioavailability of Peptide Drugs. *Molecules* **2005**, *10* (1), 65–80. <https://doi.org/10.3390/10010065>.
- (69) Shaji, J.; Patole, V. Protein and Peptide Drug Delivery: Oral Approaches. *Indian J. Pharm. Sci.* **2008**, *70* (3), 269. <https://doi.org/10.4103/0250-474X.42967>.
- (70) Hauss, D. J. Oral Lipid-Based Formulations. *Adv. Drug Deliv. Rev.* **2007**, *59* (7), 667–676. <https://doi.org/10.1016/j.addr.2007.05.006>.
- (71) Lipinski, C. A. Drug-like Properties and the Causes of Poor Solubility and Poor Permeability. *J. Pharmacol. Toxicol. Methods* **2000**, *44* (1), 235–249. [https://doi.org/10.1016/S1056-8719\(00\)00107-6](https://doi.org/10.1016/S1056-8719(00)00107-6).
- (72) Paul, S. M.; Mytelka, D. S.; Dunwiddie, C. T.; Persinger, C. C.; Munos, B. H.; Lindborg, S. R.; Schacht, A. L. How to Improve R&D Productivity: The Pharmaceutical Industry's Grand Challenge. *Nat. Rev. Drug Discov.* **2010**, *9* (MARch). <https://doi.org/10.1038/nrd3078>.
- (73) Wilson, M.; Williams, M. A.; Jones, D. S.; Andrews, G. P. Hot-Melt Extrusion Technology and Pharmaceutical Application. *Ther. Deliv.* **2012**, *3* (6), 787–797.
- (74) Paudel, A.; Worku, Z. A.; Meeus, J.; Guns, S.; Van den Mooter, G. Manufacturing of Solid Dispersions of Poorly Water Soluble Drugs by Spray Drying: Formulation and Process Considerations. *Int. J. Pharm.* **2013**, *453* (1), 253–284.

<https://doi.org/10.1016/j.ijpharm.2012.07.015>.

- (75) Loftsson, T.; Vogensen, S. B.; Brewster, M. E.; Konráðsdóttir, F. Effects of Cyclodextrins on Drug Delivery Through Biological Membranes. *J. Pharm. Sci.* **2007**, *96* (10), 2532–2546. <https://doi.org/10.1002/jps.20992>.
- (76) Ormes, J. D.; Zhang, D.; Chen, A. M.; Hou, S.; Krueger, D.; Nelson, T.; Templeton, A. Design of Experiments Utilization to Map the Processing Capabilities of a Micro-Spray Dryer: Particle Design and Throughput Optimization in Support of Drug Discovery. *Pharm. Dev. Technol.* **2013**, *18* (1), 121–129. <https://doi.org/10.3109/10837450.2011.646424>.
- (77) Huang, Y.; Dai, W.-G. Fundamental Aspects of Solid Dispersion Technology for Poorly Soluble Drugs. *Acta Pharm. Sin. B* **2014**, *4* (1), 18–25. <https://doi.org/10.1016/j.apsb.2013.11.001>.
- (78) Ting, J. M.; Tale, S.; Purchel, A. A.; Jones, S. D.; Widanapathirana, L.; Tolstyka, Z. P.; Guo, L.; Guillaudeu, S. J.; Bates, F. S.; Reineke, T. M. High-Throughput Excipient Discovery Enables Oral Delivery of Poorly Soluble Pharmaceuticals. *ACS Cent. Sci.* **2016**, *2* (10), 748–755. <https://doi.org/10.1021/acscentsci.6b00268>.
- (79) Yin, L.; Hillmyer, M. A. Preparation and Performance of Hydroxypropyl Methylcellulose Esters of Substituted Succinates for in Vitro Supersaturation of a Crystalline Hydrophobic Drug. *Mol. Pharm.* **2014**, *11* (1), 175–185. <https://doi.org/10.1021/mp4003656>.
- (80) Mundargi, R. C.; Babu, V. R.; Rangaswamy, V.; Aminabhavi, T. M. Formulation and in Vitro Evaluation of Transdermal Delivery of Zidovudine-An Anti-HIV Drug. *J. Appl. Polym. Sci.* **2011**, *119* (3), 1268–1274. <https://doi.org/10.1002/app.30832>.

- (81) Ting, J. M.; Navale, T. S.; Bates, F. S.; Reineke, T. M. Design of Tunable Multicomponent Polymers as Modular Vehicles To Solubilize Highly Lipophilic Drugs. *Macromolecules* **2014**, *47* (19), 6554–6565. <https://doi.org/10.1021/ma501839s>.
- (82) Yamashita, S.; Matsuzawa, Y. Where Are We with ProbucoL: A New Life for an Old Drug? *Atherosclerosis* **2009**, *207* (1), 16–23. <https://doi.org/10.1016/j.atherosclerosis.2009.04.002>.
- (83) Sizovs, A.; Xue, L.; Tolstyka, Z. P.; Ingle, N. P.; Wu, Y.; Cortez, M.; Reineke, T. M. Poly(Trehalose): Sugar-Coated Nanocomplexes Promote Stabilization and Effective Polyplex-Mediated SiRNA Delivery. *J. Am. Chem. Soc.* **2013**, *135* (41), 15417–15424. <https://doi.org/10.1021/ja404941p>.
- (84) Nasiri, M.; Bertrand, A.; Reineke, T. M.; Hillmyer, M. A. Polymeric Nanocylinders by Combining Block Copolymer Self-Assembly and Nanoskiving. *ACS Appl. Mater. Interfaces* **2014**, *6* (18), 16283–16288. <https://doi.org/10.1021/am504486r>.
- (85) Tale, S. R.; Yin, L.; Reineke, T. M. Trehalose-Functionalized Block Copolymers Form Serum-Stable Micelles. *Polym. Chem.* **2014**, *5* (17), 5160–5168. <https://doi.org/10.1039/C4PY00399C>.
- (86) Qian, F.; Huang, J.; Hussain, M. A. Drug–Polymer Solubility and Miscibility: Stability Consideration and Practical Challenges in Amorphous Solid Dispersion Development. *J. Pharm. Sci.* **2010**, *99* (7), 2941–2947. <https://doi.org/10.1002/jps.22074>.
- (87) Dougherty, D. A. The Cation– π Interaction. *Acc. Chem. Res.* **2013**, *46* (4), 885–893. <https://doi.org/10.1021/ar300265y>.

- (88) U.S. Food & Drug Administration. *Route of Administration*; 2006.
- (89) Huang, Y.; Dai, W.-G. Fundamental Aspects of Solid Dispersion Technology for Poorly Soluble Drugs. *Acta Pharm. Sin. B* **2014**, *4* (1), 18–25.
<https://doi.org/10.1016/j.apsb.2013.11.001>.
- (90) Leuner, C.; Dressman, J. Improving Drug Solubility for Oral Delivery Using Solid Dispersions. *Eur. J. Pharm. Biopharm.* **2000**, *50* (1), 47–60.

Chapter 3

Aggregated Solution State Morphology of Poly(acrylic acid)- Poly(styrene) Block Copolymers Improves Drug Supersaturation Maintenance and Cell Membrane Permeation*

*This manuscript was submitted to *Molecular Pharmaceutics*: Purchel, A.; Boyle, W.; Reineke, T.M. *Mol. Pharm.*, **2019**, xx(xx), xxxx-xxxx.

3.1 introduction

According to the US Food and Drug Administration (FDA), while there are more than one hundred different routes of drug administration,⁸⁸ oral drug delivery is preferred due to its non-invasive mode of administration, which promotes compliance during prolonged therapies. While advances in high-throughput screening have increased the number of new drugs that reach the formulation stage, the approval rate of new drug platforms is disproportionately low due to issues associated with achieving drug solubility and supersaturation maintenance in the gastrointestinal (GI) tract.⁶ Therefore, it is imperative to develop delivery vehicles that can enhance the GI tract solubility and oral bioavailability of lipophilic and/or rapid crystallizing drugs.

The preparation of amorphous solid dispersions, a blend of polymer excipient(s) and active pharmaceutical ingredient (API), has been identified as a method to improve solubility and bioavailability of hydrophobic drugs.^{25,89,90} To prepare SDDs, spray drying, which is scalable and circumvents the thermal degradation of the polymer and drug that may occur during melt extrusion. During spray drying, atomization of a drug/polymer solution yields a polymer matrix in which the drug is stabilized in a thermodynamically unstable amorphous state.⁸⁶ By maintaining a metastable amorphous state via a SDD, drug molecules do not need to overcome the disfavored crystal lattice energetic barrier typically needed to achieve dissolution.^{91,92}

Drugs that are lipophilic or have a high crystal lattice energy can become bottlenecked in the pharmaceutical production pipeline and there are few marketed excipients able to effectively achieve supersaturation via an amorphous SDD. For example, hydroxypropyl methyl cellulose acetate succinate (HPMCAS), a cellulose derivative and

renewable biopolymer, is a currently marketed polymer excipient for SDD. While HPMCAS has been shown to attain burst release of therapeutics with high crystal lattice energies, maintaining supersaturation for GI tract relevant residence times is often problematic.^{16,79,93} Additionally, due to its bulk manufacturing process, HPMCAS is heterogeneous in terms of its chemical composition, making it difficult to discern the mechanism of drug solubilization.

Because the efficacy of a SDD is contingent on drug/polymer matrix interactions and solution state behavior, selection of an appropriate excipient is essential. Thus, fundamental investigations of the mechanism by which polymer matrices mediate drug dissolution are needed so that informed design approaches can be employed to develop the next generation of excipients. Recently, it has been shown that assembly of the polymer excipient into nanoaggregates or micelle-like structures in aqueous solution can aid in drug solubilization maintenance. In 2013, Dalsin et al. showed that a dramatic increase in dissolution performance of probucol and phenytoin, a Biopharmaceutical Classification System (BCS) Class II pharmaceuticals, can be attained by forming polymeric micelle-like structures (50 to 100 nm) in solution prior formulation by spray drying.¹⁷ Additionally, Li et al. demonstrated that the BCS Class II drug phenytoin is partitioned into the micelle corona of a poly(*N*-isopropylacrylamide-*co*-*N,N*-dimethylacrylamide)-*b*-polystyrene (PND-*b*-PS) block copolymer excipient¹⁸ and thus can be stabilized in the amorphous state for longer time periods. Johnson et al. also reported that oligomeric NIPAM-based excipients with a C₁₂-C₁₈ hydrophobic alkyl end group self-assemble into micellar structures and increase the aqueous solubility of phenytoin.¹⁹

Poly(acrylic acid) (PAA), a biocompatible and hydrophilic polymer with multiple hydrogen bonding (H-bonding) sites, has been utilized in numerous biological and pharmaceutical applications.⁹⁴⁻⁹⁶ PAA is of interest in SDDs, as it is commercially available and approved by the FDA for human consumption.⁹⁷ Moreover, PAA is used extensively in drug delivery applications due to its ability to respond to a range of pH environments within the human body (pH = 1-7),⁹⁸ which allows for the preparation of pH-responsive drug carriers.^{97,99} For example, by encapsulating the drug inside a shell-crosslinked PAA-based micelle¹⁰⁰ or inorganic nanoparticles gated by PAA pores,¹⁰¹ controlled release can be achieved upon pH alteration. Eudragit®, a methacrylic acid-based polymer used for enteric coating and colon-targeted drug delivery, also relies on pH responsive properties.¹⁰² Additionally, PAA hydrogels show promise as tunable systems for osmotic-pressure mediated drug release, which is demonstrated by the controlled diffusion of water soluble drugs in or out of PAA polymeric networks.^{47,95,103-105} Furthermore, PAA variants have been used as drug carriers in combination with surfactants that provide further solubility enhancement of challenging formulations.¹⁰⁶

Based on the known role of nanoaggregation in drug supersaturation maintenance and the widespread use of PAA in drug delivery applications, we sought to investigate the role of PS-*b*-PAA-based SDDs in the aqueous dissolution of probucol, a BCS Class II drug. In this study, we were interested in probing the effect that polymer molecular weight and the physical aggregation behavior of the excipient in solution have on *in vitro* drug dissolution. To do so, we synthesized PS-*b*-PAA excipients with various molecular weights and monomer compositions: PS₉₀-*b*-PAA₁₅, PS₉₀-*b*-PAA₈₀, PS₃₈-*b*-PAA₂₂₀, and PS₃₈-*b*-PAA₃₂₀ (degrees of polymerization of each block are included as subscripts). PAA

homopolymers (PAA₂₀, PAA₉₆, PAA₂₂₆, and PAA₃₉₂) were synthesized as controls to probe the role of PAA-molecular weight on solubility enhancement.¹⁰⁷ Based on precedent provided by the Eisenberg group,¹⁰⁸⁻¹¹¹ the synthesized variants allowed us to target specific behaviors, such as polymer solubility, formation of micelles, and pH responsiveness. SDDs formulated with block polymers were spray dried in the presence of both selective (MeOH) and non-selective solvents (MeOH/THF) to produce aggregated and non-aggregated excipient matrices, respectively.

This study reveals that the solution state assembly of the drug-excipient prior to spray drying (pre-formulation aggregation) is induced by solvent selection and PS-*b*-PAA composition, which both play a role in promoting and maintaining supersaturation of probucol. Additionally, this work demonstrates the importance of dissolution pH in modulating drug release from PAA-based excipient platforms, while also showing that permeability through a cellular membrane *in vitro* is not hindered by the nanostructured excipient. Indeed, the ability to control drug dissolution and bioavailability via the physiochemical parameters of SDDs can be extended to a variety of small molecule drugs with solubility and oral bioavailability challenges.

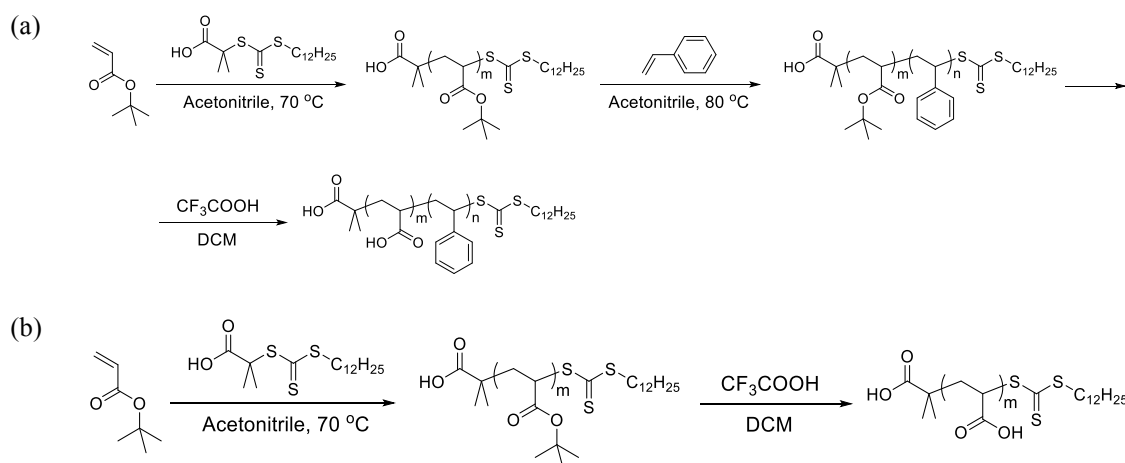
3.2 Results and Discussion

3.2.1 Polymer synthesis

To understand the role of polymer molecular weight, chemical composition, and solution state structure on drug dissolution, four amphiphilic block copolymers and four homopolymers were synthesized. PAA, which has wide application in the biomedical field,¹¹²⁻¹¹⁵ was chosen as the hydrophilic component. PS was selected as the hydrophobic constituent due to its relatively high glass transition temperature, which is important for

formation of stable aggregates that can withstand increased temperatures of spray drying.¹¹⁶ Additionally, both PAA and PS are derived from commercially available monomers and it should be noted that PAA has been FDA approved for human consumption.

First, we assessed the impact of polymer composition, namely polymer block lengths, on drug solubility enhancement. We utilized RAFT polymerization³³ to synthesize eight polymer excipient analogs in a controlled manner (Scheme 1). To study the effect of hydrophilic and hydrophobic block length on drug dissolution, the degree of polymerization of the poly(acrylic acid) and styrene blocks ranged from 15 to 320 and 38 to 90, respectively. These molecular weights allowed us to systematically probe a large variable space in terms of polymer composition and molecular weight, which has been shown to impact drug solubility and maintenance of supersaturation.¹⁰⁷ The chosen design was based on our need to target certain polymer behaviors such as solubility and ability to aggregate at specific concentration (since orally administered formulations have a limited space in how much polymer can be used and at what concentration in the GI tract). Additionally, PAA homopolymer controls were synthesized as excipients that do not exhibit aggregation behavior to clearly elucidate the role of aggregation. *Tert*-butyl-protected acrylic acid was used as the initial monomer for all polymer syntheses, which allowed for facile SEC and NMR characterization of the target block copolymers due to its solubility in a wide variety of organic solvents. After successful polymer characterization by the aforementioned techniques, the *tert*-butyl group was cleaved via hydrolysis with trifluoroacetic acid¹¹⁷ to obtain the target PAA excipients.



Scheme 1. (a) Synthetic scheme for the block copolymers (n , m – degrees of polymerization of acrylic acid and styrene respectively, $n = 90$ or 38 , $m = 15$, 80 , 220 , or 320). (b) Synthetic scheme for the homopolymers (p = degree of polymerization of acrylic acid), where $p = 20$, 96 , 226 , or 392 .

Table 3.1. Polymer Characterization Data.

Polymer	N_p^a	PAA (mol %) ^b	PAA (wt %) ^c	M_n^d	\bar{D}^e	T_g^f (°C)
PS ₉₀ - <i>b</i> -PAA ₁₅	105	10.3	9.8	11	1.05	96
PS ₉₀ - <i>b</i> -PAA ₈₀	170	38.1	28.8	20	1.03	95
PS ₃₈ - <i>b</i> -PAA ₂₂₀	260	80.0	48.8	33	1.17	59
PS ₃₈ - <i>b</i> -PAA ₃₂₀	360	85.4	50.1	46	1.08	60
PAA ₂₀	20	100	100	2.6	1.06	65
PAA ₉₆	90	100	100	12	1.09	68
PAA ₂₂₆	220	100	100	30	1.09	68
PAA ₃₉₂	290	100	100	50	1.10	66

^aDegree of polymerization. ^bMole fraction of PAA in the polymer. ^cWeight fraction of the PAA block. ^dNumber average molecular weight of the polymers as measured on a SEC before polymer deprotection. ^eDispersity as measured on a SEC using THF as the eluent at 30 °C using RI and light scattering detectors. ^fReported as the second heating with a 2.5 °C/min heating rate.

3.2.2 Polymer solution-state properties in organic solvents

PAA homopolymers are soluble in methanol and do not form aggregates in this solvent. All four block copolymers (PS₉₀-*b*-PAA₁₅, PS₉₀-*b*-PAA₈₀, PS₃₈-*b*-PAA₂₂₀, and PS₃₈-*b*-PAA₃₂₀) were screened for solubility and solution-mediated assembly/aggregation in organic solvents suitable for spray drying using dynamic light scattering (DLS) at 1 wt % polymer concentration. Specifically, we selected THF/MeOH (1:1, v/v) and methanol as spray drying solvents due to their ability to promote two disparate physical states of the amorphous solid dispersion: soluble or aggregated, respectively. The non-selective THF/MeOH (1:1, v/v) solvent system dissolves both blocks of the four PS-*b*-PAA polymers homogeneously. Dynamic light scattering analysis (Figure 3.1) shows the range of particle sizes in solution ranged from 1.4 ± 0.5 to 2.2 ± 0.4 nm, which can be attributed to free polymer chains in the solution¹⁷. A visual representation of the prepared polymer solutions is shown in Figure 3.2 (a). In methanol, which selectively dissolves only the PAA block, DLS reveals micelle-like aggregates of the PS-*b*-PAA block polymers. The longest polymer, PS₃₈-*b*-PAA₃₂₀, gives a bimodal size distribution and the hydrodynamic radius of the major particle contributing to the scattering intensity was measured to be 25 ± 1 nm, which is indicative of micelle formation.¹¹⁸ The second mode of the particle size distribution resulted from a hydrodynamic radius of 4.3 ± 0.6 nm, which may be the result

of the single chains of the PAA-*b*-PS, similar to the results of Eisneberg et al.¹¹⁶ Similarly, the PS₃₈-*b*-PAA₂₂₀ polymer, which differs from PS₃₈-*b*-PAA₃₂₀ only in the length of the PAA block, also afforded a bimodal size distribution in methanol. The main contributors to the scattering intensity of the PS₃₈-*b*-PAA₂₂₀ system were particles with a hydrodynamic radius of 13 ± 1 nm while minor contributors were 80 ± 1 nm, which may be attributed to the formation of large compound micelles.¹¹⁶ This type of micelle is common among block copolymers that form glassy cores in solutions at high concentration (more than 0.5 wt%).¹¹⁹ The PS₉₀-*b*-PAA₈₀ polymer also formed well-defined aggregates in methanol solution albeit with a smaller hydrodynamic radius of 6.8 ± 0.7 nm. The R_h of the aggregates formed by PS₉₀-*b*-PAA₂₀, the remaining block polymer, were not able to be accurately measured due to solution turbidity. However, optical turbidity measurements conducted at the same concentration used for DLS analyses (1 wt %) confirmed aggregation of PS₉₀-*b*-PAA₂₀. Overall, aggregates were formed in organic solvent suitable for spray drying at a relatively high concentration of the polymers.

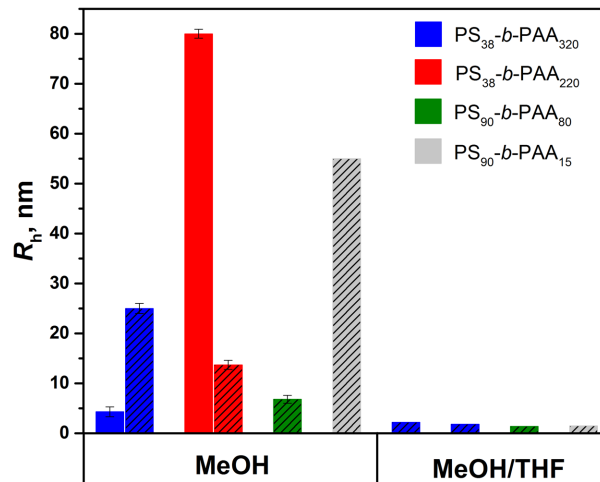


Figure 3.1. Hydrodynamic radii of PS-PAA block copolymers in methanol (selective solvent) or in methanol-THF mixture (1:1, v/v, nonselective solvent). All solutions were composed of 1 wt % polymer in solvent. Hydrodynamic radii were calculated by fitting the correlation functions using either cumulant or double exponential expansions. Linear regressions of Γ vs q^2 were performed for five angles (30° , 45° , 60° , 75° , 90°). Hashed colored bars represent the major contributing (larger particle concentration) hydrodynamic radius in the sample, and solid colored bars represent the lesser contributing second mode. * – poor solubility of this sample did not allow for the determination of a high quality correlation function. Errors bars denote the standard deviation of the linear regression (3 replicates).

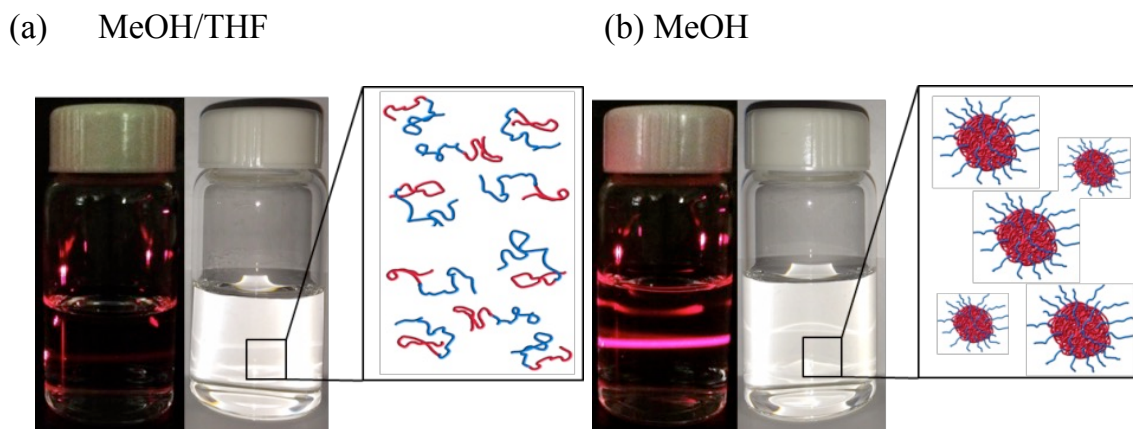


Figure 3.2. (a) Image of a 1 wt % solution of PS₃₈-*b*-PAA₃₂₀ polymer in a methanol-THF mixture (1:1, v/v) showing no laser light scattering indicating a homogeneous solution. The cartoon represents soluble unimers in solution. (b) Image of a 1 wt % solution of PS₃₈-*b*-PAA₃₂₀ polymer in methanol showing scattering of laser light denoting the aggregates. The cartoon represents the aggregation of the polymer chains into micelle-like structures, which leads to close packing of hydrophilic tails and provides a reservoir of binding sites for the drug molecule to promote solubility.

3.2.3 Solid-state properties of the spray dried dispersions

After the polymers were dispersed or dissolved in the respective pure methanol or a THF:methanol solvent systems, probucol was added such that the drug was 25 wt % of the dry component mass. This weight percent was chosen based on previous studies as higher than 10 wt % drug loading percentages are usually desired by the pharmaceutical industry and our previous studies with probucol revealed lower solubility enhancement at 25 wt%.^{82,120} The drug-polymer mixtures were then spray dried and the solid-state properties of each resultant dispersion evaluated using PXRD, MDSC, and SEM. This suite of analytical techniques enabled us to evaluate the homogeneity of the mixture and the

crystallinity of the API in the spray dried dispersion, which is pertinent information for both dissolution performance and shelf life stability.^{41,121,122}

The PXRD, a common tool to determine the presence of a crystalline drug in amorphous solid dispersions showed strong diffraction peaks for unprocessed probucol, which indicates crystallinity (and thus poor solubility).^{77,123} After spray drying probucol with the synthesized polymeric excipients at 25 wt % drug loading in the selective and nonselective solvents, PXRD patterns showed no presence of scattering peaks, which suggests that less than 5% of crystalline probucol was present in the amorphous dispersion (Figure 3.3).

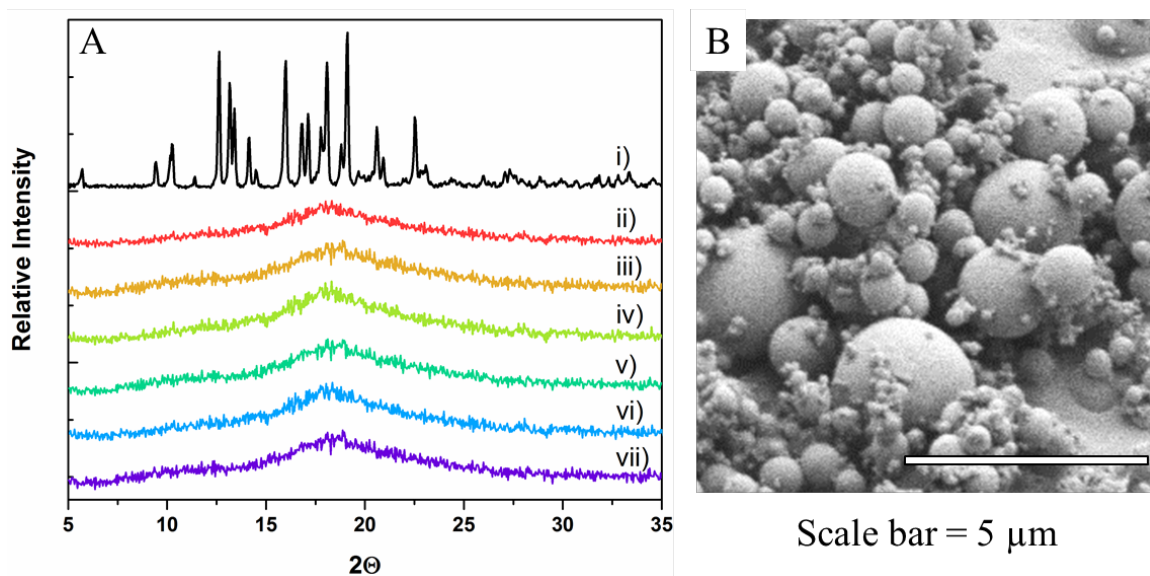


Figure 3.3. PXRD patterns (A) for SDDs with probucol loading of 25 wt % comparing (i) crystalline probucol, (ii) PS₉₀-*b*-PAA₈₀ spray dried from methanol, (iii) PS₉₀-*b*-PAA₈₀ spray dried from THF/MeOH (1:1, v/v), (iv) PS₃₈-*b*-PAA₂₂₀ spray dried from methanol, (v) PS₃₈-*b*-PAA₂₂₀ spray dried from THF/MeOH (1:1, v/v), (vi) PS₃₈-*b*-PAA₃₂₀ spray dried from methanol, (vii) PS₃₈-*b*-PAA₃₂₀ spray dried from THF/MeOH (1:1, v/v) and SEM image (B) of the SDD created by spraying a THF/MeOH (1:1) solution of probucol with PS₃₈-*b*-PAA₃₂₀.

The spray dried dispersions can be visualized via scanning electron microscopy to visualize the morphology of the particles.^{81,19} The particle size affects surface area which, in turn, can influence dissolution performance. As seen in Figure 3.11, all of the spray dried dispersions were made up of spherical particles of heterogeneous size that ranged from 0.1 to 1.0 μm with a consistent morphology across all samples tested. This result is in line with previous studies^{10,124,125} which showed that particle morphology is mainly dependent on conditions that are used for spray drying such as nebulizer temperature and solution flow rate.

3.2.4 Aqueous solution behavior of the spray dried polymer/drug dispersions

To evaluate drug solubility enhancement (and thus crystallization inhibition), we performed dissolution testing in simulated intestinal fluid under non-sink conditions (volume of the solution during dissolution test is lower than the volume of the saturated solution) at the physiological pH of the small intestine (pH = 6.5). In addition, dissolution performance was monitored through a pH transition from 1.2 to 6.5, which mimics the physiological conditions encountered through progression within the GI tract.¹²⁶ The solubilized API concentration, defined as the amount of drug content that remained in solution following centrifugation at 13,000 rpm for one minute, was measured using HPLC. The soluble API content measured during dissolution analyses consisted of dissolved drug including free drug molecules, polymer-drug assemblies, and drug molecules encapsulated inside polymer and bile salt micelles. Figure 3.4 shows dissolution curves for 25 wt % probucol-loaded SDDs at pH=6.5. For the pH transition dissolution test (Figure 3.5), PBS buffer at pH 1.2 was prepared initially and, after 90 minutes of dissolution, 18 μL of 50 wt % NaOH solution was added to increase the sample pH to 7.0.

Poor probucol solubility was initially noted for all block copolymers that were spray dried from the nonselective solvent (THF:methanol), which promotes free polymer chains in solution. This is attributed to the lack of free chain excipient solubility in the dissolution media as well as to the lower exposure of poly(acrylic acid) moieties to aqueous solution, which is discussed below. In contrast, the block copolymer formulations spray dried from methanol (selective solvent that promotes excipient aggregation) showed dramatic enhancement in probucol solubility. As shown in Figures 3.4 and 3.5, in most cases, the homopolymers showed higher solubility enhancement than the analogous block polymer systems with a similar length PAA block). However, one particular block polymer formulation, PS₉₀-*b*-PAA₈₀, which was spray dried from methanol, showed higher solubility enhancement compared to the analogous homopolymer-based SDD (PAA₉₆). We believe this is due to the additive effect of the major parameters of the system that affect drug solubility maintenance. This includes polymer-drug interaction (H-bonding, non-polar interactions, etc.), polymer behavior in the solution (formation of nanoparticles), and polymer solubility in the dissolution media (that can be tailored either by adjusting block length in the block copolymer or tailored hydrophobicity as was shown by Ting et. al.⁴¹

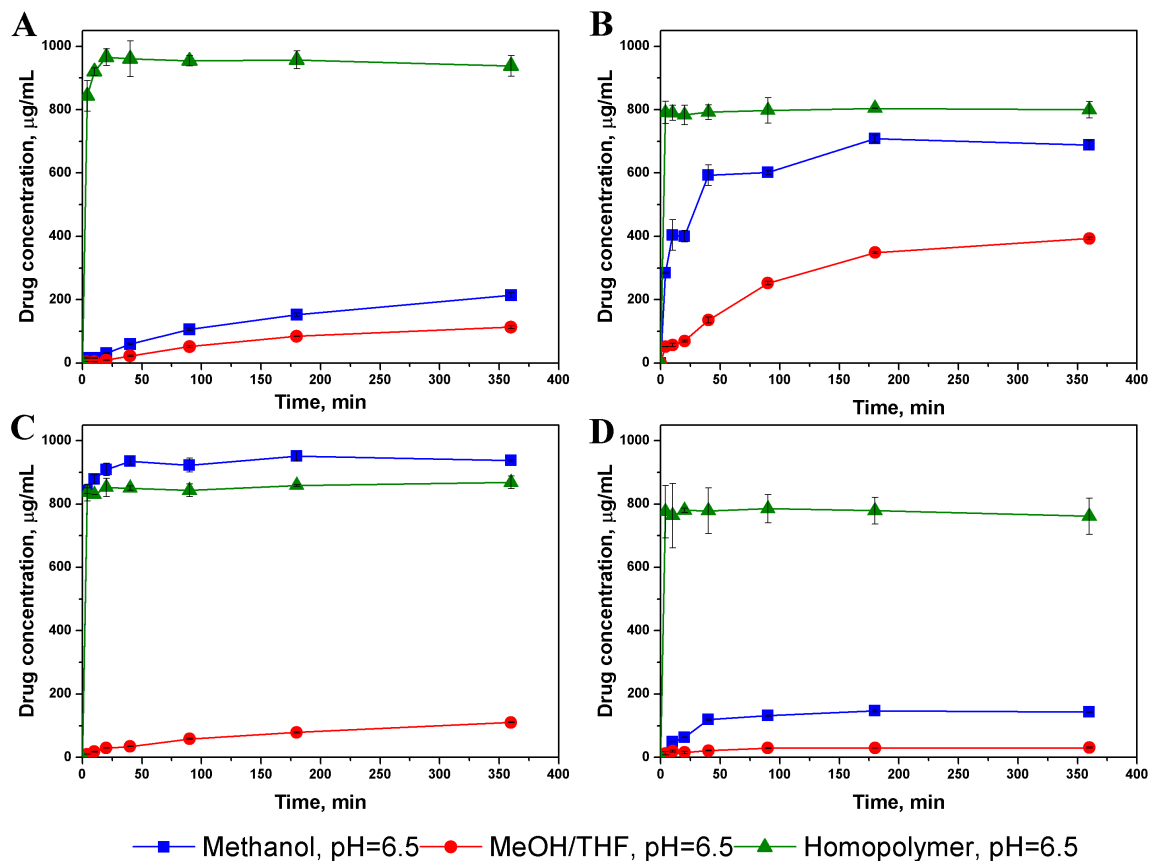


Figure 3.4. Dissolution data at pH=6.5 for the SDDs formed with the block polymers and analogous homopolymer excipients formed at 25 wt % probucol. A) PS₃₈-*b*-PAA₃₂₀ and PAA₃₉₀, B) PS₃₈-*b*-PAA₂₂₀ and PAA₂₂₆, C) PS₉₀-*b*-PAA₈₀ and PAA₉₆, D) PS₉₀-*b*-PAA₁₅ and PAA₂₀. Blue lines denote block copolymers spray dried from MeOH, red lines denote block copolymer spray dried from THF/MeOH, and green lines denote homopolymers spray dried from MeOH. Error bars denote the range of the measured data ($n=2$).

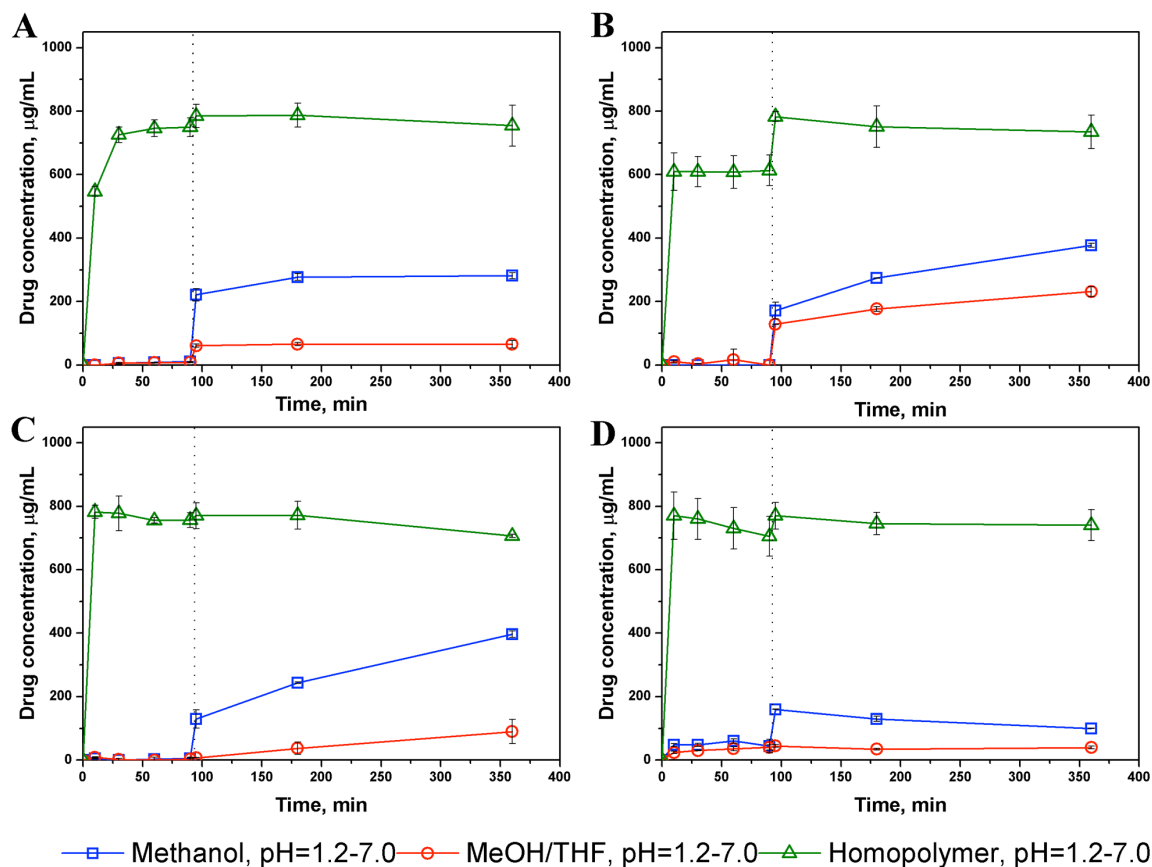


Figure 3.5. Dissolution data when the pH value of the dissolution media is changed from 1.2 to 7.0 (90 minutes time point) for the SDDs formed with the block polymers and analogous homopolymer excipients formed at 25 wt % probucol. A) PS₃₈-*b*-PAA₃₂₀ and PAA₃₉₀, B) PS₃₈-*b*-PAA₂₂₀ and PAA₂₂₆, C) PS₉₀-*b*-PAA₈₀ and PAA₉₆, D) PS₉₀-*b*-PAA₁₅ and PAA₂₀. Blue lines denote block copolymers spray dried from MeOH, red lines denote block copolymer spray dried from THF/MeOH, and green lines denote homopolymers spray dried from MeOH. Error bars denote the range of the measured data ($n=2$).

The pH responsiveness of the PAA-containing block copolymers provides a potential opportunity to control drug release and protection from the caustic environment of the stomach.¹²⁷ When the pH of the dissolution media was acidic (pH=1.2), the drug was not soluble over the initial 90 minutes. After the pH was changed to 7.0, the drug became

more solubilized and maintained supersaturated concentrations for more than four hours. This is crucial for applications where drug solubility in the stomach needs to be minimal. In contrast, the PAA homopolymer excipients are fully soluble in the aqueous dissolution media at both studied pH values. Here, PS₃₈-*b*-PAA₃₂₀ excipient achieves around 200 µg/mL probucol concentration at pH=6.5, but in a more acidic environment (pH=1.2) almost none of the probucol is soluble until pH is increased to 7.0. The analogous homopolymer control allows probucol to achieve 970 µg/mL but does not exhibit such dramatic pH dependence. PS₃₈-*b*-PAA₂₂₀ excipient maintains probucol at 750 µg/mL if spray dried from MeOH and 400 µg/mL if spray dried from THF/MeOH at pH 6.5; and in both cases, a change in probucol solubility was observed for over two orders of magnitude when the pH changes from 1.2 to 7.0. Similar behavior was observed for PS₉₀-*b*-PAA₈₀ and PS₉₀-*b*-PAA₁₅ excipients where a strong pH effect was found on probucol solubility. Overall, excipients that form aggregates in the solution (block copolymers spray dried from MeOH) allow higher probucol solubility compared to block copolymers that were spray dried from MeOH/THF mixture. A dependence of probucol solubility as a function of block copolymer molecular weight was found despite there not being a dramatic correlation to the homopolymer molecular weight.

Interestingly, during the *in vitro* dissolution tests it was noted that some dissolution vials contained more precipitate than others, especially in the dissolution vials that contained PS₃₈-*b*-PAA₃₂₀, PS₃₈-*b*-PAA₂₂₀, PS₉₀-*b*-PAA₈₀, and PS₉₀-*b*-PAA₁₅ SDDs that were spray dried from MeOH/THF as polymer unimers. This effect was attributed to overall polymeric excipient solubility in the dissolution media as it is known that polymer solubility is affected by polymer molecular composition and chain length.⁵ Precipitate was

absent for homopolymer formulations as the poly(acrylic acid) analogs were fully soluble in aqueous media. Block copolymer excipient solubility was determined by recovering as a function of time where content of dissolution vials was freeze-dried and mass of the content was recorded. Because dissolution media is a complex system (PBS buffer, simulated intestinal powder, etc.), blank solutions with no spray dried dispersions were freeze-dried as well, and then the mass difference between dissolution vials (with SDDs and without SDDs) was determined and attributed to the mass of the dissolved polymer. The homopolymers were found to be fully soluble under the dissolution test conditions. This result explains the small variability of probucol solubility when spray dried with PAA homopolymers from 970 $\mu\text{g}/\text{mL}$ for PAA₃₂₀ to 820 $\mu\text{g}/\text{mL}$ for PAA₂₂₀, PAA₉₆, and PAA₂₀. Figure 3.6 shows the general solubility of each block copolymer sample as well as the dissolution test results of the corresponding spray dried dispersions with 25 wt % probucol. This result shows that the higher the solubility of the polymeric excipient (either spray dried from MeOH or THF/MeOH mixture), the higher the concentration of probucol in solution. This result supports the conclusion that drug solubility behavior is predominantly driven by the excipient solubility in the simulated intestinal fluid.

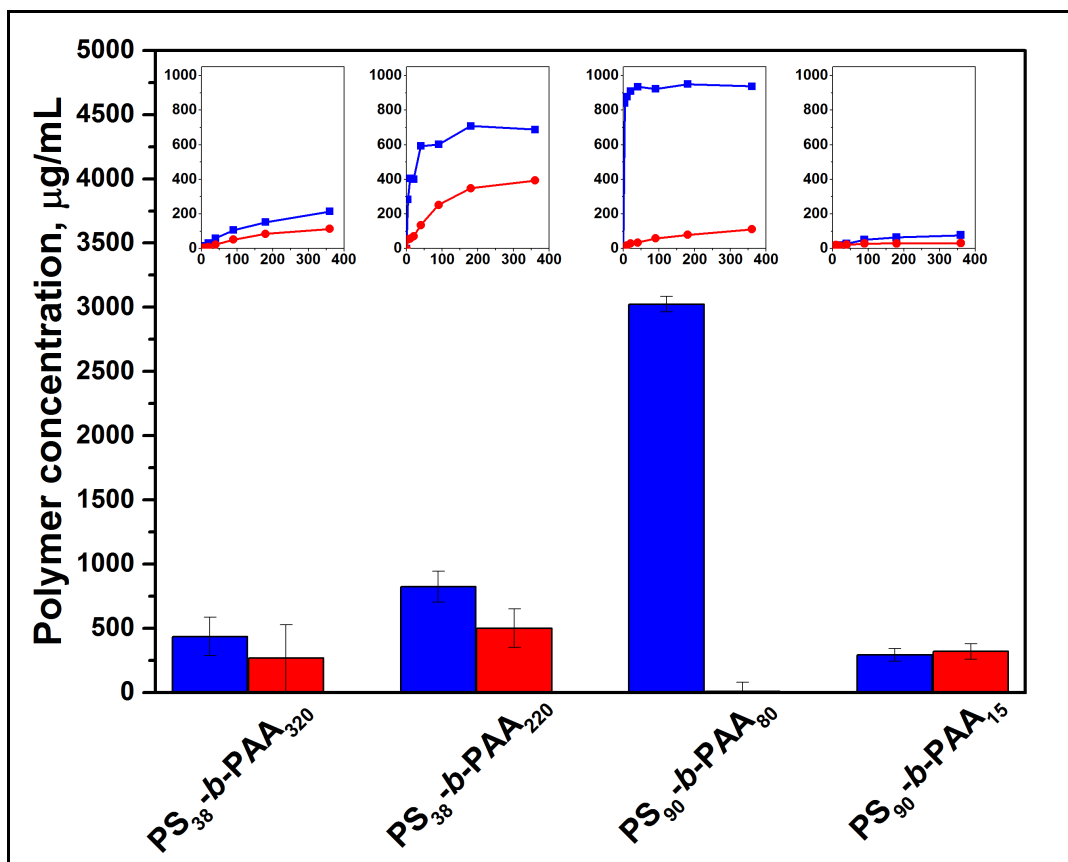


Figure 3.6. Polymer solubility data using SDDs with 25 wt % probucol at pH=6.5 and dissolution profiles (inset plots, y-axis is drug concentration, µg/mL and x-axis is time in minutes) for the same samples (see Figures 3.4 and 3.5) to demonstrate correlation between formulation performance and excipient solubility. Blue bars denote SDDs prepared in methanol (nonselective solvent) and red bars denote SDDs prepared in THF/methanol (selective solvent). Error bars denote the range of the measured data ($n=2$).

3.2.5. *In Vitro* Caco-2 cell assay permeation studies.

In order to relate dissolution performance to the bioavailability of probucol in the prepared spray dried dispersions, an immortalized line of heterogeneous human epithelial colorectal adenocarcinoma cells, Caco-2, was utilized to form a model membrane. When cultured under specific conditions, Caco-2 cells resemble enterocytes, which line the small intestine and are the site at which drug absorption predominantly occurs.⁵⁵ For this study,

Caco-2 permeation assays were performed as described previously, in which drug concentration on both sides of a Caco-2 cell layer was measured.⁶³ Due to the low solubility of probucol in the assay media, pure drug permeation could not be measured, even when a dimethyl sulfoxide (DMSO) co-solvent was added. Thus, only SDDs with probucol and the best performing polymer excipients (PS₉₀-*b*-PAA₈₀ spray dried from both solvents, MeOH and THF/MeOH, and PAA₉₆) were examined for this study. Due to the aforementioned low solubility of probucol in assay media, PAA₉₆ homopolymer was added to the receiving well to ensure that the permeated probucol stayed in solution until it was quantified via HPLC.

In this study, commercially available excipient HPMCAS (AffinisolTM) was used as a control as its effect on probucol solubility was extensively studied previously.^{16,120,128} It should be noted the presence of polymer excipient is not necessarily expected to significantly enhance the permeability of probucol. However, an increase in solubility is expected to lead to a higher permeation coefficient due to more drug available to permeate (or if the drug is bound too tightly to the excipient, it could inhibit permeation). As shown in Table 3.2, the results indicate that the presence of a polymer excipient, which promotes polymer-drug interactions, does not prevent transport of the drug across Caco-2 cultured membranes. Interestingly, the permeation coefficient for the PS₉₀-*b*-PAA₈₀ excipient was found to be $8.4 \cdot 10^6$ cm/sec when the SDD was prepared in MeOH/THF and $2.9 \cdot 10^6$ cm/sec when the SDD was prepared in MeOH, showing that promoting a specific aggregated structure prior to spray drying can have a significant effect on both supersaturation maintenance and permeation. This is particularly attractive for oral drug delivery application because even though H-bonding with excipient enhances drug solubility, it

does not hinder its cellular permeability and thus bioavailability.¹¹² Interestingly, the homopolymer model, PAA₉₆, showed probucol permeation at $1.7 \cdot 10^6$ cm/sec. As a control, a commercially used excipient, HPMCAS, was included in the Caco-2 cell assay as well. HPMCAS has been studied as a control and modeled by our group in several studies.^{41,81,120} Permeability assays also revealed that the polymer excipients do not affect intracellular junctions in the membranes, as indicated by transepithelial electrical resistance (TEER) measurements. Differentiated Caco-2 cells should maintain TEER value in a range of 600-1000 Ohm·cm². Values that are below 400 Ohm·cm² indicate that intracellular tight junctions were compromised and values above 2000 Ohm·cm² are indicative of cell multilayer formation. In a previous study, Bergstrom et al. studied how surfactants can enhance hydrophobic drug solubility and bioavailability. It was found that micellization in solution due to surfactant presence can enhance drug solubility and cell permeability. However, they also demonstrated that surfactants strongly affect intracellular tight junctions in Caco-2 cell membranes as measured by the change in trans-epithelial resistance.¹²⁹ Overall, it was determined that the PAA-containing block copolymer (PS₉₀-*b*-PAA₈₀ spray dried from methanol or MeOH/THF) offers higher performance compared to the HPMCAS or poly(acrylic acid) homopolymer (PAA₉₆).

Table 3.2. Caco-2 cell permeability assay performed using four samples: (1) PAA₉₆ spray dried with 25 wt % probucol, (2) PS₉₀-*b*-PAA₈₀ spray dried from methanol with 25 wt % probucol, (3) PS₉₀-*b*-PAA₈₀ spray dried from THF/MeOH with 25 wt % probucol, and (4) HPMCAS with 25 wt % probucol.

Sample	1	2	3	4
Polymer	PAA ₉₆	PS ₉₀ - <i>b</i> -PAA ₈₀	PS ₉₀ - <i>b</i> -PAA ₈₀	HPMCAS
Probucol loading, wt %	25	25	25	25
Solvent used for spray drying	Methanol	Methanol	THF/MeOH	Methanol
Permeation coefficient (P_{app}), $10^6 \text{ cm}\cdot\text{sec}^{-1}$	1.7	2.9	8.4	2.6
P_{app} standard error	±0.6	±0.5	±0.9	±0.7

3.3 Conclusion

We synthesized eight different polymers for this study, including four block copolymers of polystyrene and PAA of varying block lengths and four PAA homopolymers. These polymers were spray dried with the BCS Class II drug probucol using different solvents that either induced formation of aggregates in block copolymers (methanol, selective towards poly(acrylic acid) block) or suppressed aggregation (MeOH/THF mixture). We observed that block copolymers spray dried from the solution with preformed aggregates have greater probucol solubility enhancement compared to those spray dried with a non-selective solvent with free polymer chains. It is hypothesized

that this behavior is predominantly excipient-driven due to limited polymer solubility in the simulated intestinal fluid. The pH responsiveness of PAA-containing block copolymers allowed for the determination of the efficiency of drug storage and release upon a pH change from acidic (fasted stomach pH, 1.2) to neutral (small intestine pH, 6.5) pH values. Finally, the Caco-2 cell assay was used to determine the drug permeability coefficient of the block copolymer excipient PS₉₀-*b*-PAA₈₀, which was spray dried in a MeOH/THF mixture in the form of a free polymer chain with 25 wt % of probucol. This formulation showed a four-fold increase in drug permeation relative to the commercially available excipients. This is likely due to limited polymer solubility in the dissolution media, which may drive polymer-drug assemblies towards the cellular membrane. Because BCS Class II drug permeability is influenced by a myriad of different factors, we were able to show that by varying different parameters of the polymeric excipient (monomer composition, solution state behavior, etc.) we could achieve superior performance and enhance probucol bioavailability. This study reveals that utilizing preaggregated polymer excipients for formulating drug-containing spray dried dispersions plays an important role in solubilizing and maintaining supersaturated concentration of the active pharmaceutical ingredients while being a simple and controlled platform for oral drug delivery.

3.4 Materials and Methods

3.4.1 Materials

All chemicals were reagent grade and used without further purification unless otherwise noted. All solvents were HPLC or analytical grade. Styrene (99%, ACROS Organics) and *tert*-butyl acrylate (98%, Sigma-Aldrich) were purified by passing them through activated basic alumina (80-200 Mesh, Fisher Scientific) columns. 2,2'-Azobis(2-

methylpropionitrile) (AIBN, 98%, Sigma-Aldrich) was stored in a freezer at $-20\text{ }^{\circ}\text{C}$ and used as received without any further purification. Probucol (PBC), phenytoin (PTN), and danazol (DNZ) were obtained from Sigma-Aldrich (Milwaukee, WI) Acetonitrile (Fisher Scientific) and trifluoroacetic acid (ACROS Organics) were used as received. Fasted simulated intestinal fluid powder (FaSSIF) was purchased from Biorelevant (Surrey, UK). Phosphate buffered saline (PBS) consisted of 82 mM sodium chloride (99%, Fisher Scientific), 20 mM sodium phosphate dibasic heptahydrate (98%, Fisher Scientific), and 47 mM potassium phosphate monobasic (99%, J.T. Baker).

3.4.2 Polymer synthesis

These procedures are presented for one of each type of polymers that were synthesized. See the Supporting Information for specific reaction modifications to achieve different polymer molecular weights.

Poly(tert-butyl acrylate) Macro-chain Transfer Agent (CTA). 2-(Dodecylthiocarbonothioylthio)-2-methylpropionic acid (CTA) (0.246 g, 0.674 mmol), AIBN (0.0172 g, 0.105 mmol), and tert-butyl acrylate (10.0 g, 78.1 mmol) were added into a 50 mL round-bottom flask with acetonitrile, followed by three freeze-vacuum-thaw cycles. The flask was immersed into an oil bath at $70\text{ }^{\circ}\text{C}$ and stirred. After eight hours, the flask was cooled to room temperature and opened to air. The polymer was dissolved in 25 mL of tetrahydrofuran (THF) and precipitated into a methanol/water 1:1 mixture (1 L). The isolated polymer was re-dissolved in THF and precipitated twice more, to afford a yellow viscous product, which was dried in vacuum. Detailed characterization is presented in the supporting information document ($M_n = 12\text{ kg/mol}$, $D = 1.09$, yield = 85%).

Polystyrene-b-Poly(tert-butyl) Acrylate. Styrene (8.00 mL, 54.2 mmol), poly(tert-butyl acrylate) macro-CTA (500. mg, 0.125 mmol), and AIBN (6.56 mg, 0.0400 mmol) were combined in a Schlenk flask. Toluene (10 mL) was then added and mixture was purged with nitrogen gas for one hour while submerged in an ice bath. The reaction solution was placed into a 70 °C oil bath and stirred for 25 hours. The reaction was quenched by exposing to atmosphere, while cooling to room temperature. The crude polymer was concentrated *in vacuo*, dissolved in 20 mL of THF, and precipitated twice into 1 L of methanol/water (1:1, v/v) mixture. The filtered polymer was dried in a vacuum oven, yielding a yellow glassy sample ($M_n = 20$ kg/mol, $D = 1.03$, overall yield = 43%).

Hydrolysis of Polystyrene-b-poly(tert-butyl) Acrylate. Polystyrene-b-poly(tert-butyl) acrylate block copolymer (1.87 g, 0.0621 mmol) was dissolved in 5.5 mL of dichloromethane (DCM) in a 25 mL round-bottom flask equipped with a stir bar. Excess trifluoroacetic acid was then added dropwise (3.10 mL, 18.2 mmol) and the solution stirred for 24 hours at room temperature. The suspension was filtered and the resulting solid dissolved in DMF and dialyzed (ethanol-water mixture (1:1, v/v); then water). The aqueous solution was freeze-dried, yielding a yellow powder (yield = 98%). (polymer characterization results are shown in Table 3.1).

Synthesis of Poly(acrylic acid) Homopolymer. Tert-butyl acrylate (tBuA) (2.00 g, 15.6 mol), AIBN (2.57 mg, 0.0157 mmol), and 2-(Dodecylthiocarbonothioylthio)-2-methylpropionic acid (CTA, 57.1 mg, 0.156 mmol) were added to a 50 mL round-bottom flask and dissolved in dry acetonitrile (15 mL). Following three cycles of freeze-vacuum-thaw, the flask was submerged 70 °C oil bath and stirred. After four hours, the polymerization was terminated by concomitantly opening the reaction to air and cooling to

room temperature. Acetonitrile was removed under reduced pressure and the crude product re-dissolved in THF (5 mL) and precipitated twice into 1 L of methanol/water (1:1, v/v) mixture. The resulting solid was filtered and the solvent removed via vacuum oven, yielding a yellow powder (yield = 90%). (polymer characterization results are shown in Table 3.1).

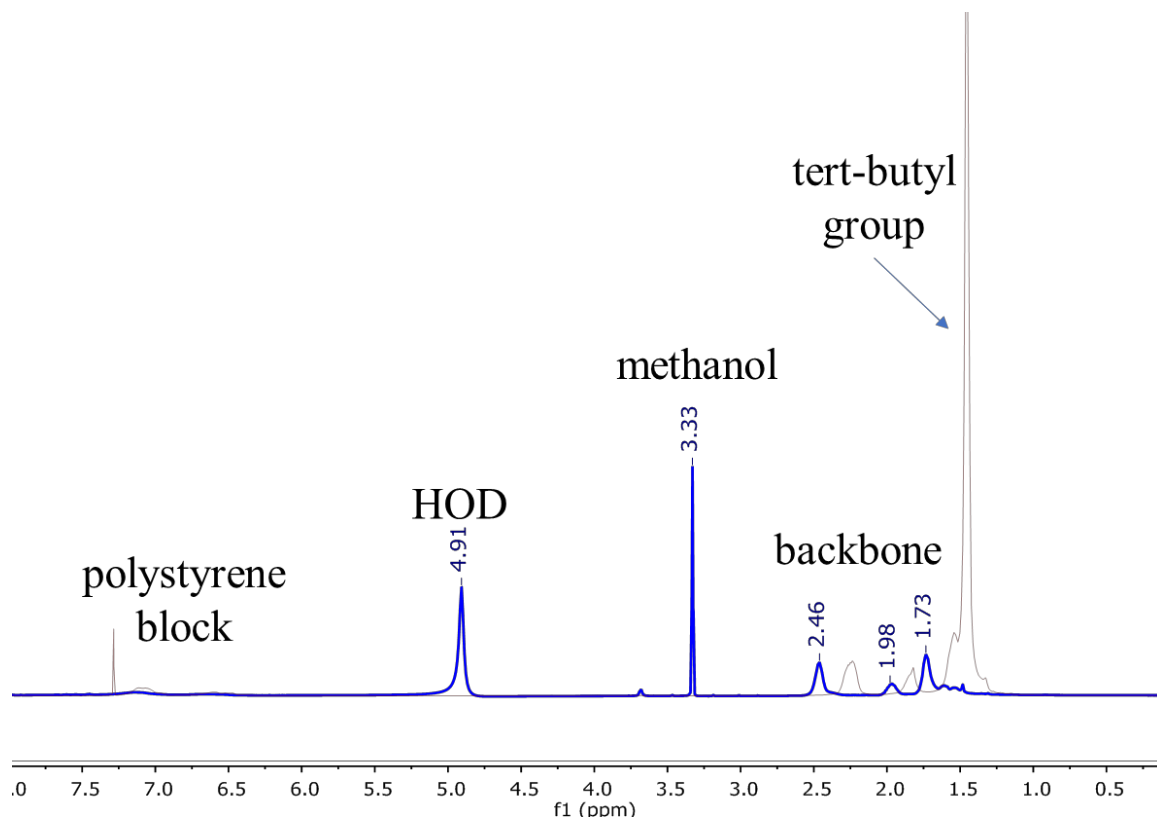


Figure 3.7. NMR spectra of the poly(acrylic acid)-b-polystyrene diblock copolymer before (brown) and after (blue) deprotection with trifluoroacetic acid from poly(tert-butyl acrylate)-b-polystyrene block copolymer. NMR shows complete disappearance of tert-butyl protecting group. NMR was recorded in deuterated methanol.

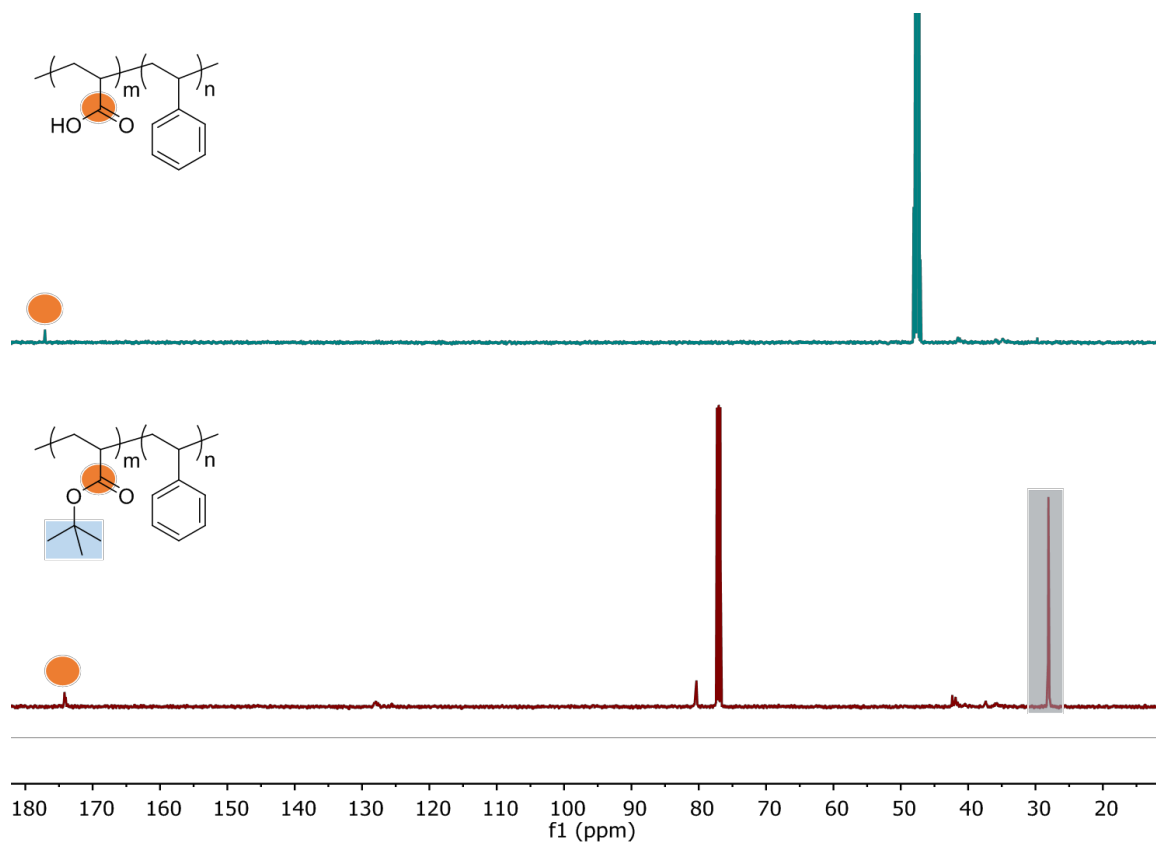


Figure 3.8. ^{13}C -NMR spectra of the poly(acrylic acid)-b-polystyrene diblock copolymer before (bottom) and after (top) deprotection with trifluoroacetic acid from poly(tert-butyl acrylate)-b-polystyrene block copolymer. NMR shows complete disappearance of tert-butyl protecting group as well as a shift in carbonyl carbon peak from 174 to 178 ppm. NMR spectra were recorded in either deuterated chloroform or deuterated methanol.

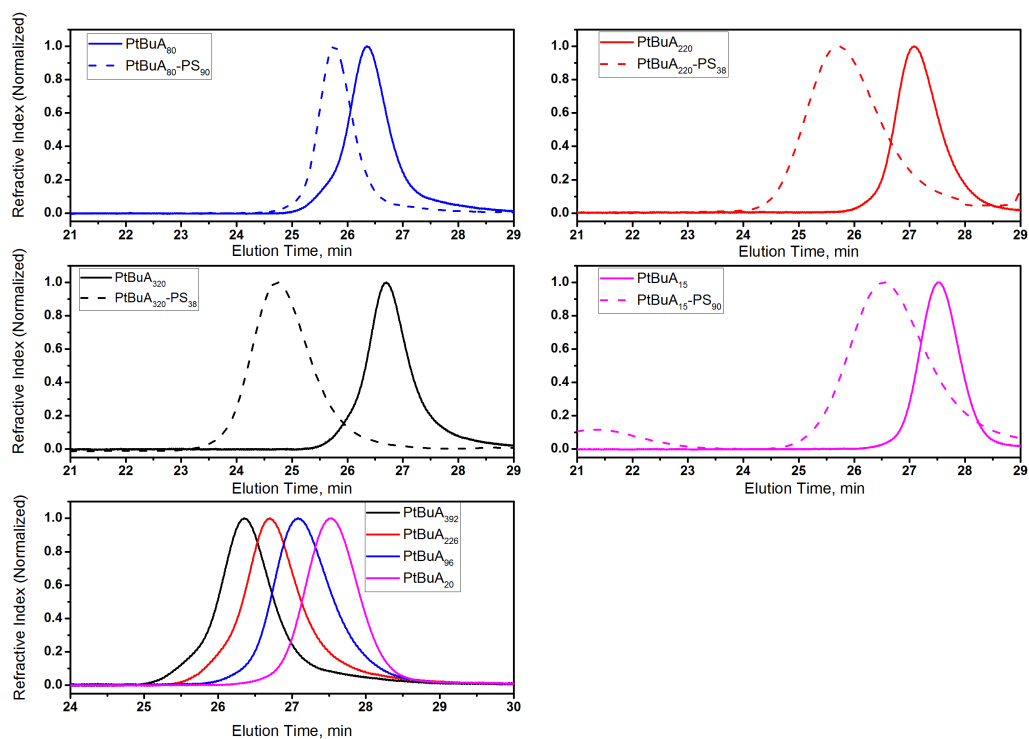
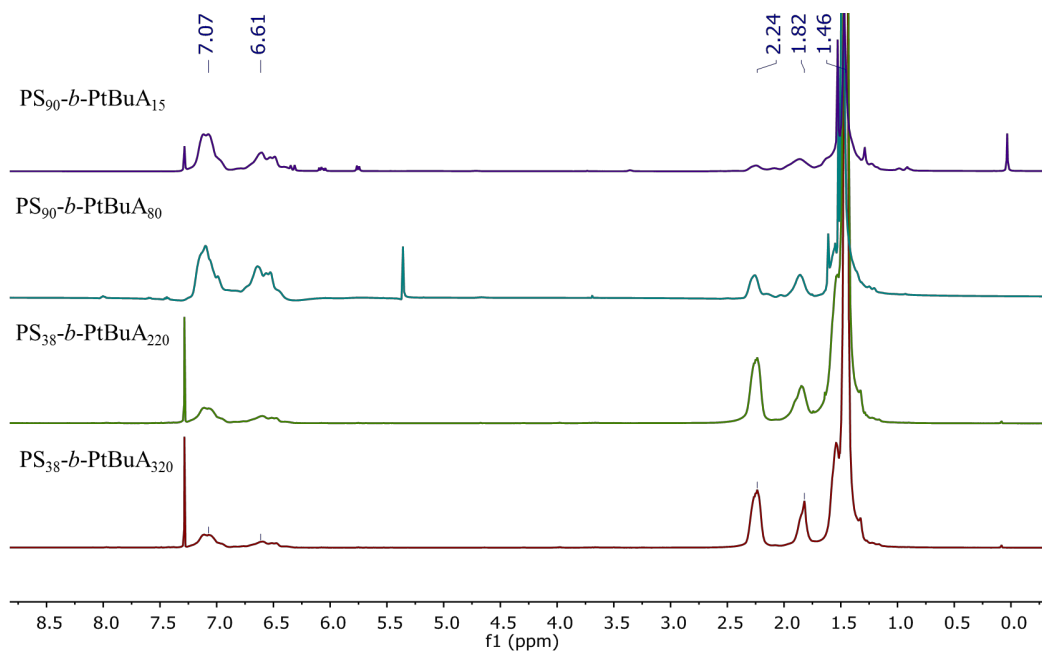


Figure 3.9. NMR spectra (top) and SEC chromatograms (bottom) of the synthesized diblock copolymers and homopolymers. Both techniques were used to determine molecular weight of the diblock copolymers and were in agreement with each other (no more than 10% difference).

3.4.3 Methods

3.4.3.1 ¹H-NMR Spectroscopy

Polymer chemical compositions and molecular weights were determined using ¹H NMR spectroscopy. ¹H NMR spectra were collected using a Bruker Avance III HD 500 spectrometer (equipped with a 5 mm Prodigy TCI cryoprobe with z-axis gradients at 22 °C using a 10 second relaxation delay and at least 16 transients).

3.4.3.2. Size exclusion chromatography (SEC) method

To determine polymer molecular weights and dispersities, SEC experiments were completed on an Agilent 1260 Infinity high performance liquid chromatography instrument equipped with a Waters Styragel guard column and three Waters Styragel columns (HR6, HR4, and HR1) with pore sizes suitable for analysis of materials with number-average molecular weights ranging from 100 to 10,000,000 g/mol. Tetrahydrofuran was used as a mobile phase with a flowrate of 1.0 mL/min at 25 °C. The SEC instrument was connected to a Wyatt Dawn Heleos II multiangle laser light scattering (MALS) detector at a laser wavelength of 663.6 nm (18 angles) and to a Wyatt Optilab T-rEX refractive index detector operating at 658.0 nm. The dn/dc value used for poly(tert-butyl acrylate) polymers was 0.043 mL/g.¹³⁰ The dn/dc for each block copolymers was measured using a Wyatt Optilab T-rEX detector in batch mode.

3.4.3.3 Dynamic light scattering

After solution preparation and dialysis of unimers and aggregates of all block copolymer samples, DLS measurements were collected. For DLS measurements, a Brookhaven Instrument system was used, which contains a mini L-30 laser source ($\lambda = 637$ nm), BI-APD avalanche photodiode detector, and BI-9000AT digital correlator, all aligned

on a BI-200SM goniometer with a decaline thermos regulating bath. For measurements, each polymer was dissolved in either MeOH or a MeOH/THF mixture until a 1 wt % concentration was reached and all samples filtered. Using the second-order scattering intensity correlation function ($g_2(t)$), each sample was measured at five different angles (30° , 60° , 90° , 120° , and 150°) and converted¹⁷ to the first-order correlation function ($g_1(t)$) by applying Siegert relation⁹⁰ $g_2(t) = 1 + |g_1(t)|$.¹³¹ The first-order correlation functions were then fit with the double exponential expansions for samples with bimodal distribution of particle sizes or with cumulant expansions for solutions with aggregates of one size. The translational diffusion coefficient was determined from linear fit for function $\Gamma(q^2)$, which was used to calculate hydrodynamic radii (R_h) of aggregates by applying the Stokes – Einstein relationship.¹³² The results are shown in the Figure 3.1.

3.4.3.4 *Spray drying*

Spray drying was conducted with a Bend Research Mini Spray Dryer (Bend, OR). Polymer and drug solutions (1 wt %) at various drug loading (10 and 25 wt % relative to the dry mass of the polymer) in either MeOH or MeOH/THF mixture (1:1, v/v) were prepared. The solutions were dissolved overnight to ensure drug homogenous distribution and were then transferred to a 20 mL syringe for spray drying under the following conditions: solution feed rate = 0.65 mL/min, inlet temperature = 72 °C, nitrogen flow rate = 12.8 L/min. The prepared spray dried dispersions (SDDs) were collected from a 1.5” Whatman filter paper and stored in a vacuum desiccator at room temperature.

3.4.3.5 *Powder X-ray diffraction (PXRD)*

PXRD characterization was carried out on a Bruker-AXS D5005 diffractometer with copper x-ray source ($KCu\alpha$, $\lambda=1.54 \text{ \AA}$), which operates at a 45 kV voltage and 40 mA

current. Approximately 500 mg of SDD was packed onto a standard glass holder with zero background. Data for each SDD, as well as pure crystalline drugs, were recorded at 2θ angles ranging from 5° to 40° at a scan step = 0.5 s and a step size = $0.02^\circ/\text{s}$. The results are shown in the Figure 3.2.

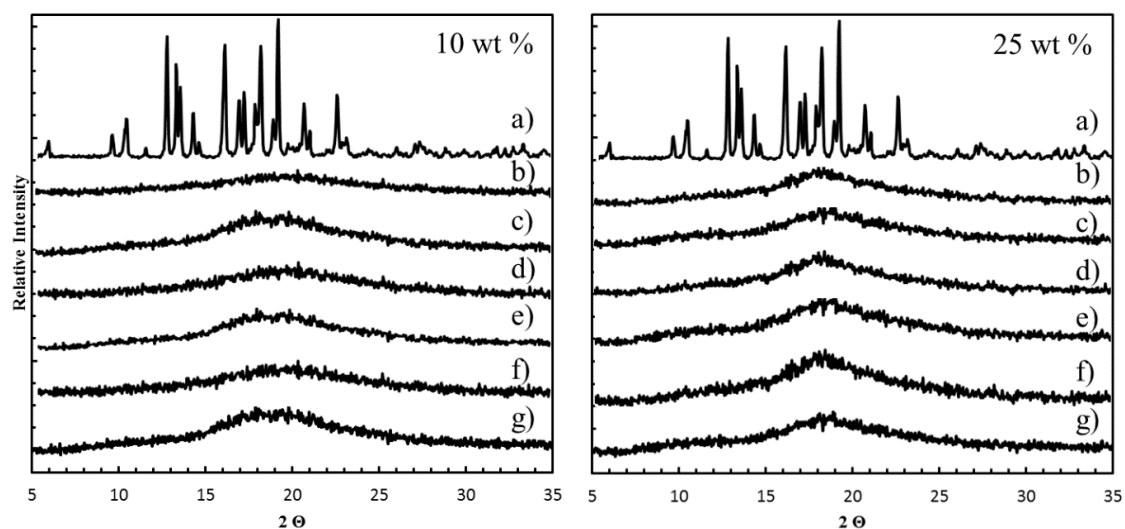


Figure 3.10. PXR D patterns for SDDs with probucol loadings of 10 and 25 wt % comparing (a) crystalline probucol, (b) PS₉₀-*b*-PAA₈₀ spray dried from methanol, (c) PS₉₀-*b*-PAA₈₀ spray dried from THF/MeOH (1:1, v/v), (d) PS₃₈-*b*-PAA₂₂₀ spray dried from methanol, (e) PS₃₈-*b*-PAA₂₂₀ spray dried from THF/MeOH (1:1, v/v), (f) PS₃₈-*b*-PAA₃₂₀ spray dried from methanol, (g) PS₃₈-*b*-PAA₃₂₀ spray dried from THF/MeOH (1:1, v/v).

3.4.3.6 Thermal analysis

To characterize the thermal properties of the SDDs, modulated differential scanning calorimetry (MDSC) equipped with an auto-sampler was utilized. Each sample (2-5 mg) was placed in a T-zero aluminum pan. MDSC analysis was performed at a heating rate of $5^\circ\text{C}/\text{min}$ from -80 to 180°C and the temperature was modulated $\pm 2^\circ\text{C}$ with a period of 40 s. The first heating scans are reported due to subsequent drug crystallization after

reaching its melting temperature. For the polymer only samples, the temperature was not modulated, but ramped from -80 to 180 °C at a rate of 5 °C/min. The second heating scans are reported in the case of the polymer-only samples. For all of the samples, TA TRIOS software was used to determine T_g values and enthalpies of transitions (ΔH). The results are shown in the Table 3.1.

3.4.3.7 Scanning electron microscopy (SEM)

SEM was conducted using a Hitachi S-4700 cold filed emission gun microscope. SDDs were placed on the SEM studs and sputter-coated with gold/palladium alloy for 30 seconds using a Denton DV-502A High Vacuum deposition system at 40 kV. Images were taken at an accelerating voltage of 3.0 kV and 10 μ A current using a backscattering detector with Au-trata modified YAG (yttrium aluminum garnet, cerium doped) crystal. The results are shown in Figure 3.2 and Figure 3.11.

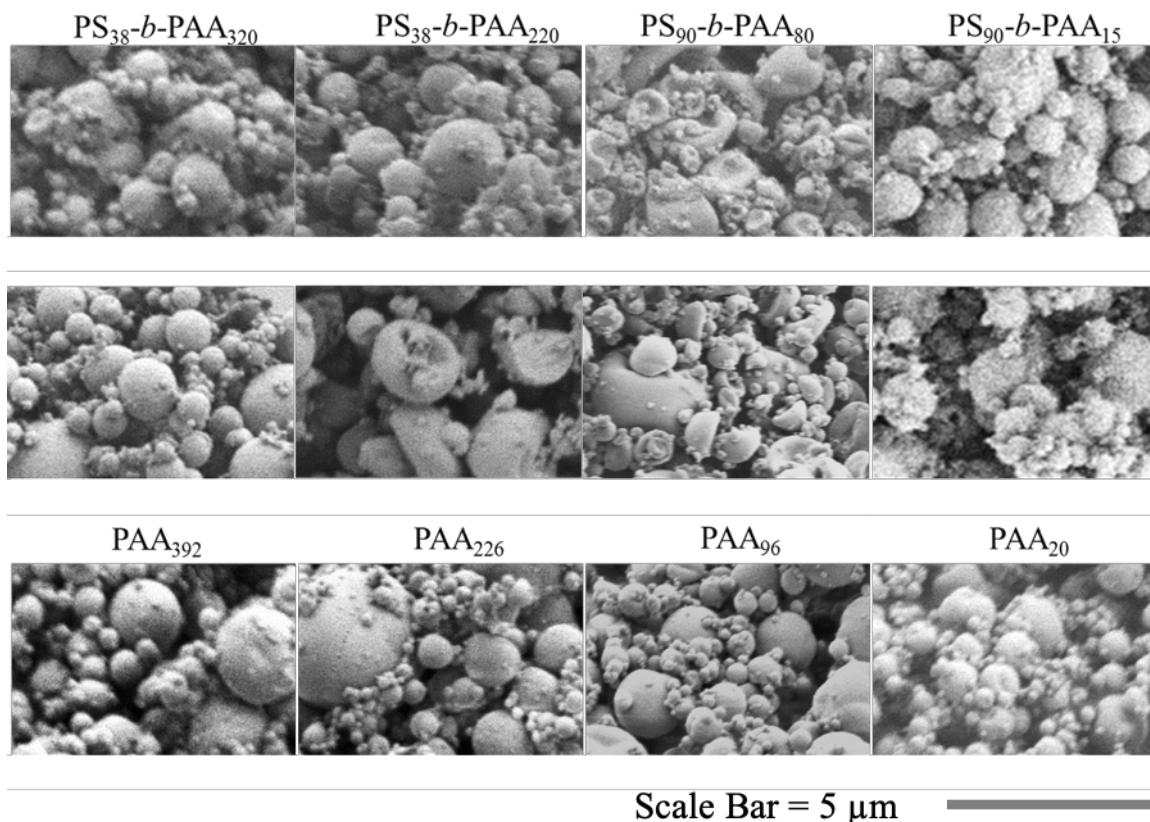


Figure 3.11. SEM images for 25 wt % probucol sprayed with block copolymers from two different solvent systems: (a) MeOH, and (b) THF/MeOH (1:1, v/v). All scale bars are equal to 5 μm

3.4.3.8 *In-vitro* dissolution test

Testing at pH 6.5 (Small Intestinal Environment Model). Dissolution testing media, containing PBS buffer and 0.5 wt % of the FaSSIF powder (3 mM sodium taurocholate, 0.2 mM lecithin, 34.8 mM sodium hydroxide, 68.62 mM sodium chloride and 19.12 mM maleic acid), was prepared. The pH of the dissolution media was 6.5, which matches that of the inside of the fasted small intestine. Dissolution testing was performed on SDDs as well as on pure crystalline drug. Each sample was weighed into a 2.0 mL Teflon microcentrifuge tube. The tests were performed with 1.00 mg/mL drug concentration when

fully dissolved (18 mg for 10 wt % SDD, 7.2 mg for 25 wt % SDD, and 3.6 mg of 50 wt % SDD). The media (1.8 mL) was preheated to 37 °C, added to a vial, and vortexed for 1 min. Samples were transferred into an aluminum heating block and kept at 37 °C. Data points were collected at 4, 10, 20, 90, 180, and 360 min, after which each sample was centrifuged at 13,000 rpm for 1 min to remove all undissolved particles. A 50 µL aliquot was then transferred into an HPLC vial and diluted with 250 µL of methanol. Dissolution vials were then vortexed for 1 min and placed back into the aluminum heating block. Drug concentration was determined via HPLC and the results are shown in Figure 3.4 and Figure 3.5.

Testing at pH 1.2 (Stomach Environment Model). Further dissolution experiments were performed at a pH of 1.2 to match the environment of a fasted stomach. These experiments were conducted using a protocol similar to the analyses at pH = 6.5. However, the initial pH of the PBS buffer was adjusted with hydrochloric acid (HCl) to achieve a pH value of 1.2.¹³³ At time points of 10, 20, 30 and 90 min, dissolution vials were centrifuged at 13,000 rpm for 1 min and a 50 µL aliquot was taken from each vial. These aliquots were then diluted with 250 µL of MeOH and analyzed via HPLC. The parent dissolution samples were then vortexed for 1 min and placed back into the aluminum heating block. After the 90 min data point was taken (approximate time of the drug residence in stomach¹³⁴), 18 µL of sodium hydroxide solution (50 %, w/w) was added to the dissolution media to return the pH to 6.5. The vials were then vortexed for 1 min, placed into the aluminum heating block for 3 min, centrifuged for 1 min, and 50 µL of the solution was transferred into the HPLC vial and diluted with 250 µL of methanol. Additional sample data points were collected at 180 and 360 min. The results are shown in the Table 3.1.

3.4.3.9 Reverse phase HPLC

Drug concentrations were determined by HPLC after supersaturation, in vitro dissolution testing, and Caco-2 permeability cell assay (*vide infra*). A diluted supersaturation, dissolution or Caco-2 permeability cell assay aliquot (10 μ L) in methanol was injected into an Agilent 1100 HPLC system equipped with a reversed-phase XDB-C18 column (Eclipse, 4.6 \times 150 mm, 5.0 μ , Agilent) connected to a diode array UV-Vis detector (1100 DAD, Agilent) at a wavelength of 254 nm. The eluent, consisting of an acetonitrile/water mixture (96/4 % v/v for probucol), was passed through the column at 1.0 mL/min and 30 °C. Each drug (10 μ L) in acetonitrile was injected onto the column and its concentration determined from the measured elution chromatogram via a linear calibration curve that was separately determined for each respective drug. The area under the dissolution curve (AUC_{360 min}) from 0 to 360 minutes was calculated for each dissolution plot.

3.4.3.10 In-vitro drug transport

Caco-2 Cell Culture. Immortalized Caco-2 cells were obtained from Sigma Aldrich (St. Luis, MO). All cells were passaged between 35 to 41 times prior to use in the drug permeation studies. Cells were cultured in 75 cm² flasks obtained from Corning (Cambridge, MA). After cultivation, cells were resuspended in Dulbecco's modified Eagle's medium (DMEM) at a concentration of 0.6 \times 10⁶ cells/mL and seeded on cell support filters pre-wetted with ~ 0.1 mL medium in 12-well cell culture clusters. Cells were seeded at densities of 2.6 \times 10⁵ cells/cm² by dispensing 0.5 mL of the resuspended cell solution on each filter. A basolateral chamber was filled with 1.5 mL DMEM solution. The plate support was incubated at 37 °C and 10% CO₂ for 6 hours. After incubation, the apical

medium was removed and replaced with 0.5 mL of fresh media to remove non-adherent cells. Cells were maintained every two days by aspirating medium from the basolateral side and then from apical side of all filters of the plate followed by addition of fresh DMEM medium. This was repeated for 28 days, by which point the cells differentiated with respect to expression of transport proteins and brush border hydrolases. Cells for permeation studies were grown in Transwell cell culture chambers (Sigma-Aldrich, St. Louis, MO, 24 mm diameter, 3.0 μm pore size, 4.71 cm^2 growth area). The integrity of the tight junction between the cells was evaluated by using mannitol as a paracellular marker and by measuring transepithelial electrical resistance (TER). For donor solutions, three spray dried dispersions were used: PS₉₀-b-PAA₈₀ with 25 wt % probucol, HPMCAS with 25 wt % probucol, and PAA₉₆ with 25 wt % probucol. Phosphate buffer (10 mL) solution was mixed with ~ 2 mg of spray dried dispersions to achieve approximately 100 μM drug concentration and the resulting solution was incubated at 37 $^\circ\text{C}$. Filter supports were washed with phosphate buffer solution and transferred to a new 12-well cluster containing Hank's buffered salt solution (HBSS, 1.5 mL per well) followed by addition of HBSS (0.5 mL) to the apical side. Filters were incubated for 20 minutes at 37 $^\circ\text{C}$ and TER values measured for each cluster.

In vitro Drug Permeation Studies. Transport experiments were performed between day 24 and 28 post-cell seeding (300,000 cells per well) as described by Hubatsch et al.⁶³ Drug permeation from apical to basolateral sites was measured in Hank's balanced salt solution (HBSS) buffer and in the presence of 1.8 mg/mL PAA in the receiving chamber. Initial solutions of SDDs in HBSS buffer contained ~ 100 μM drug concentration. SDD solutions (600 μL) were placed in donor wells and 100 μL aliquots taken at the beginning

and at the end of the assay; additionally, six aliquots of 600 μL were withdrawn from the receiving well every ten minutes. All drug concentrations were determined using HPLC. Mannitol permeability was evaluated after the completion of the Caco-2 cell assay and it remained unchanged before performing the assay and following the procedure for the drug transport experiment.

The apparent permeability coefficient (P_{app} , cm/s) was determined by measuring the amount of drug transported across the membrane as a function of time and was calculated according to the following equation (1):

$$P_{\text{app}} = (dQ/dt)(1/(AC_0)), \quad (1)$$

In Equation 1, dQ/dt is the steady-state flux of the drug ($\mu\text{mol/s}$), A is the surface area of the membrane (cm^2), and C_0 is the concentration in the donor chamber (μM).

Time points were collected every ten minutes to ensure sink conditions, in which the concentration in the basolateral site did not exceed 10% of the drug concentration in the apical site. A sample P_{app} calculation is shown in the Supporting Information.

3.5 References

- (91) Marsac, P. J.; Konno, H.; Taylor, L. S. A Comparison of the Physical Stability of Amorphous Felodipine and Nifedipine Systems. *Pharm. Res.* **2006**, *23* (10), 2306–2316. <https://doi.org/10.1007/s11095-006-9047-9>.
- (92) Liu, H.; Taylor, L. S.; Edgar, K. J. The Role of Polymers in Oral Bioavailability Enhancement; a Review. *Polymer (Guildf)*. **2015**, *77* (Supplement C), 399–415. <https://doi.org/10.1016/j.polymer.2015.09.026>.
- (93) Tanno, F.; Nishiyama, Y.; Kokubo, H.; Obara, S. Evaluation of Hypromellose Acetate Succinate (HPMCAS) as a Carrier in Solid Dispersions. *Drug Dev. Ind.*

- Pharm.* **2004**, *30* (1), 9–17. <https://doi.org/10.1081/DDC-120027506>.
- (94) Shah, P. N.; Lin, L. Y.; Smolen, J. A.; Tagaev, J. A.; Gunsten, S. P.; Han, D. S.; Heo, G. S.; Li, Y.; Zhang, F.; Zhang, S.; et al. In Vivo Efficacy of Shell Cross-Linked Nanoparticle Formulations Carrying Silver Antimicrobials as Aerosolized Therapeutics. **2013**, 4977–4987.
- (95) He, X.; Fan, J.; Zhang, F.; Li, R.; Pollack, K. a.; Raymond, J. E.; Zou, J.; Wooley, K. L. Multi-Responsive Hydrogels Derived from the Self-Assembly of Tethered Allyl-Functionalized Racemic Oligopeptides. *J. Mater. Chem. B* **2014**, *2* (46), 8123–8130. <https://doi.org/10.1039/C4TB00909F>.
- (96) Azzam, T.; Eisenberg, A.; Nedev, H.; Rosenberg, L.; Maysinger, D. Biomaterials Block-Copolymer Micelles as Carriers of Cell Signaling Modulators for the Inhibition of JNK in Human Islets of Langerhans. *Biomaterials* **2009**, *30* (21), 3597–3604. <https://doi.org/10.1016/j.biomaterials.2009.03.028>.
- (97) Liu, J.; Huang, Y.; Kumar, A.; Tan, A.; Jin, S.; Mozhi, A.; Liang, X.-J. PH-Sensitive Nano-Systems for Drug Delivery in Cancer Therapy. *Biotechnol. Adv.* **2014**, *32* (4), 693–710. <https://doi.org/10.1016/j.biotechadv.2013.11.009>.
- (98) Zheng, L.; Chai, Y.; Liu, Y.; Zhang, P. Controlled RAFT Synthesis of Polystyrene-*b*-Poly (Acrylic Acid) - *b* -Polystyrene Block Copolymers and Their Self-Assembly in an Ionic Liquid [BMIM] [PF6]. **2011**, No. 039, 1–8.
- (99) Surnar, B.; Jayakannan, M. Stimuli-Responsive Poly(Caprolactone) Vesicles for Dual Drug Delivery under the Gastrointestinal Tract. *Biomacromolecules* **2013**, *14* (12), 4377–4387. <https://doi.org/10.1021/bm401323x>.
- (100) Zhang, K.; Fang, H.; Wang, Z.; Li, Z.; Taylor, J.-S. a; Wooley, K. L. Structure-

- Activity Relationships of Cationic Shell-Crosslinked Knedel-like Nanoparticles: Shell Composition and Transfection Efficiency/Cytotoxicity. *Biomaterials* **2010**, *31* (7), 1805–1813. <https://doi.org/10.1016/j.biomaterials.2009.10.033>.
- (101) Tian, B.; Liu, S.; Wu, S.; Lu, W.; Wang, D.; Jin, L.; Hu, B.; Li, K.; Wang, Z.; Quan, Z. PH-Responsive Poly (Acrylic Acid)-Gated Mesoporous Silica and Its Application in Oral Colon Targeted Drug Delivery for Doxorubicin. *Colloids Surfaces B Biointerfaces* **2017**, *154*, 287–296. <https://doi.org/10.1016/j.colsurfb.2017.03.024>.
- (102) Thakral, S.; Thakral, N. K.; Majumdar, D. K. Eudragit®: A Technology Evaluation. *Expert Opin. Drug Deliv.* **2013**, *10* (1), 131–149. <https://doi.org/10.1517/17425247.2013.736962>.
- (103) Zhang, F.; Elsabahy, M.; Zhang, S.; Lin, L. Y.; Zou, J.; Wooley, K. L. Shell Crosslinked Knedel-like Nanoparticles for Delivery of Cisplatin: Effects of Crosslinking. *Nanoscale* **2013**, *5* (8), 3220–3225. <https://doi.org/10.1039/c3nr34320k>.
- (104) Campbell, M. L.; Waite, B. a. The Ka Values of Water and the Hydronium Ion for Comparison with Other Acids. *J. Chem. Educ.* **1990**, *67* (5), 386. <https://doi.org/10.1021/ed067p386>.
- (105) Ferrero, C.; Massuelle, D.; Jeannerat, D.; Doelker, E. Towards Elucidation of the Drug Release Mechanism from Compressed Hydrophilic Matrices Made of Cellulose Ethers. I. Pulse-Field-Gradient Spin-Echo NMR Study of Sodium Salicylate Diffusivity in Swollen Hydrogels with Respect to Polymer Matrix Physical Stru. *J. Control. Release* **2008**, *128* (1), 71–79. <https://doi.org/10.1016/j.jconrel.2008.02.006>.

- (106) Knöös, P.; Svensson, A. V.; Ulvenlund, S.; Wahlgren, M. Release of a Poorly Soluble Drug from Hydrophobically Modified Poly (Acrylic Acid) in Simulated Intestinal Fluids. *PLoS One* **2015**, *10* (10), e0140709. <https://doi.org/10.1371/journal.pone.0140709>.
- (107) Barreiro-Iglesias, R.; Bromberg, L.; Temchenko, M.; Hatton, T. A.; Alvarez-Lorenzo, C.; Concheiro, A. Pluronic-g-Poly(Acrylic Acid) Copolymers as Novel Excipients for Site Specific, Sustained Release Tablets. *Eur. J. Pharm. Sci.* **2005**, *26* (5), 374–385. <https://doi.org/10.1016/j.ejps.2005.07.014>.
- (108) Khougaz, K.; Zhong, X. F.; Eisenberg, A. Aggregation and Critical Micelle Concentrations of Polystyrene -b- Poly (Sodium Acrylate) and Polystyrene -b- Poly (Acrylic Acid) Micelles in Organic Media. *Macromolecules* **1996**, *29* (9), 3937–3949.
- (109) Shen, H.; Eisenberg, A. Morphological Phase Diagram for a Ternary System of Block Copolymer PS 310 - b -PAA 52 / Dioxane / H₂O. **1999**, 9473–9487.
- (110) Burke, S. E.; Eisenberg, A. Kinetics and Mechanisms of the Sphere-to-Rod and Rod-to-Sphere Transitions in the Ternary System PS 310 - b -PAA 52 /Dioxane/Water. *Langmuir* **2001**, *17* (21), 6705–6714. <https://doi.org/10.1021/la010640v>.
- (111) Ma, L.; Eisenberg, A. Relationship between Wall Thickness and Size in Block Copolymer Vesicles. *Langmuir* **2009**, *25* (24), 13730–13736. <https://doi.org/10.1021/la9012729>.
- (112) Rambharose, S.; Ojewole, E.; Mackraj, I.; Govender, T. Comparative Buccal Permeability Enhancement of Didanosine and Tenofovir by Potential Multifunctional Polymeric Excipients and Their Effects on Porcine Buccal

- Histology. *Pharm. Dev. Technol.* **2014**, *19* (1), 82–90.
<https://doi.org/10.3109/10837450.2012.752505>.
- (113) Lo, Y.-L.; Hsu, C.-Y.; Lin, H.-R. PH-and Thermo-Sensitive Pluronic/Poly(Acrylic Acid) in Situ Hydrogels for Sustained Release of an Anticancer Drug. *J. Drug Target.* **2013**, *21* (1), 54–66. <https://doi.org/10.3109/1061186X.2012.725406>.
- (114) Kadajji, V. G.; Betageri, G. V. Water Soluble Polymers for Pharmaceutical Applications. *Polymers (Basel)*. **2011**, *3* (4), 1972–2009.
<https://doi.org/10.3390/polym3041972>.
- (115) Tian, Y.; Tam, K. C.; Hatton, T. A.; Bromberg, L. Titration Microcalorimetry Study : Interaction of Drug and Ionic Microgel System.
- (116) Mai, Y.; Eisenberg, A. Self-Assembly of Block Copolymers. *Chem. Soc. Rev.* **2012**, *41* (18), 5969–5985. <https://doi.org/10.1039/c2cs35115c>.
- (117) Ma, Q.; Wooley, K. L. The Preparation of T-butyl Acrylate, Methyl Acrylate, and Styrene Block Copolymers by Atom Transfer Radical Polymerization: Precursors to Amphiphilic and Hydrophilic Block Copolymers and Conversion to Complex Nanostructured Materials. *J. Polym. Sci. Part A Polym. Chem.* **2000**, *38* (S1), 4805–4820.
[https://doi.org/10.1002/1099-0518\(200012\)38:1+<4805::AID-POLA180>3.3.CO;2-F](https://doi.org/10.1002/1099-0518(200012)38:1+<4805::AID-POLA180>3.3.CO;2-F).
- (118) Liu, X.; Wu, J.; Kim, J.-S.; Eisenberg, A. Self-Assembly of Mixtures of Block Copolymers of Poly(Styrene-b-Acrylic Acid) with Random Copolymers of Poly(Styrene-Co-Methacrylic Acid). *Langmuir* **2006**, *22* (1), 419–424.
<https://doi.org/10.1021/la0519610>.
- (119) Laaser, J. E.; Jiang, Y.; Sprouse, D.; Reineke, T. M.; Lodge, T. P. PH- and Ionic-

- Strength-Induced Contraction of Polybasic Micelles in Buffered Aqueous Solutions. *Macromolecules* **2015**, *48* (8), 2677–2685. <https://doi.org/10.1021/acs.macromol.5b00360>.
- (120) Ting, J. M.; Navale, T. S.; Jones, S. D.; Bates, F. S.; Reineke, T. M. Deconstructing HPMCAS: Excipient Design to Tailor Polymer-Drug Interactions for Oral Drug Delivery. *ACS Biomater. Sci. Eng.* **2015**, *1* (10), 978–990. <https://doi.org/10.1021/acsbiomaterials.5b00234>.
- (121) Taylor, L. S.; Zografi, G. Spectroscopic Characterization of Interactions between PVP and Indomethacin in Amorphous Molecular Dispersions. *Pharm. Res.* **1997**, *14* (12), 1691–1698.
- (122) Newman, A.; Engers, D.; Bates, S.; Ivanisevic, I.; Kelly, R. C.; Zografi, G. Characterization of Amorphous API:Polymer Mixtures Using X-Ray Powder Diffraction. *J. Pharm. Sci.* **2008**, *97* (11), 4840–4856. <https://doi.org/10.1002/jps.21352>.
- (123) Ilevbare, G. A.; Xu, W.; John, C. T.; D. Ormes, J.; Kuiper, J. L.; Templeton, A. C.; Bak, A. Solubility and Dissolution Considerations for Amorphous Solid Dispersions. In *Pharmaceutical Sciences Encyclopedia*; John Wiley & Sons, Inc.: Hoboken, NJ, USA, 2015; pp 1–41. <https://doi.org/10.1002/9780470571224.pse527>.
- (124) Friesen, D. T.; Shanker, R.; Crew, M.; Smithey, D. T.; Curatolo, W. J.; Nightingale, J. A. S. Hydroxypropyl Methylcellulose Acetate Succinate-Based Spray-Dried Dispersions: An Overview. *Mol. Pharm.* **2008**, *5* (6), 1003–1019. <https://doi.org/10.1021/mp8000793>.

- (125) Vehring, R. Pharmaceutical Particle Engineering via Spray Drying. *Pharm. Res.* **2008**, *25* (5), 999–1022. <https://doi.org/10.1007/s11095-007-9475-1>.
- (126) Kimura, T.; Higaki, K. Gastrointestinal Transit and Drug Absorption. *Biol. Pharm. Bull.* **2002**, *25* (2), 149–164.
- (127) Erah, P. The Stability of Amoxicillin, Clarithromycin and Metronidazole in Gastric Juice: Relevance to the Treatment of Helicobacter Pylori Infection. *J. Antimicrob. Chemother.* **1997**, *39* (1), 5–12. <https://doi.org/10.1093/jac/39.1.5>.
- (128) Ricarte, R. G.; Li, Z.; Johnson, L. M.; Ting, J. M.; Reineke, T. M.; Bates, F. S.; Hillmyer, M. A.; Lodge, T. P. Direct Observation of Nanostructures during Aqueous Dissolution of Polymer/Drug Particles. *Macromolecules* **2017**, *50* (8), 3143–3152. <https://doi.org/10.1021/acs.macromol.7b00372>.

Chapter 4

Star Architectures of Polymeric Excipients and Their Effect on Drug Supersaturation Maintenance

4.1 introduction

Star polymers represent a class of macromolecules where linear polymer 'arms' radiate from a central branching point (core). This type of structure can be further classified based on number of arms, their chemical composition, distribution around the core, core chemical makeup and molecular nature.¹³⁵ The key examples of the star architectures include block copolymer, crosslinked-core, miktoarm, and end-functionalized star polymers as shown in Figure 4.1.¹³⁶⁻¹³⁹

Star polymers have been explored previously in the realm of drug delivery.^{140,141} They possess a distinct advantage as drug delivery agents as they provide multiple functionalities with controlled composition within one molecule. For instance, star polymers have been used to encapsulate poorly water-soluble drugs such as nimodipine and achieve higher efficacy in prevention and treatment of delayed ischemic neurological disorders.¹⁴² In this work, authors used A₂B type miktoarm star polymer (see Figure 4.1) made of polyethylene glycol and polycaprolactone that could assemble into spherical micelles. Drug nimodipine was loaded into the micelles at a feed weight ratio of 5.0 %. Aqueous solubility of the drug increased ~200 fold via micelle encapsulation and in vitro release from micelles occurred at much slower rate than from its solution. Additionally, star polymers can be used as a way to increase molecular weight of the polymer where it leads to increased efficacy without sacrificing polymer solubility which tends to happen to high M_w polymers. In the case of doxorubicin delivery, poly(N-(2-hydroxypropyl)methacrylamide) (pHPMA) was attached via dithiol bonds to the NH₂-terminated dendrimer by Etrych et al. Some of the pendant hydroxypropyl groups were replaced with hydrazide groups in order to conjugate the drug via hydrazone linkage using

drug's carboxyl group. Star-shaped pHPMA – doxorubicin assembly has shown enhanced accumulation in tumors especially when higher molecular weight stars are used to formulate polymer-drug conjugates.¹⁴³ Additionally, the conjugates showed improved tumor accumulation and superior antitumor activity compared to the linear pHPMA-doxorubicin conjugates. This was due to higher molar mass (which allowed lots of drug molecules being conjugated onto one polymer) and higher solubility of the star polymer. Zhang et al.¹³⁹ investigated novel cyclodextrin-containing star polymers that were synthesized by atom transfer radical polymerization (ATRP) using the arm-first approach. A crosslinked core was produced via copolymerization of a mixture of mono- and multi-methacrylate substituted cyclodextrins and 2-(dimethylamino) ethyl methacrylate initiated by a poly(ethylene glycol) macroinitiator. Cyclodextrins that are distributed along the star polymer arms can interact with the hydrophobic drugs and form guest-host complexes that lead to stars self-assembly into nanostructures. Using these type of delivery vehicles authors showed that preformed nanoparticles could release their payload in response to a pH change.¹⁴⁴ In summary, star polymers represent a type of interesting macromolecule due to their high molecular weight, good solubility and low viscosity comparable to linear or branched polymers with relatively low molecular weight.

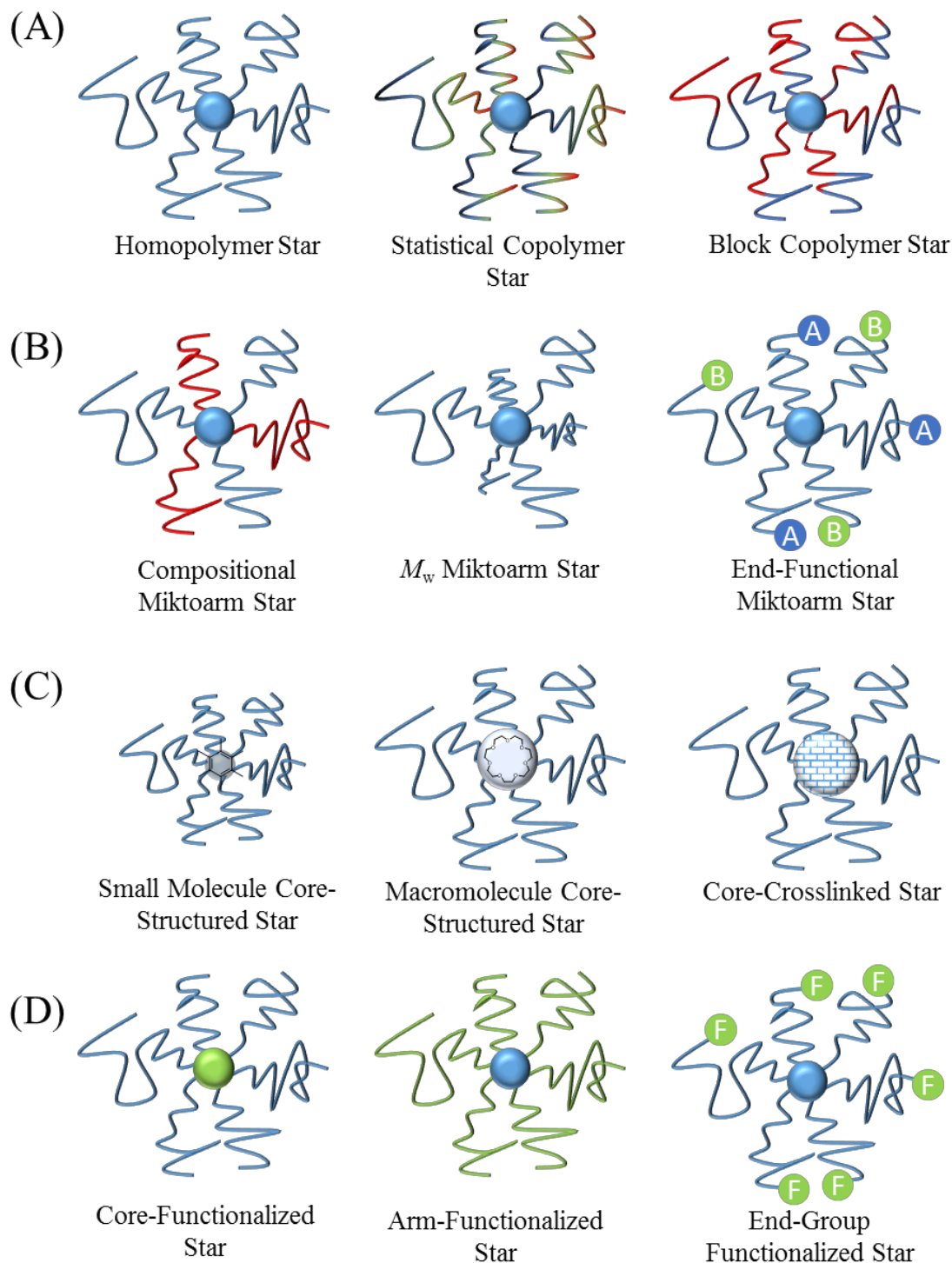


Figure 4.1. Illustration of various types of star polymers classified by (A) composition and sequence distribution of the arm polymer, (B) difference in arm species, (C) core structure, and (D) functional placement. Adapted from reference¹⁴⁵.

Star-shaped architectures are achieved via controlled polymerization techniques and three main strategies are used: core-first, arm-first, and grafting-to.¹⁴⁵ In the core-first approach star polymer arms are grown divergently from a pre-synthesized multifunctional core. For the synthesis of well-defined structures, the initiation efficiency and reactivity of the core functional groups should be equivalent.¹⁴⁶ Additionally, the rate of polymerization initiation should be much higher than the propagation and almost no termination events should occur. This is typically achieved via controlled/living polymerization techniques such that star polymers with a high level of control over functionality, structure, and composition are obtained.¹⁴⁷ The biggest advantage of this method is that the reactions are high yield and relatively facile purification since star polymers can be easily isolated from the crude monomer mixture. However, the major limitation of this approach is that a relatively low number of arms (3-8) can be achieved when compared to the number of arms that is commonly present in the stars prepared via arm-first route. Additionally, arms of these star polymers cannot be directly characterized and require the use of indirect techniques such as end-group analysis or cleaving the polymer structures from the core and measuring molecular weight.¹⁴⁸

Alternatively, arm-first star polymers can be formed by crosslinking or reacting linear polymers together in a convergent fashion around a central core. This convergent approach is usually completed by free radical or some other coupling chemistry.^{149,150} For instance, Gao et al. utilized diacrylate in ATRP polymerization to create highly-crosslinked core functionalized with Br groups as a result of ATRP polymerization. Then, monoacrylates can be added to grow 'arms' and form star polymers. Li and coworkers optimized the arm-first approach¹⁵² and were able to prepare 3, 6, and 12-arm star polymers

using copper (I)-catalyzed azide-alkyne cycloaddition reaction and clicking poly(caprolactone) arms onto alkynylated dendrimer core. One of the main advantages of this approach is that star-star intermolecular coupling is minimized compared to the core-first approach.¹⁵¹

With the grafting to approach, researchers achieve the highest structural control over each component of the star polymer because arms and core are prepared separately and can be thoroughly characterized. Then, arms are attached to the core using a variety of coupling reactions. Haddleton and coworkers¹⁵² utilized this approach to achieve star polymers of high structural complexity, using a core with two sets of functional groups. By functionalizing six cyclodextrin OH groups with thiols, two orthogonal functionalities were created for thiol-ene click and for ring opening polymerizations. Also, as it was shown by Bender et al.¹⁵³, large metal cations can be used to form star polymers. Authors prepared mikto-arm star polymers using europium chloride (EuCl_3) as a core and PLA as one type of arms and bipyridine-functionalized poly(ϵ -caprolactone) as another arm. This polymer showed unique phase behavior where it formed nanoscale assemblies with labile block junctions.

Herein, the synthesis of six well-defined star polymers using RAFT polymerization and a core-first approach is presented. Multi-substituted benzenes are used as cores and multi-functional CTAs are obtained via Steglich esterification. With this approach, the trithiocarbonate functionality of the RAFT CTA remains at the periphery of the star polymer after the polymerization. This allows potential inflexibility of end-group modification and provides an additional characterization tool – NMR end-group analysis.

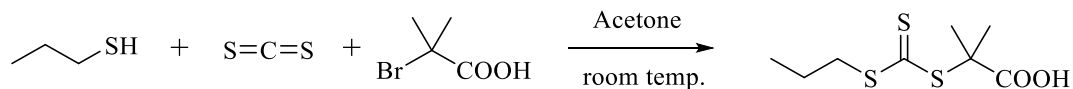
Star polymer potential application in the solubilization of poorly water-soluble will be discussed.

4.2 Results and Discussion

4.2.1 Synthesis of the chain transfer agent

It was shown previously that high drug solubility is achieved when excipient provides H-bonding sites and forms aggregates in the solution.^{17,18,40,78,120} Branched polymers like star polymers can provide a reservoir for the drug in the solution without the need of having a hydrophobic chain end in order to induce polymer aggregation. Thus, we hypothesize that star polymers may allow higher drug loadings and longer stability of the drug in the amorphous state due to their tunability and controlled polymer segregation around the central core. In order to prepare star polymers, RAFT polymerization was used with the core-first approach, where the R-group of the CTA was attached to the core. This allowed precise control of the number of arms per each star polymer. A trithiocarbonate CTA was used due to its hydrolytic stability which will be necessary for further polymer deprotection. Additionally, a C₃ R-group was chosen instead of a more commonly used C₁₂ group for decreased hydrophobicity and to promote aqueous solubility of the final polymers in water. A one-pot synthetic procedure for the CTA is shown in the Scheme 4.1. The final product has a carboxylic acid functionality that will be used for coupling to di-, tri-, and tetrahydroxy-substituted benzenes for formation of the core structures. The NMR spectrum shown in the Figure 4.2 shows the presence of the functional groups at 1.03 ppm and at 3.29 ppm that can be used for end-group analysis of the final star polymers. The procedure was adapted from the reference.¹⁵² Tert-butyl acrylate was used as a monomer

due to its solubility in organic solvents and a possibility to deprotect it under mild conditions to form the desired poly(acrylic acid) (PAA) arms.



Scheme 4.1. Reaction scheme for the CTA synthesis.

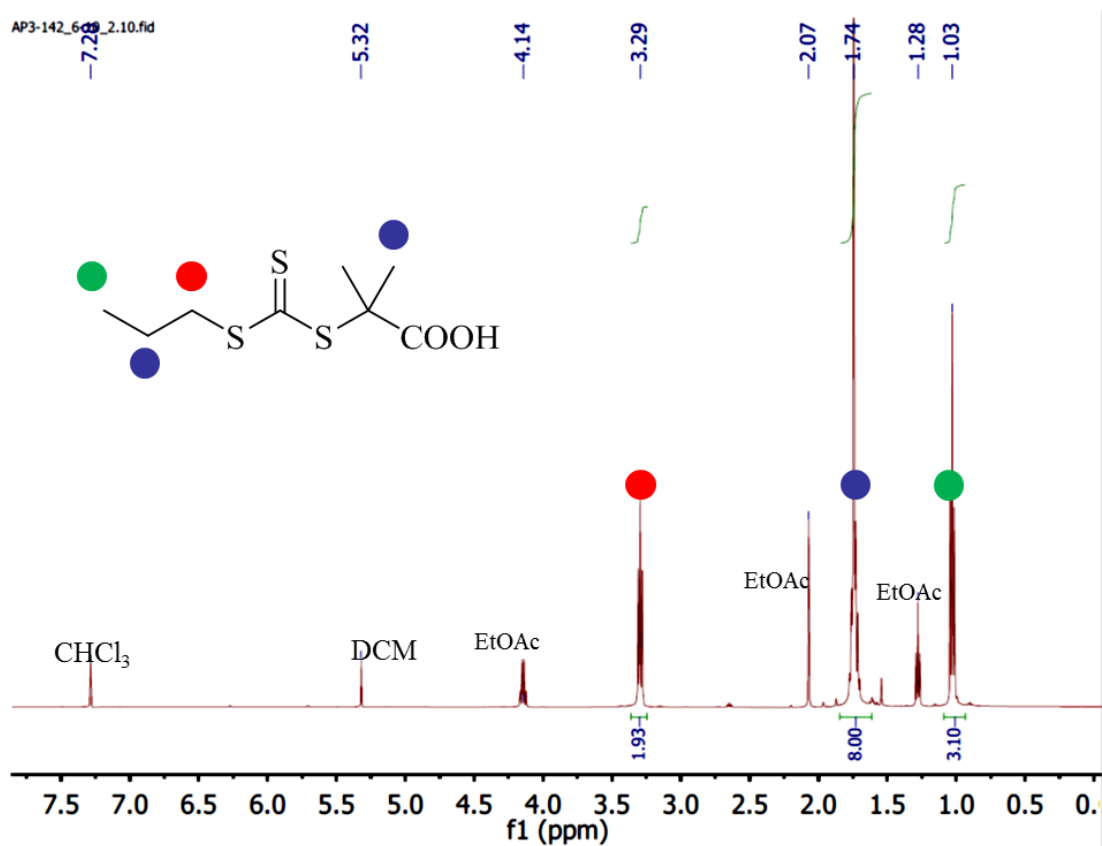


Figure 4.2. ¹H NMR spectrum of the 2-methyl-2-(((propylthio)carbonothioyl)thio)propanoic acid recorded in CDCl₃.

Monitoring of the polymerization kinetics was conducted with tert-butyl acrylate using variable temperature NMR. Thus, efficiency of the new CTA agents was evaluated,

and the results are shown in Figure 4.3. The kinetics experiment indicate that the reaction follows first-order kinetics (with the linear fit $R^2 = 0.998$) and confirms the RAFT mechanism of the *tert*-butyl acrylate polymerization.

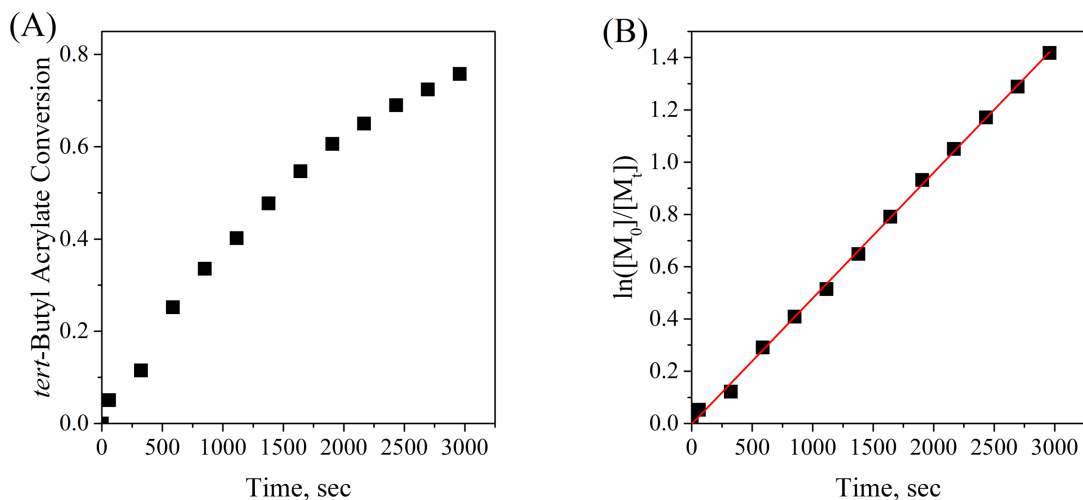


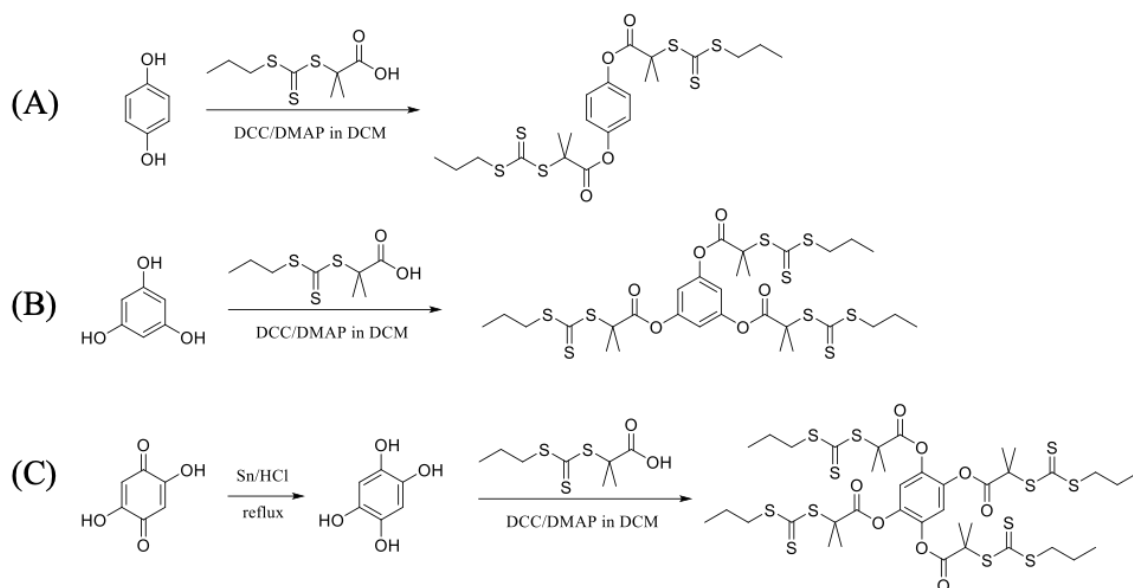
Figure 4.3. (A) Monomer conversion as a function of time, recorded using variable temperature NMR. Alpha-vinyl hydrogen on the monomer was used for the concentration determination. (B) Plot of the natural logarithm of the inverse instantaneous monomer concentration as a function of time to confirm the first order kinetics law. Reaction conducted in CD_3CN , 400 MHz.

After the starting CTA was synthesized and its reactivity was tested, carboxyl end-group was coupled via DCC coupling (Steglich esterification¹⁵³) to the hydroxy-substituted benzenes to form multi-functional CTAs for star polymer synthesis.

4.2.2 Synthesis of the multi-functional CTAs

To synthesize the star polymers, three multi-functional chain transfer agents were synthesized using *N,N'*-dicyclohexylcarbodiimide (DCC) coupling reactions with 1,4-dihydroxybenzene, 1,3,5-trihydroxy benzene, and 1,2,4,5-tetrahydroxy benzene. Multi-

substituted benzenes act as the cores structures for the star polymers. This approach was chosen to keep all polymer end-groups the same (i.e. benzene core in the center and the C₃ end-group at the periphery of the stars) as it was shown previously that end-group functionality affects drug dissolution.¹⁹ Scheme 4.2 shows the synthesis of the multifunctional CTAs used in this study. It is important to note that 1,2,4,5-tetrahydroxybenzene is not commercially available due to its air sensitivity and thus, had to be prepared from 2,5-dyhydroxy benzoquinone.



Scheme 4.2. Synthetic schemes for (A) di-functional CTA, (B) tri-functional CTA, and (C) tetra-functional CTA synthesis using coupling reactions. These CTAs structures allow consistency with the core and end-groups and are not sterically hindered to prevent RAFT polymerization of the tert-butyl acrylate monomer.

For a typical reaction, a hydroxy-substituted benzene was reacted with the 2-methyl-2-((propylthio)carbonothioyl)thio) propanoic acid for 24 hours and the final product was purified by column chromatography. Yields for the multi-functional CTA

syntheses were relatively low (20-37 %) likely due to low nucleophilicity of the hydroxy-group attached to the aromatic benzene ring.¹⁵⁴

A typical NMR spectrum of the tri-functional CTA is shown in the Figure 4.4. The phenyl CH group was found at 6.82 ppm, thionyl CH₂ group at 3.33 ppm, and methyl group at 1.04 ppm and these resonances were used for the end-group analysis as well as the means for confirming the number of arms in each star polymer.

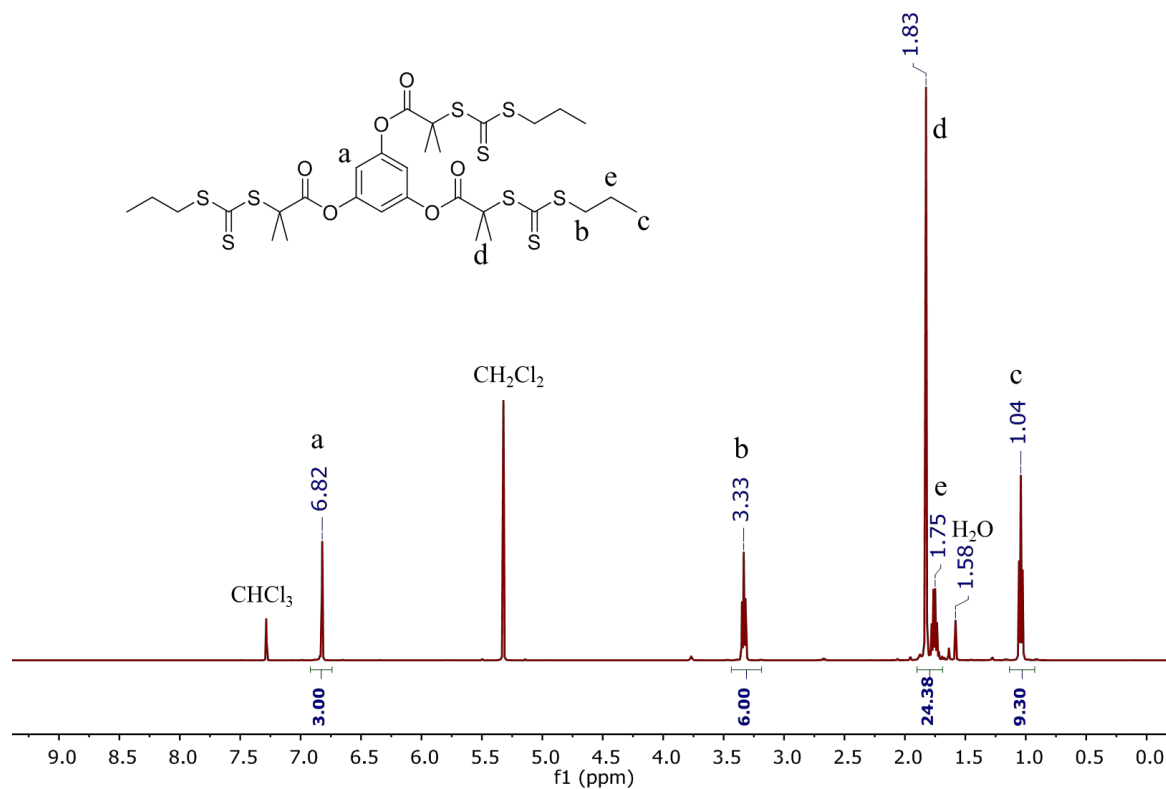


Figure 4.4. ¹H-NMR spectrum of the tri-functional CTA in CDCl₃.

4.2.3 Synthesis of the star polymers

All of the star polymers were synthesized using a tert-butyl acrylate monomer. This allowed synthesis of the poly(tert-butyl acrylate) stars that are well-soluble in most organic solvents and can be easily characterized using SEC and NMR techniques. After

polymerization,, the tert-butyl groups were cleaved and the final poly(acrylic acid) stars obtained. Two sets of star polymers (3 star polymers in each set) were synthesized. In one set, the degree of polymerization of the acrylic acid was kept the same. This meant that the more arms the star has, the shorter the arms would be. Therefore, the effect of the number of arms on drug solubility enhancement was evaluated while all other variables were kept the same (such as degree of polymerization). In the second set of star polymers, the length of each arm was kept constant, where molecular weight increased for each polymer as a function of arm length.

For a typical star polymer synthesis, the synthetic steps were as follows: Multifunctional CTA, tert-butyl acrylate, and azobisisobutyronitrile (AIBN) were added to the round-bottom flask with acetonitrile. The mixture was purged with nitrogen gas for one hour. After, the reaction mixture was sealed and submerged in an oil bath at 70 °C for six hours. When reaction was finished, the mixture was precipitated in a methanol/water mixture (1:1, v/v) and dried in vacuum. At this stage, the polymers were characterized using NMR (Figure 4.5) and SEC. After the sample was dried and characterized, tert-butyl protecting groups were removed by reacting with trifluoroacetic acid in DCM for 48 hours. The final product was dialyzed in water for three days and freeze dried to obtain a final product. The NMR spectra showed complete removal of tert-butyl protecting groups for all samples

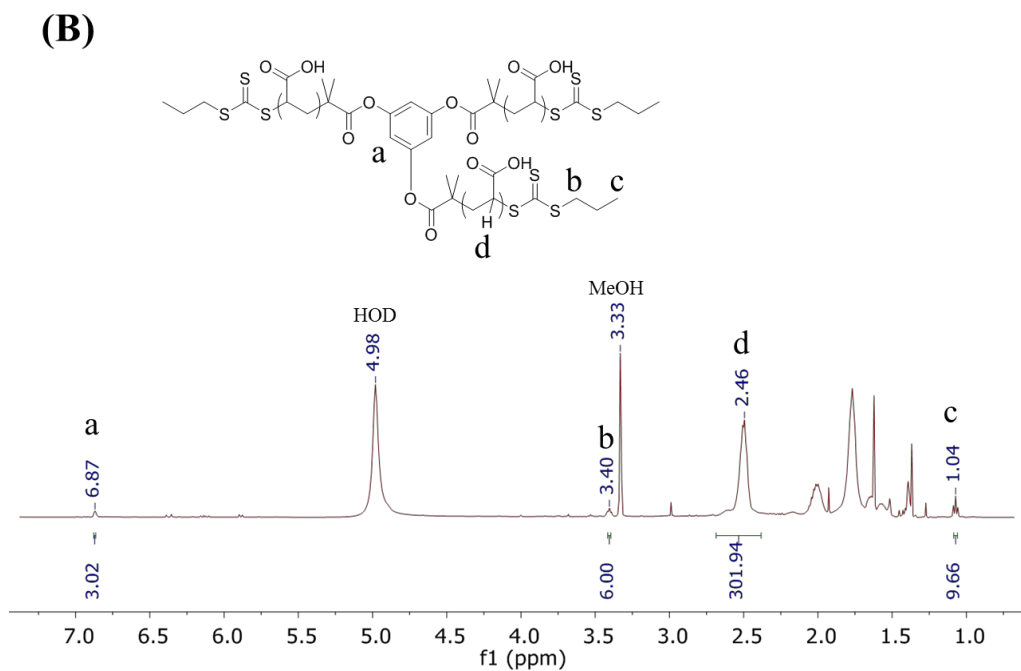
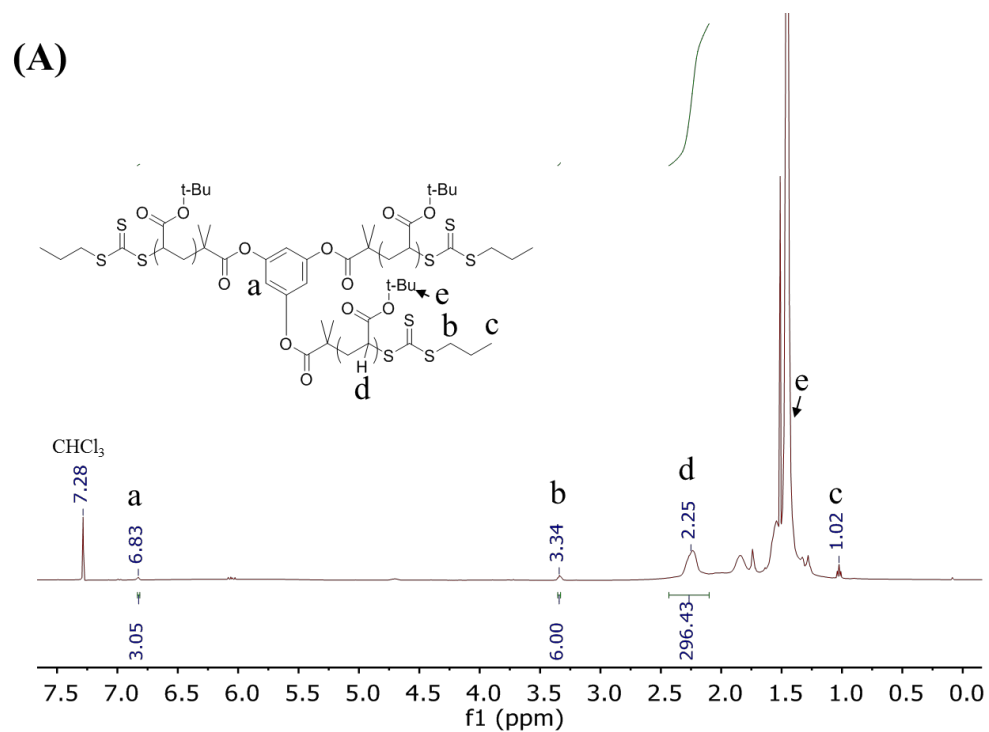


Figure 4.5. Representative NMR spectra (of the three-arm star polymer) before (A) and after (B) tert-butyl group deprotection. Spectrum (A) was recorded in CDCl₃ and (B) was recorded in MeOD. End-group analysis demonstrated that polymer architecture stays intact upon deprotection.

As shown in Figure 4.5, integral ratios between end-groups on the star periphery and end-groups in the core can elucidate degree of polymerization as well as the number of arms for each polymer. For instance, in Figure 4.5 (A), the peak area ratio of d/b = 296/6. Given that this is a three-arms star polymer, the degree of polymerization of each arm is 99 repeat units. The integral ratio between peaks b/a is shown as 6/3. This ratio is indicative that a three-arm star polymer was prepared. Table 4.1 contains all of the characterization information for the prepared star polymers.

Table 4.1. Molecular weight and dispersity data of the star polymers used in this study.

Polymer	Architecture	$M_n^{(a)}$, kDa	$M_n^{(b)}$, kDa	$M_w^{(b)}$, kDa	$\mathcal{D}^{(b)}$	RU per polymer ^(c)
[P(AA) ₁₁₈] ₁	Homopolymer	8.4	8.6	10.5	1.22	118
[P(AA) ₅₂] ₂	Diblock	7.9	7.9	8.4	1.07	104
[P(AA) ₃₈] ₃	Three-arm	8.9	9.0	9.3	1.03	114
[P(AA) ₉₇] ₃	Three-arm	21.3	21	21.8	1.04	301
[P(AA) ₂₅] ₄	Four-arm	8.4	8.2	8.9	1.09	100
[P(AA) ₉₇] ₄	Four-arm	26.4	28	30	1.07	388

In the first column, a number next to parenthesis indicates the number of repeat units per arm of the star polymer and a number next to brackets indicates number of arms in the given star polymer ^aMolecular weight was determined using NMR end-group analysis.

^bDetermined using SEC coupled with multi-angle light scattering detector.

4.2.3 Solid dispersions preparation with BCS Class II drug probucol

All samples were spray dried using a Bend Research lab scale Mini Spray Drier from MeOH. Different drug loadings were used to prepare SDDs: 25 wt % and 50 wt %; afterwards, DSC was used to evaluate their stability. In general, the physical stability of

the SDDs is a critical component for thermodynamic stability of the drug molecules.⁸⁶ The drug should be molecularly dispersed in the polymer matrix yielding an amorphous mixture. A physically-stable and amorphous SDD formulation leads to increased aqueous solubility of the drug, improved bioavailability (potentially leading to decreased costs and side effects). Probuco-polymer interactions appear to increase with the increased number of H-bonding sites in the polymer, and from the characterization data, the drug is molecularly dispersed in the polymer matrix (Table 4.2).

4.2.4 Drug dissolution testing

Next, how well the SDDs achieve and maintain the *in vitro* dissolution performance of probuocol was studied. Ideally, a dispersion of the drug and polymer should be able to maintain supersaturation levels of drug and inhibit crystal nucleation in the GI tract. Simulated intestinal fluid was added to the dissolution media to test *in vitro* performance of all the SDDs. Figure 4.6 shows the dissolution profiles of all the SDD formulations at 25 wt % probuocol loading and Figure 4.7 shows the dissolution profiles of SDDs at 50 wt % probuocol loading.

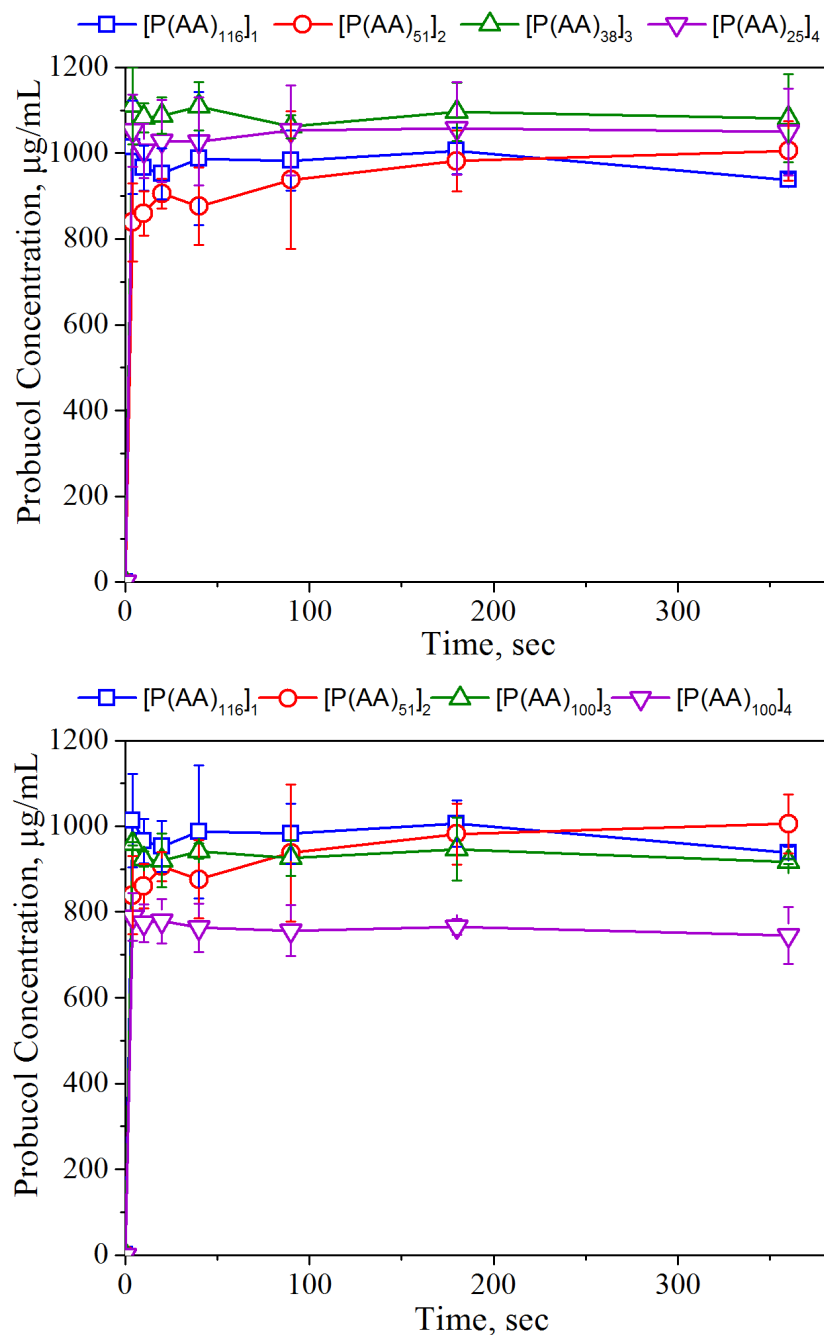


Figure 4.6. Dissolution data of the SDDs prepared at 25 wt % of probucol. The target concentration of probucol was 1000 µg/mL (denoting 100% drug solubility) whereas the aqueous solubility of crystalline probucol (without an excipient) is very poor (0.042 µg/mL). Data points denote the mean of three dissolution experiments and error bars denote the standard deviation of the measured data ($N=3$).

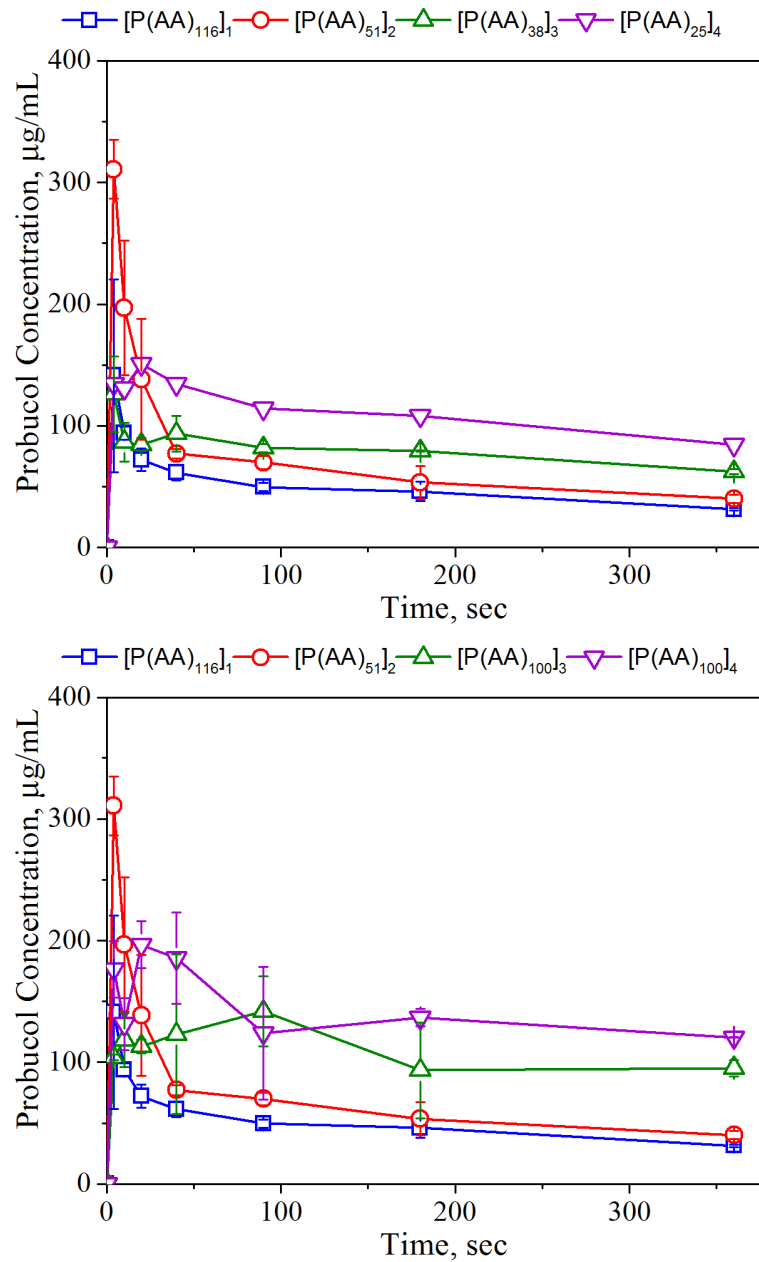


Figure 4.7. Dissolution data of the SDDs at 50 weight percent of probucol. The target concentration of probucol was 1000 µg/mL (denoting 100% drug solubility) whereas the aqueous solubility of crystalline probucol (without an excipient) is very poor (0.042 µg/mL). Data points denote the mean of three dissolution experiments and error bars denote the standard deviation of measured data ($N=3$).

The SDDs with the PAA polymers and 25 wt % drug loading (except the [(PAA)₁₀₀]₄ excipient) showed an excellent release and solubility profile with probucol in aqueous solution and maintained drug supersaturation for 360 min (6 h). We attributed the performance of the PAA stars to their ability to dissolve rapidly in aqueous solution, release probucol in the dissolution media, and inhibit crystal nucleation by potentially binding to the drug through both H-bonding and hydrophobic interactions. The [(PAA)₁₀₀]₄ four arm star did not dissolve fully because of its high molecular weight ($M_w = 28$ kDa) in the dissolution media and resulted in a lower solubilization/release profile of probucol. Due to the insolubility of the polymer matrix, the drug may be trapped and remain undissolved with the polymer in the dissolution media.

To further understand the role of the star polymer architecture, SDDs with 50 wt % of the drug were prepared. At this drug loading, the polymer concentration in the solution is low (~1 mg/mL) relative to other drug loadings. Therefore, even high molecular weight polymers tend to be soluble in aqueous media at such low concentrations. By making sure that the polymer excipient is fully soluble during the dissolution test, the effects of polymer architecture on the drug solubility enhancement can be inferred.

Two sets of polymeric excipients were tested at 50 wt % drug loading – the polymer and star variants with the same molecular weight and the polymer and star variants with the same degree of polymerization of each arm (Figure 4.7). All dissolution data were compared to the linear polymers (the homopolymer and the “deblock” polymerized with the two PAA blocks). The linear polymers ([(PAA)₁₁₆]₁ and [(PAA)₅₁]₂, controls) had the lowest solubility profile compared to other star polymers. The three-arm excipients [(PAA)₃₈]₃ and the four-arm excipient [(PAA)₂₅]₄ both allowed higher probucol solubility

maintenance leading to a conclusion that the polymer branching may the volume of space within the polymer where the drug can be partitioned into. This is further supported by literature where branched polymers are used as excipients for enhancing drug solubility.^{155,156} When star polymers of higher molecular weight were used ($[(PAA)_{100}]_3$, $M_w = 21$ kDa and $[(PAA)_{100}]_4$, $M_w = 28$ kDa), even higher amount of probucol was maintained in the solution for up to six hours. This is indicative of not only the excipient branching being important in the drug solubility maintenance, but also the excipient molecular weight as well. To further improve solubility maintenance, highly-branched and of high molecular weight (while still maintaining solubility) may create a polymer-rich phase for the drug to partition into.

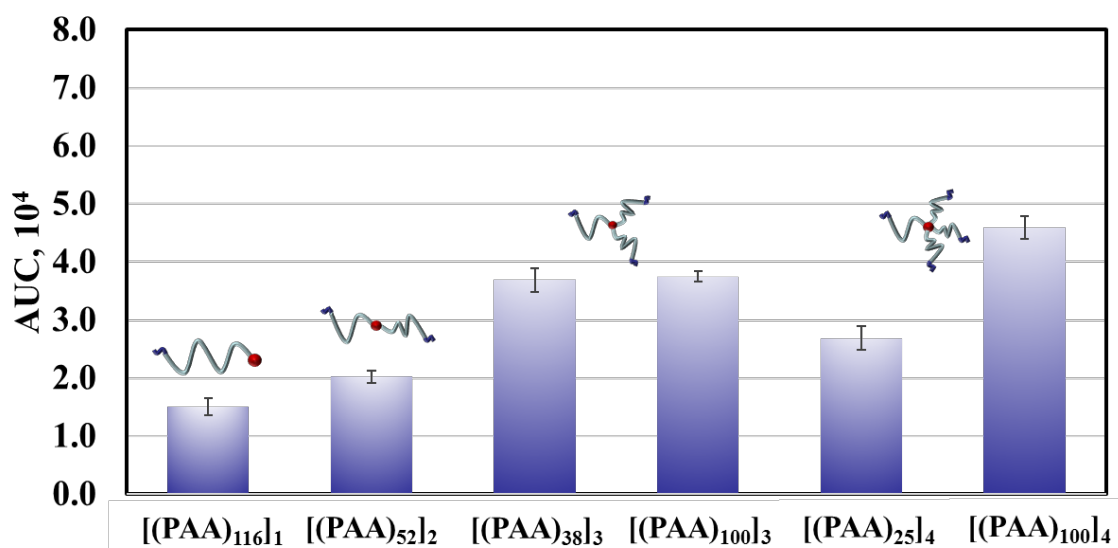


Figure 4.8. Area under the curve (AUC) as calculated at 360 min from the dissolution data of SDDs with 10, 25, and 50 weight percent probucol (PRB) loading. The calculated AUC is the average of three trials and error bars denote the standard deviation of measured data ($N=3$).

The area under the curve (AUC_{360min}) is the area under the drug concentration – time profile curves over the period of a 6 h dissolution test and represents the solubility maintenance of the excipient system for a drug. The AUC_{360max} is the theoretical maximum area under the drug concentration time profile over the period of a 6 h dissolution test, where $3.6 \times 10^5 \mu\text{g} \cdot \text{min}/\text{mL}$ denotes 100% drug solubility and supersaturation maintenance over the period of six hours. Incorporating a higher drug loading percentage in an SDD formulation is desirable; however, there is a fine interplay between higher drug loading, and the increased tendency of the drug to crystallize. Therefore, in Figure 4.8, the AUC supports the trends observed with star polymers: branching and increased molecular weight enhance drug solubility if the excipient full solubility is maintained.

Table 4.2. Percent of probucol crystallinity in SDDs formulated with 50 wt % of the drug (as determined by the DSC) and AUC_{360min} value for each of the formulations.

Polymer	% Crystallinity	AUC, 10^4
[P(AA) ₁₁₈] ₁	49	1.5±0.1
[P(AA) ₅₂] ₂	59	2.0±0.1
[P(AA) ₃₈] ₃	46	3.7±0.2
[P(AA) ₉₇] ₃	44	3.8±0.1
[P(AA) ₂₅] ₄	48	2.7±0.2
[P(AA) ₉₇] ₄	52	4.6±0.2

Finally, data in the Table 4.2 suggests that all formulations have relatively the same probucol crystallinity in each sample as determined by the DSC measurements (error of DSC crystallinity measurement is $\pm 7\%$ ¹⁵⁷). Therefore, we concluded that star polymers are

more effective at inhibiting crystal growth when the nucleation sites are already present in the solution.

4.3 Conclusion

In summary, we have synthesized two sets of well-defined architectures of the PAA-based star polymers and formulated SDDs of these materials with probucol. Our results clearly indicate that the solubility of the polymer matrices in the dissolution media and an increase in hydrogen bonding sites in the polymer matrices are critical to decrease probucol crystallization, increase drug solubility (i.e., the AUC_{360min} value), and achieve supersaturation concentration of hydrophobic drugs in the dissolution media. Our study gives new insight into the field of excipient design by demonstrating the importance of polymer architecture to maintain drug solubility of a highly hydrophobic API. The development of tunable high-performance excipients and efforts to understand the structure-activity relationships may help decrease the current high attrition rate of drugs in the pharmaceutical development pipeline.

4.4 Materials and Methods

4.4.1 Materials

All chemicals were reagent grade and used without further purification unless otherwise noted. All solvents were HPLC or analytical grade. Styrene (99%, ACROS Organics) and *tert*-butyl acrylate (98%, Sigma-Aldrich) were purified by passing them through activated basic alumina (80-200 Mesh, Fisher Scientific) columns. 2,2'-Azobis(2-methylpropionitrile) (AIBN, 98%, Sigma-Aldrich) was stored in a freezer at -20 °C and used as received without any further purification. Probucol (PBC), was obtained from

Sigma-Aldrich (Milwaukee, WI), acetonitrile (Fisher Scientific) and trifluoroacetic acid (ACROS Organics) were used as received. *N,N'*-dicyclohexylcarbodiimide (DCC, 99%, Sigma-Aldrich), 4-(dimethylamino)pyridine (DMAP, 99%, Sigma-Aldrich), 1-propanethiol (99%, Sigma-Aldrich), carbon disulfide (Sigma-Aldrich), and 2-bromo-2-methylpropanoic acid (98%, Sigma-Aldrich) were used as received without any further purification. Fasted simulated intestinal fluid powder (FaSSIF) was purchased from Biorelevant (Surrey, UK). Phosphate buffered saline (PBS) consisted of 82 mM sodium chloride (99%, Fisher Scientific), 20 mM sodium phosphate dibasic heptahydrate (98%, Fisher Scientific), and 47 mM potassium phosphate monobasic (99%, J.T. Baker).

4.4.2 Polymer synthesis

2-methyl-2-(((propylthio)carbonothioyl)thio)propanoic acid chain transfer agent synthesis. Potassium phosphate tribasic (1.1 equiv.) was dissolved in acetone and purged with nitrogen for 5 minutes. Propane thiol (1.1 equiv.) was added, and the flask was purged for 10 additional minutes. Carbon disulfide (3 equiv.) was added and stirred for 20 minutes, then 2-bromoisobutyric acid (1 equiv.) was added. After 22 hours, the reaction was stopped, was vacuum filtered to remove precipitated potassium bromide, and concentrated with a rotary evaporator to remove acetone. The reaction mixture was washed with 300 mL of 1 M hydrochloric acid, extracted with 250 mL of dichloromethane, dried with sodium sulfate, filtered, and concentrated. The reaction mixture was separated by flash column chromatography on silica gel with 3:2 hexane : ethyl acetate and concentrated to obtain a yellow oil (1) with 32% yield. ¹H NMR (500 MHz, Chloroform-*d*) δ 5.32 (d, *J* = 1.5 Hz, 0H), 4.15 (qd, *J* = 7.1, 1.6 Hz, 0H), 3.33 – 3.26 (m, 2H), 2.07 (d, *J* = 1.5 Hz, 0H), 1.80 –

1.68 (m, 8H), 1.28 (td, $J = 7.1, 1.6$ Hz, 1H), 1.03 (td, $J = 7.4, 1.6$ Hz, 3H). ^{13}C NMR (126 MHz, Chloroform-*d*) δ 220.88, 177.97, 55.53, 38.86, 25.23, 21.40, 13.51.

Difunctional CTA synthesis. 1,4-dihydroxyquinone (1 equiv.), *N,N'*-dimethyl aminopyridine (0.2 equiv.), and 2-methyl-2-(((propylthio)carbonothioyl)thio)propanoic acid (4 equiv.) were dissolved in dichloromethane and purged with nitrogen for 10 minutes before adding dicyclohexyl carbodiimide (DCC, 1.5 equiv.). After 16 hours, the reaction was stopped and concentrated. The reaction mixture was separated with flash column chromatography on silica gel with 1:1 hexanes : ethyl acetate and concentrated to obtain an orange waxy solid with 43% yield. ^1H NMR (400 MHz, Chloroform-*d*) δ 6.62 (s, 4H), 3.33 (t, $J = 7.3$ Hz, 4H), 1.83 (s, 12H), 1.75 (q, $J = 6.4$ Hz, 4H), 1.04 (s, 6H). ^{13}C NMR (126 MHz, Chloroform-*d*) δ 222.42, 173.28, 67.76, 61.01, 55.98, 38.86, 25.40, 21.44, 13.47.

Trifunctional CTA synthesis. 1,3,5-trihydroxybenzene (1 equiv.), *N,N'*-dimethyl aminopyridine (0.2 equiv.), and 2-methyl-2-(((propylthio)carbonothioyl)thio)propanoic acid (6 equiv.) were dissolved in dichloromethane and purged with nitrogen for 15 minutes before adding DCC (1.5 equiv.). After 20 hours, the reaction was stopped and concentrated. The reaction mixture was separated with flash column chromatography on silica gel with 1:1 hexanes : ethyl acetate and concentrated to obtain an orange waxy solid with 43% yield. ^1H NMR (400 MHz, Chloroform-*d*) δ 6.82 (s, 3H), 3.33 (t, $J = 7.3$ Hz, 6H), 1.83 (s, 18H), 1.75 (q, $J = 6.4$ Hz, 6H), 1.04 (s, 9H). ^{13}C NMR (126 MHz, Chloroform-*d*) δ 222.42, 173.28, 67.76, 61.01, 55.98, 38.86, 25.40, 21.44, 13.47.

1,2,4,5-tetrahydroxybenzene synthesis. To a mixture of 4.00 g of 2,5-dihydroxyquinone (28.6 mmol) and 10.16 g (85.6 mmol) of tin powder (<150 μm) 100 mL

of concentration hydrochloric acid was added (36 %) in a 1 L flask. The flask was purged with nitrogen and the mixture was stirred for 18 hours. The next day, the mixture was refluxed for 30 minutes and filtered under nitrogen atmosphere. After filtration, solution was sealed in a vial under N₂ atmosphere and cooled down to 0 °C. Recrystallized product was filtered and dried in vacuum. Yield was 36 %. ¹H NMR (400 MHz, MeOD) δ 6.36 (s, 2H). ¹³C NMR (126 MHz, MeOD) δ 137.3, 104.0.

Poly(tert-butyl acrylate) three-arm star polymer synthesis. The tri-functional CTA (0.246 g, 0.674 mmol), AIBN (0.0172 g, 0.105 mmol), and *tert*-butyl acrylate (10.0 g, 78.1 mmol) were added into a 50 mL round-bottom flask with acetonitrile, followed by three freeze-vacuum-thaw cycles. The flask was immersed into an oil bath at 70 °C and stirred. After four hours, the flask was cooled to room temperature and opened to air. The polymer was dissolved in 25 mL of tetrahydrofuran (THF) and precipitated into a methanol/water 1:1 mixture (1 L). The isolated polymer was re-dissolved in THF and precipitated twice more, to afford a yellow viscous product, which was dried in vacuum ($M_n = 8.9$ kg/mol, $\bar{D} = 1.09$, yield = 85%). ¹H NMR (400 MHz, Chloroform-*d*) δ 6.83 (s, 3H), 3.34 (bs, 6H), 2.25 (bs, 296H), 1.25 – 1.6 (bs), 1.02 (s, 9H).

Deprotection of the poly(tert-butyl acrylate) three-arm star polymer. Poly(*tert*-butyl acrylate) three-arm star polymer (1.87 g, 0.0621 mmol) was dissolved in 5.5 mL of dichloromethane (DCM) in a 25 mL round-bottom flask equipped with a stir bar. Excess trifluoroacetic acid was then added dropwise (3.10 mL, 18.2 mmol) and the solution stirred for 24 hours at room temperature. The suspension was filtered and the resulting solid dissolved in DMF and dialyzed (ethanol-water mixture (1:1, v/v); then water). The aqueous

solution was freeze-dried, yielding a yellowish powder (yield = 98%). (polymer characterization results are shown in Table 4.1).

4.4.3 Methods

4.4.3.1 Size exclusion chromatography (SEC) method

SEC measurements were carried out on an Agilent 1260 Infinity liquid chromatograph equipped with a Waters Styragel guard column and three Waters Styragel columns (HR6, HR4, and HR1; 100-10,000,000 g/mol) to provide effective separation for molecular weight determination. The detectors used were an Agilent 1260 VWD UV-vis detector, a Wyatt Dawn Heleos II light-scattering detector, and a Wyatt Optilab T-rEX refractive-index detector. Tetrahydrofuran was used as the mobile phase at 1.0 mL/min at 25 °C.

4.4.3.2 Spray drying

Spray drying was performed on a Bend Research Mini Spray Drier under the following conditions: inlet temperature of 68 °C, nitrogen flow rate of 12.8 SLPM, and a 0.65 mL/min syringe flow rate. The SDDs were collected on a 4" Whatman filter. Unless otherwise noted, the total solute content spray dried was always one weight percent. Solutions were sprayed from a THF:MeOH mixture (15:2, v/v). All diblock terpolymers were completely soluble in a THF:MeOH mixture prior to spray drying. The SDD composition is reported as the weight percent (wt %) drug in the dispersion. For example, 30 mg of probucol and 270 mg of polymer were dissolved in 29.7 g of THF:MeOH mixture to make 10 wt% probucol with (PEP-b-P(DMA-*grad*-MAT)). Three different compositions were used for the polymer/drug dispersions: 10, 25, and 50 wt % probucol relative to polymer.

4.4.3.3 Differential scanning calorimetry (DSC)

Modulated differential scanning calorimetry (MDSC) was used to determine the thermal features of the SDDs and was conducted on a TA-Instruments Discovery DSC equipped with an autosampler. Samples from 5–10 mg were placed in T-zero aluminum pans and sealed with a hermetic lid. MDSC analysis was performed with a nitrogen flow rate of 50.00 mL/min and a heating rate of 1 °C/min from 0 to 180 °C. The temperature was modulated at ± 2 °C with a period of 40 s. The first heating scans are reported. For polymer only samples (not spray dried), the temperature was not modulated, but was ramped between -50 °C and 180 °C at a rate of 10 °C/min. The second heating scans are reported for those samples. For all samples, TA TRIOS software version 2.2 was used to analyze T_g values and enthalpic components.

4.4.3.4 In-vitro dissolution test

Dissolution testing was performed on each SDD formulation and the crystalline drug to determine the concentration of drug in the dissolution media and maintenance of supersaturation. The dissolution medium consisted of phosphate buffer saline (82 mM sodium chloride, 20 mM sodium phosphate dibasic, 47 mM potassium phosphate monobasic) supplemented with 0.5 wt% FaSSIF. The medium was adjusted to pH 6.5 with NaOH. An appropriate amount of SDD or crystalline drug was weighed and added into 2.0 mL microcentrifuge tubes to yield a final total drug concentration of 1000 mg/mL (if all material is fully dissolved). For example: At 10 wt % of drug loading, we took 18.0 mg of SDD consisting of 1.8 mg of drug and 16.2 mg of polymer and diluted the SDD with 1.8 mL of PBS buffer (containing FaSSIF) solution for dissolution testing. All samples were analyzed in duplicate ($n = 2$). The first step in dissolution testing involved vortexing the

samples for 1 min in 1.8 mL of PBS+FaSSIF medium and then placing the sample into an isothermal aluminum heating block held at 37°C. At each time point (4, 10, 20, 40, 90, 180, and 360 min), tubes were removed from the heating blocks and centrifuged at 13,000 rpm, 37 °C for 1 min to remove undissolved drug from dissolved drug, and then a 50 µL aliquot of the supernatant was transferred to an HPLC vial. The samples were again vortexed for 30 s and held at 37 °C until the next time point. The supernatant in the HPLC vials was then diluted with 250 µL of methanol and analyzed for drug via HPLC.

4.4.3.5 Reverse phase HPLC

Drug concentration in each aliquot was determined by reverse phase HPLC. The HPLC consisted of a reversed-phase EC-C18 column (Poroshell 120, 4.6 × 50 mm, 2.7 µm, Agilent, USA). A mobile phase of 96:4 (v/v) acetonitrile:water was used for probucol detection with a flow rate of 1.0 mL/min at 30 °C. A 10 µL aliquot of sample was injected, and the column effluent was detected at 241 nm with a UV detector (1260 Infinity Multiple Wavelength Detector, Agilent). The probucol concentration in the samples was determined using a calibration curve of 0.1–500 µg/mL concentrations.

4.5 References

- (129) Fagerberg, J. H.; Tsinman, O.; Sun, N.; Tsinman, K.; Avdeef, A.; Bergström, C. A. S. Dissolution Rate and Apparent Solubility of Poorly Soluble Drugs in Biorelevant Dissolution Media. *Mol. Pharm.* **2010**, *7* (5), 1419–1430. <https://doi.org/10.1021/mp100049m>.
- (130) Qin, J.; Jiang, X.; Gao, L.; Chen, Y.; Xi, F. Functional Polymeric Nanoobjects by Cross-Linking Bulk Self-Assemblies of Poly(Tert -Butyl Acrylate)- Block - Poly(Glycidyl Methacrylate). *Macromolecules* **2010**, *43* (19), 8094–8100.

<https://doi.org/10.1021/ma101639w>.

- (131) Jakeš, J. Regularized Positive Exponential Sum (REPES) Program - A Way of Inverting Laplace Transform Data Obtained by Dynamic Light Scattering. *Collect. Czechoslov. Chem. Commun.* **1995**, *60* (11), 1781–1797. <https://doi.org/10.1135/cccc19951781>.
- (132) Einstein, A. Über Die von Der Molekularkinetischen Theorie Der Wärme Geforderte Bewegung von in Ruhenden Flüssigkeiten Suspendierten Teilchen. *Ann. Phys.* **1905**, *322* (8), 549–560. <https://doi.org/10.1002/andp.19053220806>.
- (133) Dressman, J. B.; Berardi, R. R.; Dermentzoglou, L. C.; Russell, T. L.; Schmaltz, S. P.; Barnett, J. L.; Jarvenpaa, K. M. Upper Gastrointestinal (GI) PH in Young, Healthy Men and Women. *Pharm. Res.* **1990**, *7* (7), 756–761.
- (134) Imura, T. K.; Igaki, K. H. Gastrointestinal Transit and Drug Absorption. **2002**, *25* (February).
- (135) Barner-Kowollik, C.; Davis, T. P.; Stenzel, M. H. Synthesis of Star Polymers Using RAFT Polymerization: What Is Possible? *Aust. J. Chem.* **2006**, *59* (10), 719–727. <https://doi.org/10.1071/CH06297>.
- (136) McKenzie, T. G.; Wong, E. H. H.; Fu, Q.; Sulistio, A.; Dunstan, D. E.; Qiao, G. G. Controlled Formation of Star Polymer Nanoparticles via Visible Light Photopolymerization. *ACS Macro Lett.* **2015**, *4* (9), 1012–1016. <https://doi.org/10.1021/acsmacrolett.5b00530>.
- (137) Park, S.; Cho, H. Y.; Wegner, K. B.; Burdynska, J.; Magenau, A. J. D.; Paik, H.; Jurga, S.; Matyjaszewski, K. Star Synthesis Using Macroinitiators via Electrochemically Mediated Atom Transfer Radical Polymerization.

- Macromolecules* **2013**, *46* (15), 5856–5860. <https://doi.org/10.1021/ma401308e>.
- (138) Liu, G.; Qiu, Q.; Shen, W.; An, Z. Aqueous Dispersion Polymerization of 2-Methoxyethyl Acrylate for the Synthesis of Biocompatible Nanoparticles Using a Hydrophilic RAFT Polymer and a Redox Initiator. *Macromolecules* **2011**, *44* (13), 5237–5245. <https://doi.org/10.1021/ma200984h>.
- (139) Zhang, C.; Miao, M.; Cao, X.; An, Z. One-Pot RAFT Synthesis of Core Cross-Linked Star Polymers of PolyPEGMA in Water by Sequential Homogeneous and Heterogeneous Polymerizations. *Polym. Chem.* **2012**, *3* (9), 2656. <https://doi.org/10.1039/c2py20442h>.
- (140) Jackson, A. W.; Fulton, D. A. PH Triggered Self-Assembly of Core Cross-Linked Star Polymers Possessing Thermoresponsive Cores. *Chem. Commun.* **2011**, *47* (24), 6807. <https://doi.org/10.1039/c1cc11785h>.
- (141) Wong, E. H. H.; Blencowe, A.; Qiao, G. G. Quantitative Formation of Core Cross-Linked Star Polymers via a One-Pot Two-Step Single Electron Transfer-Living Radical Polymerization. *Polym. Chem.* **2013**, *4* (17), 4562. <https://doi.org/10.1039/c3py00726j>.
- (142) Soliman, G. M.; Sharma, R.; Choi, A. O.; Varshney, S. K.; Winnik, F. M.; Kakkar, A. K.; Maysinger, D. Tailoring the Efficacy of Nimodipine Drug Delivery Using Nanocarriers Based on A2B Miktoarm Star Polymers. *Biomaterials* **2010**, *31* (32), 8382–8392. <https://doi.org/10.1016/j.biomaterials.2010.07.039>.
- (143) Etrych, T.; Kovář, L.; Strohalm, J.; Chytil, P.; Říhová, B.; Ulbrich, K. Biodegradable Star HPMA Polymer–Drug Conjugates: Biodegradability, Distribution and Anti-Tumor Efficacy. *J. Control. Release* **2011**, *154* (3), 241–248.

<https://doi.org/10.1016/j.jconrel.2011.06.015>.

- (144) Kostková, H.; Schindler, L.; Kotrčhová, L.; Kovář, M.; Šírová, M.; Kostka, L.; Etrych, T. Star Polymer-Drug Conjugates with PH-Controlled Drug Release and Carrier Degradation. *J. Nanomater.* **2017**, *2017*.
<https://doi.org/10.1155/2017/8675435>.
- (145) Ren, J. M.; McKenzie, T. G.; Fu, Q.; Wong, E. H. H.; Xu, J.; An, Z.; Shanmugam, S.; Davis, T. P.; Boyer, C.; Qiao, G. G. Star Polymers. *Chem. Rev.* **2016**, *116* (12), 6743–6836. <https://doi.org/10.1021/acs.chemrev.6b00008>.
- (146) Liu, J.; Duong, H.; Whittaker, M. R.; Davis, T. P.; Boyer, C. Synthesis of Functional Core, Star Polymers via RAFT Polymerization for Drug Delivery Applications. *Macromol. Rapid Commun.* **2012**, *33* (9), 760–766.
<https://doi.org/10.1002/marc.201200029>.
- (147) Kreutzer, G.; Ternat, C.; Nguyen, T. Q.; Plummer, C. J. G.; Månson, J.-A. E.; Castelletto, V.; Hamley, I. W.; Sun, F.; Sheiko, S. S.; Herrmann, A.; et al. Water-Soluble, Unimolecular Containers Based on Amphiphilic Multiarm Star Block Copolymers. *Macromolecules* **2006**, *39* (13), 4507–4516.
<https://doi.org/10.1021/ma060548b>.
- (148) Hedrick, J. L.; Trollsås, M.; Hawker, C. J.; Atthoff, B.; Claesson, H.; Heise, A.; Miller, R. D.; Mecerreyes, D.; Jérôme, R.; Dubois, P. Dendrimer-like Star Block and Amphiphilic Copolymers by Combination of Ring Opening and Atom Transfer Radical Polymerization. *Macromolecules* **1998**, *31* (25), 8691–8705.
<https://doi.org/10.1021/ma980932b>.
- (149) Barner, L.; Li, C.; Hao, X.; Stenzel, M. H.; Barner-Kowollik, C.; Davis, T. P.

- Synthesis of Core-Shell Poly(Divinylbenzene) Microspheres via Reversible Addition Fragmentation Chain Transfer Graft Polymerization of Styrene. *J. Polym. Sci. Part A Polym. Chem.* **2004**, *42* (20), 5067–5076. <https://doi.org/10.1002/pola.20328>.
- (150) Gao, H.; Matyjaszewski, K. Synthesis of Star Polymers by A New “Core-First” Method: Sequential Polymerization of Cross-Linker and Monomer. *Macromolecules* **2008**, *41* (4), 1118–1125. <https://doi.org/10.1021/ma702560f>.
- (151) Zhang, Z.; Yin, L.; Tu, C.; Song, Z.; Zhang, Y.; Xu, Y.; Tong, R.; Zhou, Q.; Ren, J.; Cheng, J. Redox-Responsive, Core Cross-Linked Polyester Micelles. *ACS Macro Lett.* **2013**, *2* (1), 40–44. <https://doi.org/10.1021/mz300522n>.
- (152) Skey, J.; O’Reilly, R. K. Facile One Pot Synthesis of a Range of Reversible Addition-Fragmentation Chain Transfer (RAFT) Agents. *Chem. Commun.* **2008**, No. 35, 4183–4185. <https://doi.org/10.1039/B804260H>.
- (153) Neises, B.; Steglich, W. Simple Method for the Esterification of Carboxylic Acids. *Angew. Chemie Int. Ed. English* **1978**, *17* (7), 522–524. <https://doi.org/10.1002/anie.197805221>.
- (154) Das, A.; Theato, P. Multifaceted Synthetic Route to Functional Polyacrylates by Transesterification of Poly(Pentafluorophenyl Acrylates). *Macromolecules* **2015**, *48* (24), 8695–8707. <https://doi.org/10.1021/acs.macromol.5b02293>.
- (155) Woodhead Publishing Series in Biomedicine. Starch and Derivatives as Pharmaceutical Excipients. In *Controlled Drug Delivery*; Elsevier, 2015; pp 21–84. <https://doi.org/10.1016/B978-1-907568-45-9.00002-0>.
- (156) Ogaji, I. J.; Nep, E. I.; Audu-Peter, J. D. Advances in Natural Polymers as

Pharmaceutical Excipients. *Pharm. Anal. Acta* **2012**, *03* (01).

<https://doi.org/10.4172/2153-2435.1000146>.

- (157) Ricarte, R. G.; Lodge, T. P.; Hillmyer, M. A. Detection of Pharmaceutical Drug Crystallites in Solid Dispersions by Transmission Electron Microscopy. *Mol. Pharm.* **2015**, *12* (3), 983–990. <https://doi.org/10.1021/mp500682x>.

Chapter 5

Summary and Outlook

5.1 Dissertation summary

Nowadays most of the pharmaceutical ingredients are coming into the innovation pipeline with poor water solubility. Thus, development of excipients is playing a crucial role in improving the solubility of poorly water-soluble compounds. The field is rapidly expanding and there had been promising progress in establishing structure-property relationships between drugs solubility enhancement and polymer microstructure/chemical functionality. The work presented here emphasized the role of non-covalent interactions like H-bonding but could significantly benefit from further investigation of electrostatic interaction that can address poor aqueous solubility of several important drug classes that exist either in cationic or anionic forms when are present in the medium of small intestine. In this dissertation, considering the imperative role of excipient development in the pharmaceutical industry, a novel class of self-assembling, stimuli-responsive polymeric excipients was described for the applications in the oral drug delivery. Chapter 1 gave an overview to this important field and Chapter 2 describes the synthesis of five well-defined architectures of diblock terpolymers PEP-*b*-P(DMA-*grad*-MAT), PNIPAm-*b*-P(DMA-*grad*-MAT) of three different molecular weights, and PDEAEMA-*b*-P(DMA-*grad*-MAT). All of the copolymers formulated as SDDs with probucol. The results demonstrate that the solubility of the polymer matrices in the dissolution media and increase in H-bonding sites in the polymer matrices are critical for lowering probucol crystallinity and for increasing its solubility. The aforementioned polymers allow orders of magnitude higher than equilibrium drug concentration maintenance for up to 6 hours. This project gives new insight into the field of excipient design by demonstrating the importance of monomer

selection and polymer composition to fine-tune drug release and maintain its solubility over prolonged periods of time in the simulated environment of the human GI tract.

Chapter 3 describes synthesis of eight different polymers, including four diblock copolymers of polystyrene and poly(acrylic acid) of varying block lengths and four poly(acrylic acid) homopolymers. Block copolymers are amphiphilic and can be formulated with the drug in a form of aggregates or in a form of unimers. We observed that block copolymers that were preaggregated have higher probucol solubility enhancement compared to those spray dried from the non-selective solvent in a form of free polymer chains. This behavior is predominantly excipient-driven due to limited polymer solubility in the simulated intestinal fluid. The pH responsiveness of poly(acrylic acid)-containing block copolymers allowed for the determination of the efficiency of drug sequestration in the aggregate corona and release upon pH change from 1.2 (stomach pH) to 6.5 (small intestine pH). Finally, the Caco-2 cell assay was used to determine the drug permeability coefficient for selected polymers and it was shown that there is a four-fold increase in drug permeability for the PS₉₀-*b*-PAA₈₀ excipient relative to the commercially-available control. This project revealed that utilizing preaggregated polymer excipients for formulating drug-containing spray dried dispersions plays an important role in solubilizing and maintaining supersaturated concentrations of certain drugs while being a simple and controlled platform for oral drug delivery.

Chapter 4 further investigates the role of polymer architecture and molar mass on drug solubility enhancement. Six poly(acrylic acid)-based star polymers were synthesized with varying number of arms and number of PAA repeat units for each arm. Because end-groups and star cores were kept consistent, this project gave an insight on the role of

polymer architecture such as varied number of arms of the star. It was revealed that higher number of arms enhances drug solubility especially at higher drug loadings (50 wt %), which is a desirable outcome for the pharmaceutical industry. This agrees with some previous research that suggests branched structures tend to increase drug solubility relative to linear excipients.

Overall, this work collectively demonstrates that the development of tunable high-performing excipients and efforts to understand the structure-activity relationships may help decrease the current high attrition rate of drugs in the pharmaceutical development pipeline.

5.2 Future directions

To further explore types of interactions that exist in a complex polymer-drug-solution system, synthesis of the drugs structural analogues should be conducted next. Previous study conducted in our group by Ting et al.⁷⁸ demonstrated presence of H-bonding and hydrophobic interaction between the excipient and the drug phenytoin. Phenytoin belongs to a class of compounds called hydantoins. By modifying hydantoin core with various H-bonding and hydrophobic functional groups we can further elucidate the role of each type of interactions between the drug and the polymer in solution. Figure 5.1 shows phenytoin drug analogues that can be used with NIPAm-*co*-DMA excipient as well as some commercially available excipients (Kollidon®, HPMCAS). For the synthesis, a versatile and green reaction between di-substituted ureas and 1,2-diketones will be used. This will enable us to prepare a library of phenytoin analogues by using starting materials with different substituents. First part of the project will study the effect of H-bonding and hydrophobic interactions between the drug analogues and the polymers. For this, nitrogens

on glycolurea ring will be substituted with methyl groups to ‘block’ their ability to hydrogen bond and phenyl groups will be replaced with tert-butyl and methyl groups. Second part of the project will determine the role of steric properties of the drug molecule: phenyl groups will be replaced with di-tertbutyl phenyl groups and then with methyl groups. We hypothesize that this systematic study will help determine specific role of each functional group on the drug molecule as well as the role of the pendant groups along the polymer backbone.

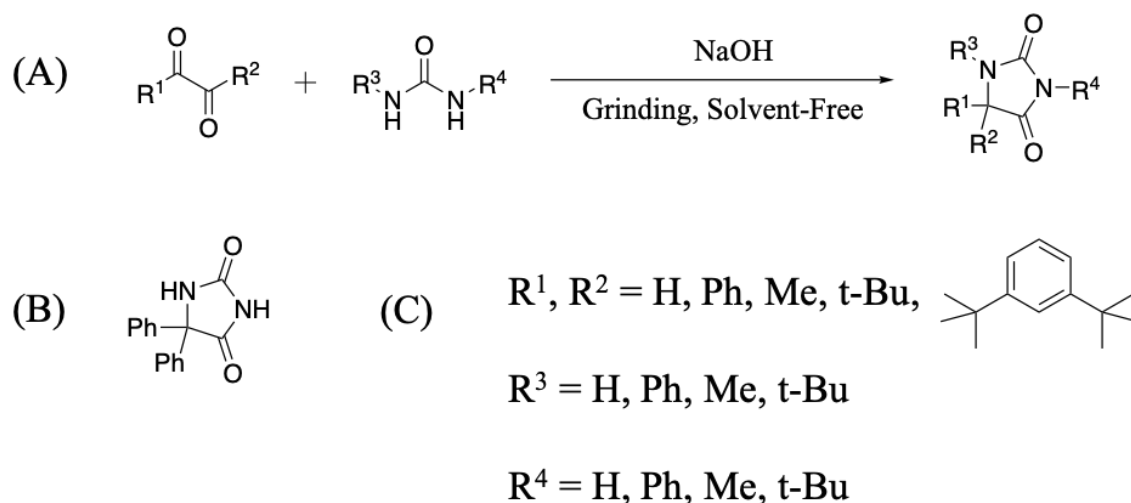


Figure 5.1. (A) Proposed synthesis method for the synthesis of hydantoin (phenytoin’s analogue), (B) Structure of the model drug phenytoin, and (C) Different substituents that will be used around hydantoin core.

Proposed structures will further our understanding of the role of non-covalent interactions between poorly water-soluble drug and a polymer. A variety of techniques that were described in this work (NOESY, DOSY, differential scanning calorimetry, IR spectroscopy) can help pinpoint the binding sites, as well as new characterization methods can be introduced. For instance, isothermal titration calorimetry should be sensitive enough

to measure the enthalpy of polymer-drug electrostatic interaction. Finally, due to biological activity of charged polymers, their role in bioavailability enhancement as well as mucoadhesive properties can be investigated. This can potentially lead to the expansion of the library of drugs to include BCS Class IV drugs that are known for their poor solubility as well as poor intestinal permeability.

Bibliography

- (1) Lipp, R. Major Advances in Oral Drug Delivery over the Past 15 Years. *American Pharmaceutical Review*. 2013.
- (2) FDA. The Biopharmaceutics Classification System (BCS) Guidance <http://www.fda.gov/AboutFDA/CentersOffices/OfficeofMedicalProductsandTobacco/CDER/ucm128219.htm>.
- (3) Morgan, S.; Grootendorst, P.; Lexchin, J.; Cunningham, C.; Greyson, D. The Cost of Drug Development: A Systematic Review. *Health Policy* **2011**, *100* (1), 4–17. <https://doi.org/10.1016/j.healthpol.2010.12.002>.
- (4) Lipp, R. The Innovator Pipeline: Bioavailability Challenges and Advanced Oral Drug Delivery Opportunities <http://www.americanpharmaceuticalreview.com/Featured-Articles/135982-The-Innovator-Pipeline-Bioavailability-Challenges-and-Advanced-Oral-Drug-Delivery-Opportunities/>.
- (5) Tale, S.; Purchel, A. A.; Dalsin, M. C.; Reineke, T. M. Diblock Terpolymers Are Tunable and PH Responsive Vehicles To Increase Hydrophobic Drug Solubility for Oral Administration. *Mol. Pharm.* **2017**, *14* (11), 4121–4127. <https://doi.org/10.1021/acs.molpharmaceut.7b00458>.
- (6) Onoue, S.; Kojo, Y.; Suzuki, H.; Yuminoki, K.; Kou, K.; Kawabata, Y.; Yamauchi, Y.; Hashimoto, N.; Yamada, S. Development of Novel Solid Dispersion of Tranilast Using Amphiphilic Block Copolymer for Improved Oral Bioavailability. *Int. J. Pharm.* **2013**, *452* (1–2), 220–226. <https://doi.org/10.1016/j.ijpharm.2013.05.022>.

- (7) Choudhary, S.; Gupta, L.; Rani, S.; Dave, K.; Gupta, U. Impact of Dendrimers on Solubility of Hydrophobic Drug Molecules. *Front. Pharmacol.* **2017**, *8* (MAY), 1–23. <https://doi.org/10.3389/fphar.2017.00261>.
- (8) Babu, N. J.; Nangia, A. Solubility Advantage of Amorphous Drugs and Pharmaceutical Cocrystals. *Cryst. Growth Des.* **2011**, *11* (7), 2662–2679. <https://doi.org/10.1021/cg200492w>.
- (9) Shimpi, S.; Chauhan, B.; Shimpi, P. Cyclodextrins: Application in Different Routes of Drug Administration. *Acta Pharm.* **2005**, *55* (2), 139–156.
- (10) Khadka, P.; Ro, J.; Kim, H.; Kim, I.; Kim, J. T.; Kim, H.; Cho, J. M.; Yun, G.; Lee, J. Pharmaceutical Particle Technologies: An Approach to Improve Drug Solubility, Dissolution and Bioavailability. *Asian J. Pharm. Sci.* **2014**, *9* (6), 304–316. <https://doi.org/10.1016/j.ajps.2014.05.005>.
- (11) Miller, J. M.; Beig, A.; Carr, R. A.; Spence, J. K.; Dahan, A. A Win – Win Solution in Oral Delivery of Lipophilic Drugs: Supersaturation via Amorphous Solid Dispersions Increases Apparent Solubility without Sacrificing Intestinal Membrane Permeability. **2012**.
- (12) Censi, R.; Di Martino, P. Polymorph Impact on the Bioavailability and Stability of Poorly Soluble Drugs. *Molecules* **2015**, *20* (10), 18759–18776. <https://doi.org/10.3390/molecules201018759>.
- (13) Hancock, B. C.; Parks, M. What Is the True Solubility Advantage for Amorphous Pharmaceuticals? *Pharm. Res.* **2000**, *17* (4), 397–404.
- (14) Guterres, S. S. Spray-Drying Technique to Prepare Innovative Nanoparticulated Formulations for Drug Administration : A Brief Overview. *Brazilian J. Phys.* **2009**,

39 (1A), 205–209.

- (15) Broadhead, J.; Edmond Rouan, S. K.; Rhodes, C. T. The Spray Drying of Pharmaceuticals. *Drug Dev. Ind. Pharm.* **1992**, *18* (11–12), 1169–1206. <https://doi.org/10.3109/03639049209046327>.
- (16) Curatolo, W.; Nightingale, J. a; Herbig, S. M. Utility of Hydroxypropylmethylcellulose Acetate Succinate (HPMCAS) for Initiation and Maintenance of Drug Supersaturation in the GI Milieu. *Pharm. Res.* **2009**, *26* (6), 1419–1431. <https://doi.org/10.1007/s11095-009-9852-z>.
- (17) Dalsin, M. C.; Tale, S.; Reineke, T. M. Solution-State Polymer Assemblies Influence BCS Class II Drug Dissolution and Supersaturation Maintenance. *Biomacromolecules* **2014**, *15* (2), 500–511. <https://doi.org/10.1021/bm401431t>.
- (18) Li, Z.; Lenk, T. I.; Yao, L. J.; Bates, F. S.; Lodge, T. P. Maintaining Hydrophobic Drug Supersaturation in a Micelle Corona Reservoir. *Macromolecules* **2018**, *51* (2), 540–551. <https://doi.org/10.1021/acs.macromol.7b02297>.
- (19) Johnson, L. M.; Li, Z.; LaBelle, A. J.; Bates, F. S.; Lodge, T. P.; Hillmyer, M. A. Impact of Polymer Excipient Molar Mass and End Groups on Hydrophobic Drug Solubility Enhancement. *Macromolecules* **2017**, *50* (3), 1102–1112. <https://doi.org/10.1021/acs.macromol.6b02474>.
- (20) Van Den Abeele, J.; Brouwers, J.; Mattheus, R.; Tack, J.; Augustijns, P. Gastrointestinal Behavior of Weakly Acidic BCS Class II Drugs in Man - Case Study Diclofenac Potassium. *J. Pharm. Sci.* **2015**, 1–11. <https://doi.org/10.1002/jps.24647>.
- (21) Kawakami, K.; Yoshikawa, T.; Hayashi, T.; Nishihara, Y.; Masuda, K.

- Microemulsion Formulation for Enhanced Absorption of Poorly Soluble Drugs. II. In Vivo Study. *J. Control. Release* **2002**, *81* (1–2), 75–82.
- (22) Guay, D. R. Micronized Fenofibrate: A New Fibric Acid Hypolipidemic Agent. *Ann. Pharmacother.* **1999**, *33* (10), 1083–1103.
- (23) Kalepu, S.; Manthina, M.; Padavala, V. Oral Lipid-Based Drug Delivery Systems – an Overview. *Acta Pharm. Sin. B* **2013**, *3* (6), 361–372. <https://doi.org/10.1016/j.apsb.2013.10.001>.
- (24) Subudhi, B. B.; Mandal, S. Self-Microemulsifying Drug Delivery System: Formulation and Study Intestinal Permeability of Ibuprofen in Rats. *J. Pharm.* **2013**, *2013*, 1–6. <https://doi.org/10.1155/2013/328769>.
- (25) Kushida, I.; Ichikawa, M.; Asakawa, N. Improvement of Dissolution and Oral Absorption of ER-34122, a Poorly Water-Soluble Dual 5-Lipoxygenase/Cyclooxygenase Inhibitor with Anti-Inflammatory Activity by Preparing Solid Dispersion. *J. Pharm. Sci.* **2002**, *91* (1), 258–266.
- (26) Godfroy, I. Polymeric Micelles – The Future of Oral Drug Delivery. *J. Biomater. Appl. Rev.* **2009**, *3*, 216–232.
- (27) Kurkuri, M. D.; Aminabhavi, T. M. Poly(Vinyl Alcohol) and Poly(Acrylic Acid) Sequential Interpenetrating Network PH-Sensitive Microspheres for the Delivery of Diclofenac Sodium to the Intestine. *J. Control. Release* **2004**, *96* (1), 9–20. <https://doi.org/10.1016/j.jconrel.2003.12.025>.
- (28) Jenkins, A. D.; Kratochvíl, P.; Stepto, R. F. T.; Suter, U. W. Glossary of Basic Terms in Polymer Science (IUPAC Recommendations 1996). *Pure Appl. Chem.* **1996**, *68* (12). <https://doi.org/10.1351/pac199668122287>.

- (29) Szwarc, M. 'Living' Polymers. *Nature* **1956**, *178* (4543), 1168–1169. <https://doi.org/10.1038/1781168a0>.
- (30) Braunecker, W. a.; Matyjaszewski, K. Controlled/Living Radical Polymerization: Features, Developments, and Perspectives. *Prog. Polym. Sci.* **2007**, *32* (1), 93–146. <https://doi.org/10.1016/j.progpolymsci.2006.11.002>.
- (31) Lowe, A. B.; McCormick, C. L. Reversible Addition–Fragmentation Chain Transfer (RAFT) Radical Polymerization and the Synthesis of Water-Soluble (Co)Polymers under Homogeneous Conditions in Organic and Aqueous Media. *Prog. Polym. Sci.* **2007**, *32* (3), 283–351. <https://doi.org/10.1016/j.progpolymsci.2006.11.003>.
- (32) Zetterlund, P. B.; Kagawa, Y.; Okubo, M. Controlled/Living Radical Polymerization in Dispersed Systems. *Chem. Rev.* **2008**, *108* (9), 3747–3794. <https://doi.org/10.1021/cr800242x>.
- (33) Keddie, D. J. A Guide to the Synthesis of Block Copolymers Using Reversible-Addition Fragmentation Chain Transfer (RAFT) Polymerization. *Chem. Soc. Rev.* **2014**, *43* (2), 496–505. <https://doi.org/10.1039/c3cs60290g>.
- (34) Science, C. M. RAFT – Choosing the Right Agent. **2005**, 1–19.
- (35) Bromberg, L. Polymeric Micelles in Oral Chemotherapy. *J. Control. Release* **2008**, *128* (2), 99–112. <https://doi.org/10.1016/j.jconrel.2008.01.018>.
- (36) Tale, S. R.; Yin, L.; Reineke, T. M. Trehalose-Functionalized Block Copolymers Form Serum-Stable Micelles. *Polym. Chem.* **2014**, *5* (17), 5160. <https://doi.org/10.1039/C4PY00399C>.
- (37) Torchilin, V. P. Micellar Nanocarriers: Pharmaceutical Perspectives. *Pharm. Res.* **2007**, *24* (1), 1–16. <https://doi.org/10.1007/s11095-006-9132-0>.

- (38) Gil, E.; Hudson, S. Stimuli-Responsive Polymers and Their Bioconjugates. *Prog. Polym. Sci.* **2004**, *29* (12), 1173–1222. <https://doi.org/10.1016/j.progpolymsci.2004.08.003>.
- (39) Mondon, K.; Gurny, R.; Möller, M. Colloidal Drug Delivery Systems – Recent Advances With Polymeric Micelles. *Chim. Int. J. Chem.* **2008**, *62* (10), 832–840. <https://doi.org/10.2533/chimia.2008.832>.
- (40) Johnson, L. M.; Li, Z.; LaBelle, A. J.; Bates, F. S.; Lodge, T. P.; Hillmyer, M. A. Impact of Polymer Excipient Molar Mass and End Groups on Hydrophobic Drug Solubility Enhancement. *Macromolecules* **2017**, *50* (3), 1102–1112. <https://doi.org/10.1021/acs.macromol.6b02474>.
- (41) Ting, J. M.; Tale, S.; Purchel, A. A.; Jones, S. D.; Widanapathirana, L.; Tolstyka, Z. P.; Guo, L.; Guillaudeu, S. J.; Bates, F. S.; Reineke, T. M. High-Throughput Excipient Discovery Enables Oral Delivery of Poorly Soluble Pharmaceuticals. *ACS Cent. Sci.* **2016**, *2* (10), 748–755. <https://doi.org/10.1021/acscentsci.6b00268>.
- (42) Lu, Y.; Park, K. Polymeric Micelles and Alternative Nanonized Delivery Vehicles for Poorly Soluble Drugs. *Int. J. Pharm.* **2013**, *453* (1), 198–214. <https://doi.org/10.1016/j.ijpharm.2012.08.042>.
- (43) Camilleri, M.; Colemont, L. J.; Phillips, S. F.; Brown, M. L.; Thomforde, G. M.; Chapman, N.; Zinsmeister, A. R. Human Gastric Emptying and Colonic Filling of Solids Characterized by a New Method. *Am. J. Physiol. Liver Physiol.* **1989**, *257* (2), G284–G290. <https://doi.org/10.1152/ajpgi.1989.257.2.G284>.
- (44) Ould-Ouali, L.; Noppe, M.; Langlois, X.; Willems, B.; Te Riele, P.; Timmerman, P.; Brewster, M. E.; Ariën, A.; Pr at, V. Self-Assembling PEG-p(CL-Co-TMC)

- Copolymers for Oral Delivery of Poorly Water-Soluble Drugs: A Case Study with Risperidone. *J. Control. Release* **2005**, *102* (3), 657–668. <https://doi.org/10.1016/j.jconrel.2004.10.022>.
- (45) Pierri, E.; Avgoustakis, K. Poly(Lactide)-Poly(Ethylene Glycol) Micelles as a Carrier for Griseofulvin. *J. Biomed. Mater. Res. Part A* **2005**, *75A* (3), 639–647. <https://doi.org/10.1002/jbm.a.30490>.
- (46) Chen, W.; Zhong, P.; Meng, F.; Cheng, R.; Deng, C.; Feijen, J.; Zhong, Z. Redox and PH-Responsive Degradable Micelles for Dually Activated Intracellular Anticancer Drug Release. *J. Control. Release* **2013**, *169* (3), 171–179. <https://doi.org/10.1016/j.jconrel.2013.01.001>.
- (47) Kim, S.; Kim, J. Y.; Huh, K. M.; Acharya, G.; Park, K. Hydrotropic Polymer Micelles Containing Acrylic Acid Moieties for Oral Delivery of Paclitaxel. *J. Control. Release* **2008**, *132* (3), 222–229. <https://doi.org/10.1016/j.jconrel.2008.07.004>.
- (48) Sant, V. P.; Smith, D.; Leroux, J.-C. Novel PH-Sensitive Supramolecular Assemblies for Oral Delivery of Poorly Water Soluble Drugs: Preparation and Characterization. *J. Control. Release* **2004**, *97* (2), 301–312. <https://doi.org/10.1016/j.jconrel.2004.03.026>.
- (49) Choonara, B. F.; Choonara, Y. E.; Kumar, P.; Bijukumar, D.; du Toit, L. C.; Pillay, V. A Review of Advanced Oral Drug Delivery Technologies Facilitating the Protection and Absorption of Protein and Peptide Molecules. *Biotechnol. Adv.* **2014**, *32* (7), 1269–1282. <https://doi.org/10.1016/j.biotechadv.2014.07.006>.
- (50) Park, K.; Kwon, I. C.; Park, K. Oral Protein Delivery: Current Status and Future

- Prospect. *React. Funct. Polym.* **2011**, *71* (3), 280–287.
<https://doi.org/10.1016/j.reactfunctpolym.2010.10.002>.
- (51) DEACON, M. P.; MCGURK, S.; ROBERTS, C. J.; WILLIAMS, P. M.; TENDLER, S. J. B.; DAVIES, M. C.; DAVIS, S. S. (Bob); HARDING, S. E. Atomic Force Microscopy of Gastric Mucin and Chitosan Mucoadhesive Systems. *Biochem. J.* **2000**, *348* (3), 557–563. <https://doi.org/10.1042/bj3480557>.
- (52) Lehr, C. M.; Bouwstra, J. A.; Schacht, E. H.; Junginger, H. E. In Vitro Evaluation of Mucoadhesive Properties of Chitosan and Some Other Natural Polymers. *Int. J. Pharm.* **1992**, *78* (1–3), 43–48. [https://doi.org/10.1016/0378-5173\(92\)90353-4](https://doi.org/10.1016/0378-5173(92)90353-4).
- (53) Bromberg, L.; Temchenko, M.; Alakhov, V.; Hatton, T. A. Bioadhesive Properties and Rheology of Polyether-Modified Poly(Acrylic Acid) Hydrogels. *Int. J. Pharm.* **2004**, *282* (1–2), 45–60. <https://doi.org/10.1016/j.ijpharm.2004.05.030>.
- (54) Schulz, J. D.; Gauthier, M. A.; Leroux, J.-C. Improving Oral Drug Bioavailability with Polycations? *Eur. J. Pharm. Biopharm.* **2015**, *97*, 427–437. <https://doi.org/10.1016/j.ejpb.2015.04.025>.
- (55) Hidalgo, I. J.; Raub, T. J.; Borchardt, R. T. Characterization of the Human Colon Carcinoma Cell Line (Caco-2) as a Model System for Intestinal Epithelial Permeability. *Gastroenterology* **1989**, *96* (3), 736–749. [https://doi.org/10.1016/0016-5085\(89\)90897-4](https://doi.org/10.1016/0016-5085(89)90897-4).
- (56) Juergenliemk, G.; Boje, K.; Huewel, S.; Lohmann, C.; Galla, H. J.; Nahrstedt, A. In Vitro Studies Indicate That Miquelianin (Quercetin 3-O-β-D-Glucuronopyranoside) Is Able to Reach the CNS from the Small Intestine. *Planta Med.* **2003**, *69* (11), 1013–1017. <https://doi.org/10.1055/s-2003-45148>.

- (57) Fagerholm, U. Prediction of Human Pharmacokinetics -Gastrointestinal Absorption. *J. Pharm. Pharmacol.* **2007**, *59* (7), 905–916. <https://doi.org/10.1211/jpp.59.7.0001>.
- (58) Li, C.; Wainhaus, S.; Uss, A. S.; Cheng, K.-C. High-Throughput Screening Using Caco-2 Cell and PAMPA Systems. In *Drug Absorption Studies*; Springer US: Boston, MA; pp 418–429. https://doi.org/10.1007/978-0-387-74901-3_18.
- (59) Schumann, R. The Seventh Amendment to the Cosmetics Directive: What Does DG Enterprise Want from ECVAM? *Altern. Lab. Anim.* **2002**, *30 Suppl 2*, 213–214.
- (60) Hubbard, D.; Bond, T.; Ghandehari, H. Regional Morphology and Transport of PAMAM Dendrimers Across Isolated Rat Intestinal Tissue. *Macromol. Biosci.* **2015**, 1–9. <https://doi.org/10.1002/mabi.201500225>.
- (61) Uchiyama, H.; Tozuka, Y.; Imono, M.; Takeuchi, H. Transglycosylated Stevia and Hesperidin as Pharmaceutical Excipients: Dramatic Improvement in Drug Dissolution and Bioavailability. *Eur. J. Pharm. Biopharm.* **2010**, *76* (2), 238–244. <https://doi.org/10.1016/j.ejpb.2010.07.006>.
- (62) Li, A. In Vitro Approaches to Evaluate ADMET Drug Properties. *Curr. Top. Med. Chem.* **2004**, *4* (7), 701–706. <https://doi.org/10.2174/1568026043451050>.
- (63) Hubatsch, I.; Ragnarsson, E. G. E.; Artursson, P. Determination of Drug Permeability and Prediction of Drug Absorption in Caco-2 Monolayers. *Nat. Protoc.* **2007**, *2* (9), 2111–2119. <https://doi.org/10.1038/nprot.2007.303>.
- (64) Joshi, G.; Kumar, A.; Sawant, K. Bioavailability Enhancement, Caco-2 Cells Uptake and Intestinal Transport of Orally Administered Lopinavir-Loaded PLGA Nanoparticles. *Drug Deliv.* **2016**, *23* (9), 3492–3504. <https://doi.org/10.1080/10717544.2016.1199605>.

- (65) Li, P.; Nielsen, H. M.; Müllertz, A. Impact of Lipid-Based Drug Delivery Systems on the Transport and Uptake of Insulin Across Caco-2 Cell Monolayers. *J. Pharm. Sci.* **2016**, *105* (9), 2743–2751. <https://doi.org/10.1016/j.xphs.2016.01.006>.
- (66) Obringer, C.; Manwaring, J.; Goebel, C.; Hewitt, N. J.; Rothe, H. Suitability of the in Vitro Caco-2 Assay to Predict the Oral Absorption of Aromatic Amine Hair Dyes. *Toxicol. Vitro.* **2016**, *32*, 1–7. <https://doi.org/10.1016/j.tiv.2015.11.007>.
- (67) Gaucher, G.; Satturwar, P.; Jones, M. C.; Furtos, A.; Leroux, J. C. Polymeric Micelles for Oral Drug Delivery. *Eur. J. Pharm. Biopharm.* **2010**, *76* (2), 147–158. <https://doi.org/10.1016/j.ejpb.2010.06.007>.
- (68) Delie, F.; Blanco-Prieto, M. J. Polymeric Particulates to Improve Oral Bioavailability of Peptide Drugs. *Molecules* **2005**, *10* (1), 65–80. <https://doi.org/10.3390/10010065>.
- (69) Shaji, J.; Patole, V. Protein and Peptide Drug Delivery: Oral Approaches. *Indian J. Pharm. Sci.* **2008**, *70* (3), 269. <https://doi.org/10.4103/0250-474X.42967>.
- (70) Hauss, D. J. Oral Lipid-Based Formulations. *Adv. Drug Deliv. Rev.* **2007**, *59* (7), 667–676. <https://doi.org/10.1016/j.addr.2007.05.006>.
- (71) Lipinski, C. A. Drug-like Properties and the Causes of Poor Solubility and Poor Permeability. *J. Pharmacol. Toxicol. Methods* **2000**, *44* (1), 235–249. [https://doi.org/10.1016/S1056-8719\(00\)00107-6](https://doi.org/10.1016/S1056-8719(00)00107-6).
- (72) Paul, S. M.; Mytelka, D. S.; Dunwiddie, C. T.; Persinger, C. C.; Munos, B. H.; Lindborg, S. R.; Schacht, A. L. How to Improve R&D Productivity: The Pharmaceutical Industry's Grand Challenge. *Nat. Rev. Drug Discov.* **2010**, *9* (MARch). <https://doi.org/10.1038/nrd3078>.

- (73) Wilson, M.; Williams, M. A.; Jones, D. S.; Andrews, G. P. Hot-Melt Extrusion Technology and Pharmaceutical Application. *Ther. Deliv.* **2012**, *3* (6), 787–797.
- (74) Paudel, A.; Worku, Z. A.; Meeus, J.; Guns, S.; Van den Mooter, G. Manufacturing of Solid Dispersions of Poorly Water Soluble Drugs by Spray Drying: Formulation and Process Considerations. *Int. J. Pharm.* **2013**, *453* (1), 253–284. <https://doi.org/10.1016/j.ijpharm.2012.07.015>.
- (75) Loftsson, T.; Vogensen, S. B.; Brewster, M. E.; Konráðsdóttir, F. Effects of Cyclodextrins on Drug Delivery Through Biological Membranes. *J. Pharm. Sci.* **2007**, *96* (10), 2532–2546. <https://doi.org/10.1002/jps.20992>.
- (76) Ormes, J. D.; Zhang, D.; Chen, A. M.; Hou, S.; Krueger, D.; Nelson, T.; Templeton, A. Design of Experiments Utilization to Map the Processing Capabilities of a Micro-Spray Dryer: Particle Design and Throughput Optimization in Support of Drug Discovery. *Pharm. Dev. Technol.* **2013**, *18* (1), 121–129. <https://doi.org/10.3109/10837450.2011.646424>.
- (77) Huang, Y.; Dai, W.-G. Fundamental Aspects of Solid Dispersion Technology for Poorly Soluble Drugs. *Acta Pharm. Sin. B* **2014**, *4* (1), 18–25. <https://doi.org/10.1016/j.apsb.2013.11.001>.
- (78) Ting, J. M.; Tale, S.; Purchel, A. A.; Jones, S. D.; Widanapathirana, L.; Tolstyka, Z. P.; Guo, L.; Guillaudeu, S. J.; Bates, F. S.; Reineke, T. M. High-Throughput Excipient Discovery Enables Oral Delivery of Poorly Soluble Pharmaceuticals. *ACS Cent. Sci.* **2016**, *2* (10), 748–755. <https://doi.org/10.1021/acscentsci.6b00268>.
- (79) Yin, L.; Hillmyer, M. A. Preparation and Performance of Hydroxypropyl Methylcellulose Esters of Substituted Succinates for in Vitro Supersaturation of a

- Crystalline Hydrophobic Drug. *Mol. Pharm.* **2014**, *11* (1), 175–185.
<https://doi.org/10.1021/mp4003656>.
- (80) Mundargi, R. C.; Babu, V. R.; Rangaswamy, V.; Aminabhavi, T. M. Formulation and in Vitro Evaluation of Transdermal Delivery of Zidovudine-An Anti-HIV Drug. *J. Appl. Polym. Sci.* **2011**, *119* (3), 1268–1274. <https://doi.org/10.1002/app.30832>.
- (81) Ting, J. M.; Navale, T. S.; Bates, F. S.; Reineke, T. M. Design of Tunable Multicomponent Polymers as Modular Vehicles To Solubilize Highly Lipophilic Drugs. *Macromolecules* **2014**, *47* (19), 6554–6565.
<https://doi.org/10.1021/ma501839s>.
- (82) Yamashita, S.; Matsuzawa, Y. Where Are We with Probucol: A New Life for an Old Drug? *Atherosclerosis* **2009**, *207* (1), 16–23.
<https://doi.org/10.1016/j.atherosclerosis.2009.04.002>.
- (83) Sizovs, A.; Xue, L.; Tolstyka, Z. P.; Ingle, N. P.; Wu, Y.; Cortez, M.; Reineke, T. M. Poly(Trehalose): Sugar-Coated Nanocomplexes Promote Stabilization and Effective Polyplex-Mediated siRNA Delivery. *J. Am. Chem. Soc.* **2013**, *135* (41), 15417–15424. <https://doi.org/10.1021/ja404941p>.
- (84) Nasiri, M.; Bertrand, A.; Reineke, T. M.; Hillmyer, M. A. Polymeric Nanocylinders by Combining Block Copolymer Self-Assembly and Nanoskiving. *ACS Appl. Mater. Interfaces* **2014**, *6* (18), 16283–16288. <https://doi.org/10.1021/am504486r>.
- (85) Tale, S. R.; Yin, L.; Reineke, T. M. Trehalose-Functionalized Block Copolymers Form Serum-Stable Micelles. *Polym. Chem.* **2014**, *5* (17), 5160–5168.
<https://doi.org/10.1039/C4PY00399C>.
- (86) Qian, F.; Huang, J.; Hussain, M. A. Drug–Polymer Solubility and Miscibility:

- Stability Consideration and Practical Challenges in Amorphous Solid Dispersion Development. *J. Pharm. Sci.* **2010**, *99* (7), 2941–2947. <https://doi.org/10.1002/jps.22074>.
- (87) Dougherty, D. A. The Cation– π Interaction. *Acc. Chem. Res.* **2013**, *46* (4), 885–893. <https://doi.org/10.1021/ar300265y>.
- (88) U.S. Food & Drug Administration. *Route of Administration*; 2006.
- (89) Huang, Y.; Dai, W.-G. Fundamental Aspects of Solid Dispersion Technology for Poorly Soluble Drugs. *Acta Pharm. Sin. B* **2014**, *4* (1), 18–25. <https://doi.org/10.1016/j.apsb.2013.11.001>.
- (90) Leuner, C.; Dressman, J. Improving Drug Solubility for Oral Delivery Using Solid Dispersions. *Eur. J. Pharm. Biopharm.* **2000**, *50* (1), 47–60.
- (91) Marsac, P. J.; Konno, H.; Taylor, L. S. A Comparison of the Physical Stability of Amorphous Felodipine and Nifedipine Systems. *Pharm. Res.* **2006**, *23* (10), 2306–2316. <https://doi.org/10.1007/s11095-006-9047-9>.
- (92) Liu, H.; Taylor, L. S.; Edgar, K. J. The Role of Polymers in Oral Bioavailability Enhancement; a Review. *Polymer (Guildf)*. **2015**, *77* (Supplement C), 399–415. <https://doi.org/10.1016/j.polymer.2015.09.026>.
- (93) Tanno, F.; Nishiyama, Y.; Kokubo, H.; Obara, S. Evaluation of Hypromellose Acetate Succinate (HPMCAS) as a Carrier in Solid Dispersions. *Drug Dev. Ind. Pharm.* **2004**, *30* (1), 9–17. <https://doi.org/10.1081/DDC-120027506>.
- (94) Shah, P. N.; Lin, L. Y.; Smolen, J. A.; Tagaev, J. A.; Gunsten, S. P.; Han, D. S.; Heo, G. S.; Li, Y.; Zhang, F.; Zhang, S.; et al. In Vivo Efficacy of Shell Cross-Linked Nanoparticle Formulations Carrying Silver Antimicrobials as Aerosolized

Therapeutics. **2013**, 4977–4987.

- (95) He, X.; Fan, J.; Zhang, F.; Li, R.; Pollack, K. a.; Raymond, J. E.; Zou, J.; Wooley, K. L. Multi-Responsive Hydrogels Derived from the Self-Assembly of Tethered Allyl-Functionalized Racemic Oligopeptides. *J. Mater. Chem. B* **2014**, 2 (46), 8123–8130. <https://doi.org/10.1039/C4TB00909F>.
- (96) Azzam, T.; Eisenberg, A.; Nedev, H.; Rosenberg, L.; Maysinger, D. Biomaterials Block-Copolymer Micelles as Carriers of Cell Signaling Modulators for the Inhibition of JNK in Human Islets of Langerhans. *Biomaterials* **2009**, 30 (21), 3597–3604. <https://doi.org/10.1016/j.biomaterials.2009.03.028>.
- (97) Liu, J.; Huang, Y.; Kumar, A.; Tan, A.; Jin, S.; Mozhi, A.; Liang, X.-J. PH-Sensitive Nano-Systems for Drug Delivery in Cancer Therapy. *Biotechnol. Adv.* **2014**, 32 (4), 693–710. <https://doi.org/10.1016/j.biotechadv.2013.11.009>.
- (98) Zheng, L.; Chai, Y.; Liu, Y.; Zhang, P. Controlled RAFT Synthesis of Polystyrene-*b*-Poly (Acrylic Acid) - *b*-Polystyrene Block Copolymers and Their Self-Assembly in an Ionic Liquid [BMIM] [PF6]. **2011**, No. 039, 1–8.
- (99) Surnar, B.; Jayakannan, M. Stimuli-Responsive Poly(Caprolactone) Vesicles for Dual Drug Delivery under the Gastrointestinal Tract. *Biomacromolecules* **2013**, 14 (12), 4377–4387. <https://doi.org/10.1021/bm401323x>.
- (100) Zhang, K.; Fang, H.; Wang, Z.; Li, Z.; Taylor, J.-S. a; Wooley, K. L. Structure-Activity Relationships of Cationic Shell-Crosslinked Knedel-like Nanoparticles: Shell Composition and Transfection Efficiency/Cytotoxicity. *Biomaterials* **2010**, 31 (7), 1805–1813. <https://doi.org/10.1016/j.biomaterials.2009.10.033>.
- (101) Tian, B.; Liu, S.; Wu, S.; Lu, W.; Wang, D.; Jin, L.; Hu, B.; Li, K.; Wang, Z.; Quan,

- Z. PH-Responsive Poly (Acrylic Acid)-Gated Mesoporous Silica and Its Application in Oral Colon Targeted Drug Delivery for Doxorubicin. *Colloids Surfaces B Biointerfaces* **2017**, *154*, 287–296. <https://doi.org/10.1016/j.colsurfb.2017.03.024>.
- (102) Thakral, S.; Thakral, N. K.; Majumdar, D. K. Eudragit®: A Technology Evaluation. *Expert Opin. Drug Deliv.* **2013**, *10* (1), 131–149. <https://doi.org/10.1517/17425247.2013.736962>.
- (103) Zhang, F.; Elsabahy, M.; Zhang, S.; Lin, L. Y.; Zou, J.; Wooley, K. L. Shell Crosslinked Knedel-like Nanoparticles for Delivery of Cisplatin: Effects of Crosslinking. *Nanoscale* **2013**, *5* (8), 3220–3225. <https://doi.org/10.1039/c3nr34320k>.
- (104) Campbell, M. L.; Waite, B. a. The Ka Values of Water and the Hydronium Ion for Comparison with Other Acids. *J. Chem. Educ.* **1990**, *67* (5), 386. <https://doi.org/10.1021/ed067p386>.
- (105) Ferrero, C.; Massuelle, D.; Jeannerat, D.; Doelker, E. Towards Elucidation of the Drug Release Mechanism from Compressed Hydrophilic Matrices Made of Cellulose Ethers. I. Pulse-Field-Gradient Spin-Echo NMR Study of Sodium Salicylate Diffusivity in Swollen Hydrogels with Respect to Polymer Matrix Physical Stru. *J. Control. Release* **2008**, *128* (1), 71–79. <https://doi.org/10.1016/j.jconrel.2008.02.006>.
- (106) Knöös, P.; Svensson, A. V.; Ulvenlund, S.; Wahlgren, M. Release of a Poorly Soluble Drug from Hydrophobically Modified Poly (Acrylic Acid) in Simulated Intestinal Fluids. *PLoS One* **2015**, *10* (10), e0140709. <https://doi.org/10.1371/journal.pone.0140709>.

- (107) Barreiro-Iglesias, R.; Bromberg, L.; Temchenko, M.; Hatton, T. A.; Alvarez-Lorenzo, C.; Concheiro, A. Pluronic-g-Poly(Acrylic Acid) Copolymers as Novel Excipients for Site Specific, Sustained Release Tablets. *Eur. J. Pharm. Sci.* **2005**, *26* (5), 374–385. <https://doi.org/10.1016/j.ejps.2005.07.014>.
- (108) Khougaz, K.; Zhong, X. F.; Eisenberg, A. Aggregation and Critical Micelle Concentrations of Polystyrene -b- Poly (Sodium Acrylate) and Polystyrene -b- Poly (Acrylic Acid) Micelles in Organic Media. *Macromolecules* **1996**, *29* (95), 3937–3949.
- (109) Shen, H.; Eisenberg, A. Morphological Phase Diagram for a Ternary System of Block Copolymer PS 310 - b -PAA 52 / Dioxane / H₂O. **1999**, 9473–9487.
- (110) Burke, S. E.; Eisenberg, A. Kinetics and Mechanisms of the Sphere-to-Rod and Rod-to-Sphere Transitions in the Ternary System PS 310 - b -PAA 52 /Dioxane/Water. *Langmuir* **2001**, *17* (21), 6705–6714. <https://doi.org/10.1021/la010640v>.
- (111) Ma, L.; Eisenberg, A. Relationship between Wall Thickness and Size in Block Copolymer Vesicles. *Langmuir* **2009**, *25* (24), 13730–13736. <https://doi.org/10.1021/la9012729>.
- (112) Rambharose, S.; Ojewole, E.; Mackraj, I.; Govender, T. Comparative Buccal Permeability Enhancement of Didanosine and Tenofovir by Potential Multifunctional Polymeric Excipients and Their Effects on Porcine Buccal Histology. *Pharm. Dev. Technol.* **2014**, *19* (1), 82–90. <https://doi.org/10.3109/10837450.2012.752505>.
- (113) Lo, Y.-L.; Hsu, C.-Y.; Lin, H.-R. PH-and Thermo-Sensitive Pluronic/Poly(Acrylic Acid) in Situ Hydrogels for Sustained Release of an Anticancer Drug. *J. Drug*

- Target*. **2013**, *21* (1), 54–66. <https://doi.org/10.3109/1061186X.2012.725406>.
- (114) Kadajji, V. G.; Betageri, G. V. Water Soluble Polymers for Pharmaceutical Applications. *Polymers (Basel)*. **2011**, *3* (4), 1972–2009. <https://doi.org/10.3390/polym3041972>.
- (115) Tian, Y.; Tam, K. C.; Hatton, T. A.; Bromberg, L. Titration Microcalorimetry Study : Interaction of Drug and Ionic Microgel System.
- (116) Mai, Y.; Eisenberg, A. Self-Assembly of Block Copolymers. *Chem. Soc. Rev.* **2012**, *41* (18), 5969–5985. <https://doi.org/10.1039/c2cs35115c>.
- (117) Ma, Q.; Wooley, K. L. The Preparation of T-butyl Acrylate, Methyl Acrylate, and Styrene Block Copolymers by Atom Transfer Radical Polymerization: Precursors to Amphiphilic and Hydrophilic Block Copolymers and Conversion to Complex Nanostructured Materials. *J. Polym. Sci. Part A Polym. Chem.* **2000**, *38* (S1), 4805–4820. [https://doi.org/10.1002/1099-0518\(200012\)38:1+<4805::AID-POLA180>3.3.CO;2-F](https://doi.org/10.1002/1099-0518(200012)38:1+<4805::AID-POLA180>3.3.CO;2-F).
- (118) Liu, X.; Wu, J.; Kim, J.-S.; Eisenberg, A. Self-Assembly of Mixtures of Block Copolymers of Poly(Styrene-*b*-Acrylic Acid) with Random Copolymers of Poly(Styrene-*Co*-Methacrylic Acid). *Langmuir* **2006**, *22* (1), 419–424. <https://doi.org/10.1021/la0519610>.
- (119) Laaser, J. E.; Jiang, Y.; Sprouse, D.; Reineke, T. M.; Lodge, T. P. PH- and Ionic-Strength-Induced Contraction of Polybasic Micelles in Buffered Aqueous Solutions. *Macromolecules* **2015**, *48* (8), 2677–2685. <https://doi.org/10.1021/acs.macromol.5b00360>.
- (120) Ting, J. M.; Navale, T. S.; Jones, S. D.; Bates, F. S.; Reineke, T. M. Deconstructing

- HPMCAS: Excipient Design to Tailor Polymer-Drug Interactions for Oral Drug Delivery. *ACS Biomater. Sci. Eng.* **2015**, *1* (10), 978–990. <https://doi.org/10.1021/acsbiomaterials.5b00234>.
- (121) Taylor, L. S.; Zografi, G. Spectroscopic Characterization of Interactions between PVP and Indomethacin in Amorphous Molecular Dispersions. *Pharm. Res.* **1997**, *14* (12), 1691–1698.
- (122) Newman, A.; Engers, D.; Bates, S.; Ivanisevic, I.; Kelly, R. C.; Zografi, G. Characterization of Amorphous API:Polymer Mixtures Using X-Ray Powder Diffraction. *J. Pharm. Sci.* **2008**, *97* (11), 4840–4856. <https://doi.org/10.1002/jps.21352>.
- (123) Ilevbare, G. A.; Xu, W.; John, C. T.; D. Ormes, J.; Kuiper, J. L.; Templeton, A. C.; Bak, A. Solubility and Dissolution Considerations for Amorphous Solid Dispersions. In *Pharmaceutical Sciences Encyclopedia*; John Wiley & Sons, Inc.: Hoboken, NJ, USA, 2015; pp 1–41. <https://doi.org/10.1002/9780470571224.pse527>.
- (124) Friesen, D. T.; Shanker, R.; Crew, M.; Smithey, D. T.; Curatolo, W. J.; Nightingale, J. A. S. Hydroxypropyl Methylcellulose Acetate Succinate-Based Spray-Dried Dispersions: An Overview. *Mol. Pharm.* **2008**, *5* (6), 1003–1019. <https://doi.org/10.1021/mp8000793>.
- (125) Vehring, R. Pharmaceutical Particle Engineering via Spray Drying. *Pharm. Res.* **2008**, *25* (5), 999–1022. <https://doi.org/10.1007/s11095-007-9475-1>.
- (126) Kimura, T.; Higaki, K. Gastrointestinal Transit and Drug Absorption. *Biol. Pharm. Bull.* **2002**, *25* (2), 149–164.

- (127) Erah, P. The Stability of Amoxicillin, Clarithromycin and Metronidazole in Gastric Juice: Relevance to the Treatment of Helicobacter Pylori Infection. *J. Antimicrob. Chemother.* **1997**, *39* (1), 5–12. <https://doi.org/10.1093/jac/39.1.5>.
- (128) Ricarte, R. G.; Li, Z.; Johnson, L. M.; Ting, J. M.; Reineke, T. M.; Bates, F. S.; Hillmyer, M. A.; Lodge, T. P. Direct Observation of Nanostructures during Aqueous Dissolution of Polymer/Drug Particles. *Macromolecules* **2017**, *50* (8), 3143–3152. <https://doi.org/10.1021/acs.macromol.7b00372>.
- (129) Fagerberg, J. H.; Tsinman, O.; Sun, N.; Tsinman, K.; Avdeef, A.; Bergström, C. A. S. Dissolution Rate and Apparent Solubility of Poorly Soluble Drugs in Biorelevant Dissolution Media. *Mol. Pharm.* **2010**, *7* (5), 1419–1430. <https://doi.org/10.1021/mp100049m>.
- (130) Qin, J.; Jiang, X.; Gao, L.; Chen, Y.; Xi, F. Functional Polymeric Nanoobjects by Cross-Linking Bulk Self-Assemblies of Poly(Tert -Butyl Acrylate)- Block - Poly(Glycidyl Methacrylate). *Macromolecules* **2010**, *43* (19), 8094–8100. <https://doi.org/10.1021/ma101639w>.
- (131) Jakeš, J. Regularized Positive Exponential Sum (REPES) Program - A Way of Inverting Laplace Transform Data Obtained by Dynamic Light Scattering. *Collect. Czechoslov. Chem. Commun.* **1995**, *60* (11), 1781–1797. <https://doi.org/10.1135/cccc19951781>.
- (132) Einstein, A. Über Die von Der Molekularkinetischen Theorie Der Wärme Geforderte Bewegung von in Ruhenden Flüssigkeiten Suspendierten Teilchen. *Ann. Phys.* **1905**, *322* (8), 549–560. <https://doi.org/10.1002/andp.19053220806>.
- (133) Dressman, J. B.; Berardi, R. R.; Dermentzoglou, L. C.; Russell, T. L.; Schmaltz, S.

- P.; Barnett, J. L.; Jarvenpaa, K. M. Upper Gastrointestinal (GI) PH in Young, Healthy Men and Women. *Pharm. Res.* **1990**, *7* (7), 756–761.
- (134) Imura, T. K.; Igaki, K. H. Gastrointestinal Transit and Drug Absorption. **2002**, *25* (February).
- (135) Barner-Kowollik, C.; Davis, T. P.; Stenzel, M. H. Synthesis of Star Polymers Using RAFT Polymerization: What Is Possible? *Aust. J. Chem.* **2006**, *59* (10), 719–727. <https://doi.org/10.1071/CH06297>.
- (136) McKenzie, T. G.; Wong, E. H. H.; Fu, Q.; Sulistio, A.; Dunstan, D. E.; Qiao, G. G. Controlled Formation of Star Polymer Nanoparticles via Visible Light Photopolymerization. *ACS Macro Lett.* **2015**, *4* (9), 1012–1016. <https://doi.org/10.1021/acsmacrolett.5b00530>.
- (137) Park, S.; Cho, H. Y.; Wegner, K. B.; Burdynska, J.; Magenau, A. J. D.; Paik, H.; Jurga, S.; Matyjaszewski, K. Star Synthesis Using Macroinitiators via Electrochemically Mediated Atom Transfer Radical Polymerization. *Macromolecules* **2013**, *46* (15), 5856–5860. <https://doi.org/10.1021/ma401308e>.
- (138) Liu, G.; Qiu, Q.; Shen, W.; An, Z. Aqueous Dispersion Polymerization of 2-Methoxyethyl Acrylate for the Synthesis of Biocompatible Nanoparticles Using a Hydrophilic RAFT Polymer and a Redox Initiator. *Macromolecules* **2011**, *44* (13), 5237–5245. <https://doi.org/10.1021/ma200984h>.
- (139) Zhang, C.; Miao, M.; Cao, X.; An, Z. One-Pot RAFT Synthesis of Core Cross-Linked Star Polymers of PolyPEGMA in Water by Sequential Homogeneous and Heterogeneous Polymerizations. *Polym. Chem.* **2012**, *3* (9), 2656. <https://doi.org/10.1039/c2py20442h>.

- (140) Jackson, A. W.; Fulton, D. A. PH Triggered Self-Assembly of Core Cross-Linked Star Polymers Possessing Thermoresponsive Cores. *Chem. Commun.* **2011**, 47 (24), 6807. <https://doi.org/10.1039/c1cc11785h>.
- (141) Wong, E. H. H.; Blencowe, A.; Qiao, G. G. Quantitative Formation of Core Cross-Linked Star Polymers via a One-Pot Two-Step Single Electron Transfer-Living Radical Polymerization. *Polym. Chem.* **2013**, 4 (17), 4562. <https://doi.org/10.1039/c3py00726j>.
- (142) Soliman, G. M.; Sharma, R.; Choi, A. O.; Varshney, S. K.; Winnik, F. M.; Kakkar, A. K.; Maysinger, D. Tailoring the Efficacy of Nimodipine Drug Delivery Using Nanocarriers Based on A2B Miktoarm Star Polymers. *Biomaterials* **2010**, 31 (32), 8382–8392. <https://doi.org/10.1016/j.biomaterials.2010.07.039>.
- (143) Etrych, T.; Kovář, L.; Strohalm, J.; Chytil, P.; Říhová, B.; Ulbrich, K. Biodegradable Star HPMA Polymer–Drug Conjugates: Biodegradability, Distribution and Anti-Tumor Efficacy. *J. Control. Release* **2011**, 154 (3), 241–248. <https://doi.org/10.1016/j.jconrel.2011.06.015>.
- (144) Kostková, H.; Schindler, L.; Kotrchová, L.; Kovář, M.; Šírová, M.; Kostka, L.; Etrych, T. Star Polymer-Drug Conjugates with PH-Controlled Drug Release and Carrier Degradation. *J. Nanomater.* **2017**, 2017. <https://doi.org/10.1155/2017/8675435>.
- (145) Ren, J. M.; McKenzie, T. G.; Fu, Q.; Wong, E. H. H.; Xu, J.; An, Z.; Shanmugam, S.; Davis, T. P.; Boyer, C.; Qiao, G. G. Star Polymers. *Chem. Rev.* **2016**, 116 (12), 6743–6836. <https://doi.org/10.1021/acs.chemrev.6b00008>.
- (146) Liu, J.; Duong, H.; Whittaker, M. R.; Davis, T. P.; Boyer, C. Synthesis of Functional

- Core, Star Polymers via RAFT Polymerization for Drug Delivery Applications. *Macromol. Rapid Commun.* **2012**, *33* (9), 760–766. <https://doi.org/10.1002/marc.201200029>.
- (147) Kreutzer, G.; Ternat, C.; Nguyen, T. Q.; Plummer, C. J. G.; Månson, J.-A. E.; Castelletto, V.; Hamley, I. W.; Sun, F.; Sheiko, S. S.; Herrmann, A.; et al. Water-Soluble, Unimolecular Containers Based on Amphiphilic Multiarm Star Block Copolymers. *Macromolecules* **2006**, *39* (13), 4507–4516. <https://doi.org/10.1021/ma060548b>.
- (148) Hedrick, J. L.; Trollsås, M.; Hawker, C. J.; Atthoff, B.; Claesson, H.; Heise, A.; Miller, R. D.; Mecerreyes, D.; Jérôme, R.; Dubois, P. Dendrimer-like Star Block and Amphiphilic Copolymers by Combination of Ring Opening and Atom Transfer Radical Polymerization. *Macromolecules* **1998**, *31* (25), 8691–8705. <https://doi.org/10.1021/ma980932b>.
- (149) Barner, L.; Li, C.; Hao, X.; Stenzel, M. H.; Barner-Kowollik, C.; Davis, T. P. Synthesis of Core-Shell Poly(Divinylbenzene) Microspheres via Reversible Addition Fragmentation Chain Transfer Graft Polymerization of Styrene. *J. Polym. Sci. Part A Polym. Chem.* **2004**, *42* (20), 5067–5076. <https://doi.org/10.1002/pola.20328>.
- (150) Gao, H.; Matyjaszewski, K. Synthesis of Star Polymers by A New “Core-First” Method: Sequential Polymerization of Cross-Linker and Monomer. *Macromolecules* **2008**, *41* (4), 1118–1125. <https://doi.org/10.1021/ma702560f>.
- (151) Zhang, Z.; Yin, L.; Tu, C.; Song, Z.; Zhang, Y.; Xu, Y.; Tong, R.; Zhou, Q.; Ren, J.; Cheng, J. Redox-Responsive, Core Cross-Linked Polyester Micelles. *ACS Macro*

- Lett.* **2013**, 2 (1), 40–44. <https://doi.org/10.1021/mz300522n>.
- (152) Skey, J.; O'Reilly, R. K. Facile One Pot Synthesis of a Range of Reversible Addition-Fragmentation Chain Transfer (RAFT) Agents. *Chem. Commun.* **2008**, No. 35, 4183–4185. <https://doi.org/10.1039/B804260H>.
- (153) Neises, B.; Steglich, W. Simple Method for the Esterification of Carboxylic Acids. *Angew. Chemie Int. Ed. English* **1978**, 17 (7), 522–524. <https://doi.org/10.1002/anie.197805221>.
- (154) Das, A.; Theato, P. Multifaceted Synthetic Route to Functional Polyacrylates by Transesterification of Poly(Pentafluorophenyl Acrylates). *Macromolecules* **2015**, 48 (24), 8695–8707. <https://doi.org/10.1021/acs.macromol.5b02293>.
- (155) Woodhead Publishing Series in Biomedicine. Starch and Derivatives as Pharmaceutical Excipients. In *Controlled Drug Delivery*; Elsevier, 2015; pp 21–84. <https://doi.org/10.1016/B978-1-907568-45-9.00002-0>.
- (156) Ogaji, I. J.; Nep, E. I.; Audu-Peter, J. D. Advances in Natural Polymers as Pharmaceutical Excipients. *Pharm. Anal. Acta* **2012**, 03 (01). <https://doi.org/10.4172/2153-2435.1000146>.
- (157) Ricarte, R. G.; Lodge, T. P.; Hillmyer, M. A. Detection of Pharmaceutical Drug Crystallites in Solid Dispersions by Transmission Electron Microscopy. *Mol. Pharm.* **2015**, 12 (3), 983–990. <https://doi.org/10.1021/mp500682x>.